Supercurrent through grain boundaries in the presence of strong correlations

Masterarbeit im Fach Physik
vorgelegt der
mathematisch-naturwissenschaflichen Fakultät
der Universität Augsburg von

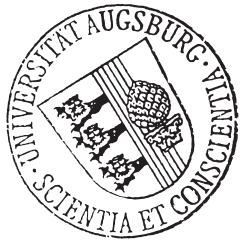

Fabian Alexander Wolf

Juni 2011

angefertigt am Lehrstuhl für Experimentalphysik VI
Zentrum für elektronische Korrelationen und Magnetismus
Institut für Physik der Universität Augsburg
bei Prof. Dr. T. Kopp
Zweitprüfer: Prof. Dr. D. Vollhardt

Abstract

Strong correlations are known to severely reduce the mobility of charge carriers near half-filling and thus have an important influence on the current carrying properties of grain boundaries in the high-T_c cuprates. In order to analyze this influence, we derive an extension of the Gutzwiller projection approach capable to treat general strongly inhomogeneous systems. An application of the method to grain boundaries yields an exponential reduction of the critical supercurrent with increasing misalignment angle. Our results are in quantitative agreement with experimental data.

We furthermore provide a detailed comparison to an analogous weak-coupling evaluation, as well as derivations and discussions of the Bogoliubov - de Gennes (BdG) framework, the renormalized mean-field theory (RMFT) and the super-cell method.

Thanks to

I am grateful to S. Graser and T. Kopp for being great supervisors during the time of this thesis, as well as to F. Loder for lots of helping advice. This work would not have been possible without the almost two years of practical learning before: I owe much to M. Kollar and M. Rigol who guided my first steps in doing research in theoretical physics as well as to D. Vollhardt who always helped in practical issues and gave great lectures. Finally I thank Andrea — who unexpectedly saw herself confronted with me doing physics all the time — and my parents for their continuous support.

Contents

1. Introduction

The design of high-temperature superconducting cables as well as the characterization of well-defined interfaces and contacts for superconducting microwave electronics has been optimized over the last 20 years so that they are now found in applications ranging from short range power supply to medical instrumentation. This has been made possible by intensive experimental and theoretical research which lead to a better understanding of the bulk as well as the interface properties of high-T_c materials.[1] One of the most complex and puzzling problems in this respect is the strong reduction of the critical current j_c as a function of the grain boundary (GB) angle. This problem is furthermore of particular practical relevance (Freericks 2010). Among the various potential and realized technical applications of superconductors[2] the largest application of conventional superconductors in industry has come in the form of superconducting wires for magnets, such as those used for most magnetic resonance imaging machines. But exactly for this purpose, unconventional (high-temperature) superconductors fall short due to the exponential reduction of the current at GBs.

For these reasons, artificially fabricated, well defined GBs, have been extensively studied (Hilgenkamp and Mannhart 2002). Although great progress has been made to reduce the influence of large angle GBs on the total current (Hammerl *et al.* 2002) and to locally improve their current carrying properties (Hammerl *et al.* 2000) a full theoretical understanding of the grain boundary problem is hampered by the complexity of the physics involved. In a recent study by Graser *et al.* (2010), the experimentally observed decay of j_c with increasing misalignment angle was reproduced in a microscopic model in which charge inhomogeneities at the grain boundary were identified as the main source for the suppression of j_c. But still the overall magnitude of j_c could not be correctly determined and it was speculated that strong electronic correlations present in the high-T_c materials might be responsible for this discrepancy.[3]

The main aim of this thesis is to present an analysis of the supercurrent through GBs that takes into account the presence of strong Coulomb interactions. In order to capture generic defects of the lattice for a certain GB angle, a theoretically reconstructed sample of a GB should include at least several hundred lattice sites. Due to numerical limitations, this can only be modeled by an effective one-particle description. To incorporate static correlations nevertheless we employ a Gutzwiller approximation (Zhang *et al.* 1988) that should already

[1] Hilgenkamp and Mannhart (2002), Dimos *et al.* (1988), Gurevich and Pashitskii (1998), Stolbov *et al.* (1999), Pennycook *et al.* (2000), Tanaka and Kashiwaya (1995), Freericks (2006), Yokoyama *et al.* (2007), Schwingenschlögl and Schuster (2009).

[2] For example, low-cost current-carrying wires, passive electronic devices, and high-speed active digital electronics.

[3] Andersen *et al.* (2008) made the assertion based on a non-microscopic calcualtion for the special case of (110) junctions. In contrast to that, in this thesis a microscopic calculation is employed.

capture an important part of the GB physics.

The Gutzwiller approach had a lot of success for the description of homogeneous models of cuprate high-T_c superconductors (Anderson *et al.* 2004). In the last years it could be rigorously extended to inhomogeneous systems (Wang *et al.* 2006, Ko *et al.* 2007) and is now an established method to e.g. capture important aspects of the interplay between impurities and superconductivity (Garg *et al.* 2008). In this thesis, we employ an extended implementation ot the Gutzwiller projection approach that is able to account for the very strong inhomogeneities present in GBs, which is otherwise not possible. Using this method we obtain excellent agreement with experimental data.

The thesis is structured into three parts. In Sec. 2, the extended Gutzwiller approximation scheme is derived in detail. Sec. 3 is dedicated to the employed methods, the Bogoliubov - de Gennes (BdG) framework and the renormalized mean field theory (RMFT). In Sec. 4, these tools are employed to discuss the supercurrent through GBs in the presence of strong correlations.

2. Gutzwiller approximation for strongly inhomogeneous systems

The Hubbard model,[1] given by the hamiltonian

$$H_{\text{Hubbard}} = -\sum_{\langle ij\rangle s} t_{ij}(c^{\dagger}_{is}c_{js} + \text{h.c.}) + U\sum_{i}(\hat{n}_{i\uparrow} - \tfrac{1}{2})(\hat{n}_{i\downarrow} - \tfrac{1}{2}) \tag{2.1}$$

allows to address several aspects of unconventional superconductivity. In the half filled case and with an interaction U stronger than a certain critical value, the system is in a Mott insulating state.[2] For very large U this state can be thought to be a Heisenberg antiferromagnet, the effective spin coupling constant of which originates from virtual hopping processes and has a value of $J = t^2/U$. Anderson (1987) proposed that upon doping, the antiferromagnetic Néel lattice is melted and a spin liquid groundstate emerges. This spin liquid state is called the resonating valence bond (RVB) state,[3] in which the neutral magnetic singlet pairs of the insulator have become charged superconducting pairs.

For the functional form of the RVB state different propositions were made, the most successfull one turned out to be the one proposed by Anderson (1987)

$$|\psi\rangle \equiv |\text{RVB}\rangle \equiv \mathcal{P}|\psi\rangle_0 \quad \text{where} \quad |\psi_0\rangle \equiv |\text{BCS}\rangle \equiv \prod_{\boldsymbol{k}}(u_{\boldsymbol{k}} + v_{\boldsymbol{k}}c^{\dagger}_{\boldsymbol{k}\uparrow}c^{\dagger}_{\boldsymbol{k}\downarrow})|\text{vac}\rangle \tag{2.2}$$

$$\mathcal{P} \equiv \prod_{i}(1 - \hat{n}_{i\uparrow}\hat{n}_{i\downarrow}) \tag{2.3}$$

and $|\text{vac}\rangle$ is the state devoid of all particles. It is meant to be viewed as a natural extension of the usual BCS state for strongly correlated systems. Indeed this state is capable to describe several physical properties of cuprate superconductors. For reviews about this see e.g. Anderson *et al.* (2004) or Edegger *et al.* (2007).

The problem with the state in Eq. (2.2) is that the form of the projection operator makes it very hard to calculate analytical results. Following the original idea of Gutzwiller (1965),[4] Zhang *et al.* (1988) introduced a version of the Gutzwiller approximation that evaluates expectation values within the RVB state by taking into account the projection operator in an approximate way via classical statistical weights. For this they used techniques developed

[1] The Hubbard model was introduced simultaneously by Hubbard (1963), Kanamori (1963) and Gutzwiller (1963).

[2] Confer Mott (1949) and Brinkman and Rice (1970).

[3] Earlier ideas concerning a realization of the RVB state were formulated already by Anderson (1973) and Fazekas and Anderson (1974).

[4] The original formulation of the Gutzwiller approximation (Gutzwiller 1965) was introduced in order to approximate an exact evaluation of the Gutzwiller wave function (Gutzwiller 1963; 1964).

and clarified by Ogawa *et al.* (1975) and Vollhardt (1984). Zhang *et al.* (1988) showed by comparison with variational Monte Carlo calculations that their evaluation yields results that are in good qualitative agreement with a numerically exact calculation. Although the Gutzwiller approximation neglects all quantum correlations[5] and only retains combinatorial ones.

2.1. Basic theoretical concept

The argumentation used by Zhang *et al.* (1988) to introduce their Gutzwiller approximation is so short and instructive that it is presented here. The reader will get an intuition for the physical and technical implications which will make it easier to later follow the derivation of an extended version of the Gutzwiller approximation.

The key idea to evaluate expectation values in the RVB state is to assume complete statistical independence of the populations on different sites. This assumption is of course a very crude one and means basically to treat certain important aspects of the quantum electronic system like a classical, ideal gas. This can only lead to physical results in special situations and for special observables. We keep this in mind and stress that the Gutzwiller approximation is far from being a correct microscopic description of the system, but may rather be viewed as a phenomenological description that can lead to physical insights.

This thesis will focus on the t-J-model which is well established to describe superconduction in Cu oxides (Zhang and Rice 1988). It can be directly derived from an analyzation of the physical processes in the Cu oxides[6] or from a strong coupling expansion of the Hubbard model. Its hamiltonian is given by[7]

$$H = -t \sum_{(ij)s} (c_{is}^{\dagger} c_{js} + \text{h.c.}) + J \sum_{\langle ij \rangle} \boldsymbol{S}_i \cdot \boldsymbol{S}_j \tag{2.4}$$

We are interested in the two expectation values that characterize the two microscopic processes captured in Eq. (2.4). This is the hopping and the spin-interaction process. Their expectation value corresponds to their probability of occurrence in the system state.

The Gutzwiller approximated probability for a hopping process in a state that allows double occupation $|\psi_0\rangle$ is calculated as follows. One neglects spatial correlations but still considers non-distinguishable electrons that obey the Pauli principle. Furthermore the probability for a process is calculated as the product of the probability amplitudes of its start and end configuration. The four possible start configurations[8] for an $\uparrow$-spin hopping process

[5] Dynamical correlations are already excluded due to the variational wave function ansatz. Spatial correlations are neglected when employing the Gutzwiller approximation. This will become clearer later on.

[6] For this issue and further information, see the review by Ogata and Fukuyama (2008).

[7] The no-double occupancy condition for the hopping term that is usually present in the t-J-hamiltonian is not taken into account in Eq. (2.4) as the Gutzwiller projector in the wave function makes it redundant. In other words, the no-double occupancy condition of the full t-J-hamiltonian is already implemented in the variational wave function. As we focus solely either on Gutzwiller evaluations or on completely uncorrelated Hartree-Fock evaluations that simply neglect the no-double occupancy condition, we employ the hamiltonian as given in Eq. (2.4).

[8] We classify configurations with respect to the kind of occupation of a site: empty (holon), occupied with

from site i to site j must have a site i occupied with an $\uparrow$-spin electron and a site j not occupied by an $\uparrow$-spin electron, due to the Pauli principle. The end configuration is then just inverted with respect to the site indices i, j, such that the probability for the process reads

$$\langle c^\dagger_{i\uparrow} c_{j\uparrow}\rangle_0 \sim \underbrace{\left(n_{i\uparrow}(1-n_{j\uparrow})\right)^{1/2}}_{\sqrt{P(\text{end configuration})}} \underbrace{\left((1-n_{i\uparrow})n_{j\uparrow}\right)^{1/2}}_{\sqrt{P(\text{start configuration})}} \tag{2.8}$$

Consider now a system that does not allow for double occupancies but has the same density (one simply adjusts μ accordingly). Such a system corresponds to the wave function $|\psi\rangle$, in which doublons are projected out. In such a system only three types of occupations are possible: occupation by a hole, an $\uparrow$-spin or $\downarrow$-spin electron. This changes the probabilities for the different populations Eq. (2.6) and thus the probability for the start and end configuration of a $\uparrow$-spin hopping process. The probability for the whole process in $|\psi\rangle$ then reads

$$\langle c^\dagger_{i\uparrow} c_{j\uparrow}\rangle \sim \left(n_{i\uparrow}(1-n_j)(1-n_i)n_{j\uparrow}\right)^{1/2} \tag{2.9}$$

where $n_i \equiv n_{i\uparrow} + n_{i\downarrow}$.

The derivation of these probabilities makes sense only for a homogeneous system where $n_i \equiv n$. Only then the approximation of the system as a non-correlated gas is reasonable. One is only interested in the paramagnetic case such that $n_{i\uparrow} = n_{i\downarrow} = \frac{n}{2}$ holds true. With this we can give the ratio for the probabilities of a hopping process in a strongly correlated system being one in which doublons are projected out, compared to a non-correlated system in which doublons are present

$$\frac{\langle c^\dagger_{i\uparrow} c_{j\uparrow}\rangle}{\langle c^\dagger_{i\uparrow} c_{j\uparrow}\rangle_0} \sim \frac{\left(n_{i\uparrow}(1-n_j)(1-n_i)n_{j\uparrow}\right)^{1/2}}{\left(n_{i\uparrow}(1-n_{j\uparrow})(1-n_{i\uparrow})n_{j\uparrow}\right)^{1/2}} = \frac{2(1-n)}{2-n} \tag{2.10}$$

---

a $\uparrow$-spin electron, occupied with a $\downarrow$-spin electron, doubly occupied (doublon).

To make the following arguments more clear we give the probabilities for the just mentioned different populations of a site i when spatial correlations are neglected, i.e. populations are treated as in a classical, ideal gas on a lattice. We furthermore consider results in the thermodynamic limit ($L, N \to \infty$ where L is the number of lattice sites and N the number of particles). For a Hilbert space that allows double occupancies the probabilities are

$$P_i(\uparrow) = n_{i\uparrow}(1-n_{i\downarrow}) \tag{2.5a}$$
$$P_i(\downarrow) = n_{i\downarrow}(1-n_{i\uparrow}) \tag{2.5b}$$
$$P_i(0) = (1-n_{i\uparrow})(1-n_{i\downarrow}) \tag{2.5c}$$
$$P_i(\uparrow\downarrow) = n_{i\uparrow}n_{i\downarrow} \tag{2.5d}$$

and for a Hilbert space that only allows empty and singly occupied sites

$$P_i(\uparrow) = n_{i\uparrow} \qquad P_i(\downarrow) = n_{i\downarrow} \qquad P_i(0) = 1 - n_{i\uparrow} - n_{i\downarrow} \tag{2.6}$$

The site index i is merely given to distinguish start and end configuration of the processes discussed in the text above. We consider a homogeneous system where all sites are equivalent.

As it will be needed later, below the probabilities for a Hilbert space that does not allow for holes are given. For simplicity, here are only the results for the spin-symmetric case $n_{i\uparrow} = n_{i\downarrow} = \frac{n_i}{2}$

$$P_i(\uparrow) = (1 - \frac{n_i}{2}) = P_i(\downarrow) \qquad P_i(\uparrow\downarrow) = n_i - 1 \tag{2.7}$$

This ratio defines the Gutzwiller factor g^t

$$\langle c_{is}^\dagger c_{js}\rangle \overset{\text{Gutzw.}}{\simeq} g^t(n)\langle c_{is}^\dagger c_{js}\rangle_0 \quad , \qquad g^t(n) \equiv \frac{2(1-n)}{2-n} \tag{2.11}$$

This is an approximate expression for the probability of a hopping process in the complicated state $|\psi\rangle$ in dependence of the probability of a hopping process in the simple product state $|\psi_0\rangle = |\text{BCS}\rangle$ describing non-interacting pairs of electrons. We note that for both, neither the free $|\psi_0\rangle = |\text{BCS}\rangle$ nor the exactly evaluated projected state $|\psi\rangle$ the assumption of statistical independence of site populations holds true[9] such that the approximation of equation Eq. (2.11) certainly contains spatial correlations also on the right hand side. This makes the approximation a non-trivial one. It is therefore wrong to think that the Gutzwiller approximation amounts to fully neglecting spatial correlations[10] — it is only in the derivation of the statistical weighting factors that they are neglected. Realizing this we would now rather say that the Gutzwiller approximation in the form just introduced makes the assumption that the description of expectation values in $|\psi\rangle$ is possible with a product state of non-interacting particles for $|\psi\rangle$, if the latter is appropriately renormalized. This can be a good approximation if the expectation value under consideration does not depend on the details of the complicated form of $|\psi\rangle$ but rather on general energetic considerations.

For the spin exchange process between an $\uparrow$-spin electron on site i and a $\downarrow$-spin electron on site j, start and end configuration have to consist of two singly occupied sites. All other configurations imply a contradiction with the Pauli Principle. The probability for the spin interaction process[11] in the states $|\psi_0\rangle$ and $|\psi\rangle$ can then be given in analogy to the above derivation

$$\langle \boldsymbol{S}_i \cdot \boldsymbol{S}_j\rangle_0 \sim \left(n_{i\uparrow}(1-n_{i\downarrow})n_{j\downarrow}(1-n_{j\uparrow})n_{i\downarrow}(1-n_{i\uparrow})n_{j\uparrow}(1-n_{j\downarrow})\right)^{1/2} \tag{2.12}$$

$$\langle \boldsymbol{S}_i \cdot \boldsymbol{S}_j\rangle \sim \left(n_{i\uparrow}n_{j\downarrow}n_{i\downarrow}n_{j\uparrow}\right)^{1/2} \tag{2.13}$$

The ratio of these probabilities defines the Gutzwiller factor for the spin interaction process

$$\langle \boldsymbol{S}_i \cdot \boldsymbol{S}_j\rangle \overset{\text{Gutzw.}}{\simeq} g^J(n)\langle \boldsymbol{S}_i \cdot \boldsymbol{S}_j\rangle_0 \quad , \qquad g_J(n) \equiv \frac{4}{(2-n)^2} \tag{2.14}$$

Finally the limiting cases $n \to 1$ and $n \to 0$ are briefly discussed. Clearly $g_t(n=1) = 0$, i.e. the probability for a hopping process in a system at half filling in which doublons are projected out. This situation is an immediate consequence of the Pauli exclusion principle

[9] Otherwise, of course, the result would be Eq. (2.9), the hopping probability in the approximation of complete statistical independence of site populations.

[10] This would be the case for a so-called Gutzwiller type wave function that is constructed such that $\langle A_i B_j\rangle = \langle A_i\rangle\langle B_j\rangle$ holds true exactly for any local operators A_i and B_i. Above the neglected spatial correlation is recuperated on the r.h.s. of Eq. (2.11) by using a wave function $|\psi_0\rangle$ that allows spatial correlations such that here way employ a better approximation. Nevertheless, even approximations with Gutzwiller-type wave functions are very successfully employed (e.g. for the description of cold gases Jaksch *et al.* (1998) and Jaksch *et al.* (2002)).

[11] Note here that also other processes than the spin exchange process are involved in the spin interaction, e.g. the charge density interaction. Historically this was ignored — the issue will be discussed in detail in Sec. 2.2.

for a Coulomb interaction higher than a critical value and the corresponding state is the Mott insulator already mentioned above. One calculates furthermore $g^J(n=1)=4$ which reflects the fact that in a half filled system without double occupations spin-exchange processes can happen between much more sites than in a system of the same density allowing double occupations. For zero filling we have $g^t(n=0)=g^J(n=0)=1$. This means that for fillings close to zero filling, the effects of combinatorial correlation can be neglected. This is also in correspondence with the trivial physical insight, that almost no electrons will almost never meet and therefore almost never interact. With this we already captured some important physical aspects of a strongly correlated system though it is not obvious that this is right beyond the qualitative level.

Particle-hole transformation Consider now what happens in a system that is electron doped, i.e. $n>1$. One can define an operator that creates a hole as

$$h_{is}^\dagger \equiv c_{is} \tag{2.15}$$

with its hermitian conjugate. If all $c_{is}^\dagger$ operators in the hamiltonian of the Hubbard model, now including a term with a chemical potential,

$$H_{\text{Hubbard}}(t,U,\mu) = -\sum_{\langle ij\rangle s} t_{ij}(c_{is}^\dagger c_{js} + \text{h.c.}) + U\sum_i (n_{i\uparrow}-\tfrac{1}{2})(n_{i\downarrow}-\tfrac{1}{2}) - \mu\sum_i n_i \tag{2.16}$$

are expressed in terms of the $h_{is}^\dagger$ operators one sees that the expression remains invariant up to a minus sign for the kinetic energy and the chemical potential term.[12] Without any problem one can absorb an overall minus sign to produce a hamiltonian $H_{\text{Hubbard}}(t,-U,\mu)$ being equivalent to $H_{\text{Hubbard}}(-t,U,-\mu)$. This procedure is called a particle-hole transformation.

Without being concerned with mathematical issues here, the question arises what a system above half filling behaves like and if the idea of a particle-hole transformation can be useful for its inspection. Take the interaction term: When $n>1$ in a snapshot of the system state there are at least $n-1$ double occupations. Starting from this situation, one realizes that any creation of an empty site costs the energy of a further double occupation, as these processes can only happen simultaneously. In this situation empty sites have taken the role of double occupations. This is just the physics described by the transformation from $H_{\text{Hubbard}}(t,U)$ to $H_{\text{Hubbard}}(t,-U)$ if we take the transformed hamiltonian as consisting of particle operators $c^\dagger$ again.

In a pragmatic sense, we use the projection operator in the Gutzwiller wave function to reintroduce the neglected no-double occupancy condition in the t-J-model hamiltonian. This no-double occupancy condition is a result of the strong-coupling theory that leads from the Hubbard model to the t-J-model by considering processes that take place only in the lower Hubbard band, i.e. the set of local states with doublons excluded. As already mentioned,

[12] For the interaction term we have $(n_{is}-\frac{1}{2}) = (c_{is}^\dagger c_{is}-\frac{1}{2}) = (\frac{1}{2}-c_{is}c_{is}^\dagger) = -(h_{is}^\dagger h_{is}-\frac{1}{2})$. Such that the product of the two spin terms cancels the minus sign. For the kinetic energy and the chemical potential term we perform one simple commutation that yields the minus sign.

this is no longer the right way to describe the system if the chemical potential is so large that the system is above half filling. Then one is forced to consider only the upper Hubbard band. In order to choose a physical t-J-model, one then has to choose a projection operator that projects out holes in the wave function, i.e. take the setting of Eq. (2.2) but define the projection operator as

$$\mathcal{P}_h \equiv \prod_i (1 - E_i) \quad \text{where} \quad E_i = (1 - \hat{n}_{i\uparrow})(1 - \hat{n}_{i\downarrow}) \tag{2.17}$$

Then the Gutzwiller factors can be calculated using Eq. (2.7)

$$\langle c_{is}^\dagger c_{js} \rangle \sim g_t(n) \langle c_{is}^\dagger c_{js} \rangle_0 \quad , \qquad g_t(n) \equiv \frac{2(n-1)}{n} \tag{2.18}$$

$$\langle \boldsymbol{S}_i \cdot \boldsymbol{S}_j \rangle \sim g_J(n) \langle \boldsymbol{S}_i \cdot \boldsymbol{S}_j \rangle_0 \quad , \qquad g_J(n) \equiv \frac{4}{n^2} \tag{2.19}$$

This result can be directly obtained by performing a local particle hole transformation in the expressions Eqs. (2.11) and (2.14) by replacing the spin-dependent densities $n_{is} \to 1 - n_{is}$ or for a homogeneous paramagnet $n \to 2 - n$.

2.2. Standard application for inhomogeneous systems

One may wonder why the preceding derivation of the Gutzwiller factors is not valid for inhomogeneous systems. This is due to the fact that upon projecting with the operator $\mathcal{P}$ defined in Eq. (2.2) the local densities n_i will not coincide in the two states $|\psi\rangle$ and $|\psi_0\rangle$. Another reason is the justification of the calculations for the occupancies in footnote 8 which rely completely on the picture of a classical, ideal gas. It is hard to believe that this should be valid in an inhomogeneous system. Nevertheless it will turn out that a quantum mechanical evaluation of expectation values will yield the same result as a naive application of the results of the preceding section to inhomogeneous systems.

Only recently, a mathematically clear derivation of the Gutzwiller factors for inhomogeneous systems was presented by Wang *et al.* (2006). They again referred to the t-J-model which includes now an additional term with local impurity potentials ϵ_i

$$H = -t \sum_{(ij)s} (c_{is}^\dagger c_{js} + \text{h.c.}) + J \sum_{\langle ij \rangle} \boldsymbol{S}_i \cdot \boldsymbol{S}_j + \sum_{is} (\epsilon_i - \mu) c_{is}^\dagger c_{is} \tag{2.20}$$

Here their derivation is briefly sketched to provide an appropiate introduction to Sec. 2.3. There an extension of their work will be derived in order to describe strongly inhomogeneous systems, e.g. grain boundaries (Sec. 4). For the clarification of certain additional aspects in this section Ko *et al.* (2007) will be consulted.[13]

[13] Further remarks:
(i) A clear improvement of the method that is presented here is given by Fukushima (2008). As in this thesis the aim is not to work with the best Gutzwiller approximation possible, but rather to use a phenomenological tool that allows to describe the problem of interest (Sec. 4), these details are not given.
(ii) Successfull applications of the inhomogeneous theory presented here come from Garg *et al.* (2008) and Li *et al.* (2006).

The derivation of the Gutzwiller factors by Wang *et al.* (2006) is based on the definition of a generalized projection operator

$$\mathcal{P} \equiv \prod_i \mathcal{P}_i \quad \text{where} \quad \mathcal{P}_i \equiv y_i^{\hat{n}_i}(1 - D_i) \quad \text{where} \quad D_i \equiv \hat{n}_{i\uparrow}\hat{n}_{i\downarrow} \tag{2.21}$$

that includes the fugacities y_i in order to fulfill the constraint that the density on each site remains unchanged upon projection.

$$\langle \hat{n}_i \rangle \stackrel{!}{=} \langle \hat{n}_i \rangle_0 \tag{2.22}$$

It is this constraint that leads to the explicit form of the Gutzwiller factors we employ as pointed out by Ko *et al.* (2007).

As before, the Gutzwiller factors are derived as the ratios of the expectation values of the process of interest in the projected $\langle\cdot\rangle$ and the preprojected state $\langle\cdot\rangle_0$. But now, it is aimed to perform this evaluation in a more rigorous manner than just stating that non-correlation between different sites is assumed. An expectation value in the projected state $|\psi\rangle = \mathcal{P}|\psi_0\rangle$ is defined as

$$\langle\cdot\rangle = \frac{1}{Z}\langle\psi_0|\mathcal{P}\cdot\mathcal{P}|\psi_0\rangle \quad \text{where} \quad Z = \langle\psi_0|\mathcal{P}^2|\psi_0\rangle \tag{2.23}$$

As $|\psi_0\rangle$ is a non-interacting state one can in principle use Wick's theorem to evaluate such an expectation value exactly. But clearly, for a bigger system the number of $c_i^\dagger$ and c_i operators already present in $\prod_i \mathcal{P}_i$ becomes so immense that evaluation by contraction is a task that is in practice not feasible. When restating the idea of the Gutzwiller approximation in this language one formulates: inter-site contractions $\langle c_i^\dagger c_j\rangle_0$ yield a much smaller contribution then on-site contractions $\langle c_i^\dagger c_i\rangle$ when calculating the expectation value.[14] Therefore one can approximate the evaluation by just accounting for on-site contractions.[15] This formulation of the Gutzwiller approximation is stated in a different way by Ko *et al.* (2007) who consider canonical wave functions. We are interested in describing a system with states that are BCS type variational wave functions, and therefore grand-canonical wave functions. This is the case treated by Wang *et al.* (2006). A detailed discussion, though interesting,[16]

(iii) Noteworthy is also the article of Ogata and Himeda (2003) who presented an elaborate derivation of Gutzwiller factors that include also non-local contributions for homogeneous systems (similar to Fukushima (2008)). Their expressions are also used in a form appropriate for inhomogeneous systems as e.g. in Tsuchiura *et al.* (2001), but this form is only "speculated" (Fukushima *et al.* 2009) from the homogeneous case, not rigorously derived. (This happened also in several other cases with different authors and different expressions.) Needless to say that Ogata has made some important contributions, for one of the early articles see e.g. Tsuchiura *et al.* (1999).

[14] This statement is taken from Fukushima (2008), the formulation of which allows him to systematically improve the approximation by taking more and more non-local terms into account using the method introduced by Metzner and Vollhardt (1988).

[15] Take e.g. a product of occupation numbers, which is the operator which will be most frequently needed as it appears in the expansion of $\prod_i \mathcal{P}^2$. The approximation then reads:

$$\langle \prod_i \hat{n}_i \rangle \stackrel{\text{Gutzw.}}{\simeq} \prod_i \langle \hat{n}_i \rangle \tag{2.24}$$

[16] (i) The formulation of the condition to neglect inter-site correlations of Ko *et al.* (2007) is different from

will not be presented.

The Gutzwiller approximation in our formulation is now used to evaluate all expectation valuers of interest. In particular the normalization constant:

$$Z = \langle \mathcal{P}^2 \rangle = \left\langle \prod_i \mathcal{P}_i^2 \right\rangle \sim \prod_i \langle \mathcal{P}_i^2 \rangle \equiv \prod_i z_i \tag{2.28}$$

and e.g. the spin-interaction process,

$$\langle \boldsymbol{S}_i \cdot \boldsymbol{S}_j \rangle = \frac{1}{Z} \langle \psi_0 | \mathcal{P} \boldsymbol{S}_i \cdot \boldsymbol{S}_j \mathcal{P} | \psi_0 \rangle = \frac{1}{z_i z_j} \langle \psi_0 | \mathcal{P}_i \mathcal{P}_j \boldsymbol{S}_i \cdot \boldsymbol{S}_j \mathcal{P}_i \mathcal{P}_j | \psi_0 \rangle \tag{2.29}$$

To evaluate this we have to find an expression for $\mathcal{P}_i \mathcal{P}_j \boldsymbol{S}_i \cdot \boldsymbol{S}_j \mathcal{P}_i \mathcal{P}_j$. This is easy for the spin-exchange component of the interaction $\boldsymbol{S}_i \cdot \boldsymbol{S}_j$. As Eq. (C.8) shows, only the x, y-components of the spin-interaction describe a spin-exchange process while the z-component describes a spin density interaction. Only the exchange is projective as is immediately clear when noting that it is strongly restricted by the Pauli principle. It can only happen in the sub-space of singly-occupied sites and therefore there exists a simple expression for $\mathcal{P}_i \mathcal{P}_j \boldsymbol{S}_i \cdot \boldsymbol{S}_j \mathcal{P}_i \mathcal{P}_j$ that will be explicitly derived in the following section.

For the z-component of the spin-interaction the property of projectiveness does not hold true. In particular, in the system where double occupancy is forbidden this interaction acts in the same way as in the preprojected system. Thus the Gutzwiller factor for the z-component would therefore be $g_{iz}^J = 1$. This of course breaks rotational invariance which is not astonishing as configuration counting requires a fixed spin basis (Ko *et al.* 2007). This breaking of rotational invariance turned out to lead to unphysical results, which are avoided if the complete spin-spin interaction is renormalized in the same way. In the paramagnetic

---

what we do as stated above. They consider the explicit form of a canonical wave function

$$|\psi_0\rangle = \prod_{k'}^{N_\downarrow} \alpha_{k'\downarrow}^\dagger \prod_k^{N_\uparrow} \alpha_{k\uparrow}^\dagger |vac\rangle \qquad \text{where} \qquad \alpha_{ks}^\dagger = \sum_i \alpha_{kis} c_{is}^\dagger \tag{2.25}$$

describe one-particle states. They can then derive the Gutzwiller factors by configuration counting on a lattice in an approach that is similar to the one of Metzner and Vollhardt (1988). In particular they can perform all Wick contractions analytically to obtain determinants that are then approximated by their diagonal elements.

(ii) There is another very interesting and successful concept to introduce a Gutzwiller type approximation. It consists in the introduction of a so-called Gutzwiller-type wave function, which is of grand-canonical type and has the following form for spin-less fermions

$$|\psi_0\rangle = \prod_i^L |i\rangle \qquad \text{where} \qquad |i\rangle = (\beta_{i0} + \beta_{i1} c_i^\dagger)|vac\rangle \tag{2.26}$$

This wave function does not describe a product of one-particle states but a product of local states or configurations of each lattice site i. In such a state obviously, the above factorization Eq. (2.24) condition holds true exactly. Consider for example the projector on occupied sites:

$$\langle \prod_i^L \hat{n}_i \rangle = \prod_i^L \langle \hat{n}_i \rangle = \prod_i^L \langle i | \hat{n}_i | i \rangle = \prod_i^L n_i \tag{2.27}$$

We will later on refer to this to make certain points of the general interpretation of such a Gutzwiller approach clear.

phase it is adequate to identify the spin-interaction process solely by the spin-exchange process. Then

$$\langle \boldsymbol{S}_i \cdot \boldsymbol{S}_j \rangle = g_i^J g_j^J \, \langle \boldsymbol{S}_i \cdot \boldsymbol{S}_j \rangle_0 \tag{2.30}$$

2.3. Particle-hole symmetric Gutzwiller factors

In this section a derivation of Gutzwiller factors that are symmetric around half filling is presented. These renormalization coefficients will then be used in the description of grain boundaries in Sec. 4. They might as well be useful for other examples of strongly inhomogeneous systems, though this question is not investigated in this thesis. Also in Sec. 4, a phenomenological argumentation for the need of particle-hole symmetric Gutzwiller factors will be given. Here it is only briefly summarized. Imagine a system that has lattice sites on which particles can gain more potential energy than the interaction energy on single sites, i.e. $\epsilon_i < -U$. On such a site the empty state plays the role of the doubly occupied state in the sense that it is energetically as unfavorable as the latter on a site with $\epsilon_i \sim 0$. One can therefore conclude that a better wave function modeling is obtained if on such a site the holon instead of the doublon contributions are projected out. This leads to Gutzwiller factors which perform a renormalization that is symmetric with respect to half filling, i.e. particle-hole symmetric. The derivation is presented in the following.

For this we further generalize the projection operator of Eq. (2.21). The operator to be defined below, locally projects out either doublons (double occupations) or holons (empty sites) depending on the local density. The derivation is in complete analogy to the one presented by Wang *et al.* (2006). For clarity and comparison their results are restated while introducing the new form of Gutzwiller factors.

2.3.1. A generalized projection operator

The following notation is used where the preprojected state $|\psi_0\rangle$ is assumed to be normalized

$$\langle \cdot \rangle_0 = \langle \psi_0 | \cdot | \psi_0 \rangle \tag{2.31}$$

$$\langle \cdot \rangle = \frac{1}{Z} \langle \psi_0 | \mathcal{P} \cdot \mathcal{P} | \psi_0 \rangle \quad \text{where} \quad Z = \langle \psi_0 | \mathcal{P}^2 | \psi_0 \rangle \tag{2.32}$$

$$\langle \hat{n}_{is} \rangle_0 \equiv n_{is} \quad \text{and} \quad \langle \hat{n}_i \rangle_0 \equiv n_i \tag{2.33}$$

We consider a generalized projection operator $\mathcal{P} \equiv \prod_i \mathcal{P}_i$

$$\mathcal{P}_i \equiv \begin{cases} \mathcal{P}_i^d \equiv y_i^{\hat{n}_i}(1 - D_i) & \text{if} \quad n_i \leq 1 \\ \mathcal{P}_i^h \equiv y_i^{\hat{n}_i}(1 - E_i) & \text{if} \quad n_i > 1 \end{cases} \tag{2.34}$$

and introduce at the same time the local projectors

$$E_i \equiv (1-\hat{n}_{i\uparrow})(1-\hat{n}_{i\downarrow}) \tag{2.35a}$$
$$Q_{i\uparrow} \equiv \hat{n}_{i\uparrow}(1-\hat{n}_{i\downarrow}) \tag{2.35b}$$
$$Q_{i\downarrow} \equiv (1-\hat{n}_{i\uparrow})\hat{n}_{i\downarrow} \qquad \Rightarrow \qquad Q_i \equiv Q_{i\uparrow} + Q_{i\downarrow} \tag{2.35c}$$
$$D_i \equiv \hat{n}_{i\uparrow}\hat{n}_{i\downarrow} \tag{2.35d}$$

The latter have projector properties. The identity is given as $\mathrm{Id} = E_i + Q_i + D_i$. They are orthogonal $E_iQ_i = 0, \ldots$ and they are equal to their square $E_i = E_i^2, \ldots$.

We then can immediately give an alternative expression for $\mathcal{P}_i$

$$\begin{cases} \mathcal{P}_i^d = E_i + y_iQ_i \\ \mathcal{P}_i^h = y_i(Q_i + y_iD_i) \end{cases} \tag{2.36}$$

To derive the following expressions, we will frequently use the Gutzwiller assumption of contracting only on-site contributions in expectation values (refer to the preceding section and e.g. Eq. (2.24)). We will also use the fact, that the BCS type state $|\psi\rangle_0$ is a mean-field state for which expectation values of four-operator terms decouple into expectation values of two-operator terms.

We introduce a last additional piece of notation to make the book-keeping simpler. As we work in the Gutzwiller approximation and approximate expectation values only by on-site contractions, for general operators A_i and B_j that are expressed in terms of $c_i^\dagger$ and c_i it holds $\langle A_iB_j\rangle \overset{\text{Gutzw.}}{=} \langle A_i\rangle\langle B_j\rangle$ for $i \neq j$. We can therefore express all expectation values taken in the global wave function in terms of local expectation values $\langle\cdot\rangle_i$ defined as

$$\langle A_i\rangle \overset{\text{Gutzw.}}{\simeq} \langle A_i\rangle_i \quad \text{where} \quad \langle . \rangle_i \equiv \begin{cases} \langle . \rangle_{di} = \frac{1}{z_{di}}\langle \mathcal{P}_{di}\cdot\mathcal{P}_{di}\rangle_0 & \text{if} \quad n_i \leq 1 \\ \langle . \rangle_{hi} = \frac{1}{z_{hi}}\langle \mathcal{P}_{hi}\cdot\mathcal{P}_{hi}\rangle_0 & \text{if} \quad n_i > 1 \end{cases} \tag{2.37}$$

Finally we note that we are only interested in a non-magnetic system in which $n_{i\uparrow} = n_{i\downarrow} = \frac{n_i}{2}$ holds true.

2.3.2. Calculation of expectation values

For the normalization constant Z we have

$$Z = \langle \mathcal{P}^2\rangle = \left\langle \prod_i \mathcal{P}_i^2 \right\rangle \overset{\text{Gutzw.}}{\simeq} \prod_i \langle \mathcal{P}_i^2\rangle \equiv \prod_i z_i \tag{2.38}$$

where

$$z_i = \begin{cases} z_{di} = \langle \mathcal{P}_{di}^2\rangle_0 = \langle E_i\rangle_0 + y_i^2\langle Q_i\rangle_0 & \text{if} \quad n_i \leq 1 \\ z_{hi} = \langle \mathcal{P}_{hi}^2\rangle_0 = y_i^2(\langle Q_i\rangle_0 + y_i^2\langle D_i\rangle_0) & \text{if} \quad n_i > 1 \end{cases} \tag{2.39}$$

We further need the expectation values for the different local projectors:

$$\langle E_i\rangle_0 = (1-n_{i\uparrow})(1-n_{i\downarrow}) = (1-\tfrac{n_i}{2})^2 \tag{2.40a}$$

$$\langle Q_{i\uparrow}\rangle_0 = n_{i\uparrow}(1-n_{i\downarrow}) = \tfrac{n_i}{2}(1-\tfrac{n_i}{2}) \tag{2.40b}$$

$$\langle Q_{i\downarrow}\rangle_0 = (1-n_{i\uparrow})n_{i\downarrow} = \tfrac{n_i}{2}(1-\tfrac{n_i}{2}) \tag{2.40c}$$

$$\langle D_i\rangle_0 = n_{i\uparrow}n_{i\downarrow} = \tfrac{n_i^2}{4} \tag{2.40d}$$

where we used the property of the mean-field state that four-operator terms can be decoupled and for the second equal sign the assumption of a non-magnetic system.

We also need the expectation values of these local projectors in the projected state.[17] To derive them we employ the explicit expressions of $\mathcal{P}_i^d$ and $\mathcal{P}_i^h$ of Eq. (2.36) and use the orthogonality of the local projectors. The result is

$$\begin{cases} \langle E_i\rangle_{di} = \frac{1}{z_{di}}\langle\psi_0|E_i|\psi_0\rangle \\ \langle E_i\rangle_{hi} = 0 \end{cases} \tag{2.41}$$

$$\begin{cases} \langle Q_i\rangle_{di} = \frac{y_i^2}{z_{di}}\langle\psi_0|Q_i|\psi_0\rangle \\ \langle Q_i\rangle_{hi} = \frac{y_i^2}{z_{hi}}\langle\psi_0|Q_i|\psi_0\rangle \end{cases} \tag{2.42}$$

$$\begin{cases} \langle D_i\rangle_{di} = 0 \\ \langle D_i\rangle_{hi} = \frac{y_i^4}{z_{hi}}\langle\psi_0|D_i|\psi_0\rangle \end{cases} \tag{2.43}$$

As already discussed in the preceding section, the fugacity is determined by enforcing the same value of the local occupation number in the projected as in the preprojected state Eq. (2.22). We can again directly express it in terms of the local expectation value

$$\langle\hat{n}_i\rangle_i \stackrel{!}{=} n_i \tag{2.44}$$

This equation is most easily evaluated by employing the identities

$$\hat{n}_i = Q_i + 2D_i \quad \text{in the case of} \quad \langle\hat{n}_i\rangle_{di} \tag{2.45}$$

$$\hat{n}_i = 2 - 2E_i - Q_i \quad \text{in the case of} \quad \langle\hat{n}_i\rangle_{hi} \tag{2.46}$$

As $\langle D_i\rangle_{di} = 0$ and $\langle E_i\rangle_{hi} = 0$ these identities lead to simple equivalent expressions for Eq. (2.44)

$$\langle\hat{n}_i\rangle_{di} = \frac{y_{di}^2}{z_{di}}\langle Q_i\rangle_0 \stackrel{!}{=} n_i \tag{2.47a}$$

$$\langle\hat{n}_i\rangle_{hi} = 2 - \frac{y_{hi}^2}{z_{hi}}\langle Q_i\rangle_0 \stackrel{!}{=} n_i \tag{2.47b}$$

[17] For example $\langle E_i\rangle = \frac{1}{Z}\langle\psi_0|\mathcal{P}E_i\mathcal{P}|\psi_0\rangle \stackrel{\text{Gutzw.}}{=} \frac{1}{z_i}\langle\psi_0|\mathcal{P}_iE_i\mathcal{P}_i|\psi_0\rangle = \langle E_i\rangle_i$ with the just introduced notation of Eq. (2.37).

which can be immediately evaluated to give

$$\frac{y_{di}^2}{z_{di}} = \frac{2}{2-n_i} \tag{2.48a}$$

$$\frac{y_{hi}^2}{z_{hi}} = \frac{2}{n_i} \tag{2.48b}$$

We can evaluate the terms appearing in

$$\langle \boldsymbol{S}_i \cdot \boldsymbol{S}_j \rangle = \frac{1}{Z} \langle \psi_0 | \mathcal{P} \boldsymbol{S}_i \cdot \boldsymbol{S}_j \mathcal{P} | \psi_0 \rangle = \frac{1}{z_i z_j} \langle \psi_0 | \mathcal{P}_i \mathcal{P}_j \boldsymbol{S}_i \cdot \boldsymbol{S}_j \mathcal{P}_i \mathcal{P}_j | \psi_0 \rangle \tag{2.49}$$

using the projectiveness property of the spin-interaction term and restoring rotational invariance as discussed in the preceding section.[18] We obtain

$$\mathcal{P}_i \mathcal{P}_j \boldsymbol{S}_i \cdot \boldsymbol{S}_j \mathcal{P}_i \mathcal{P}_j \overset{\text{rot. Inv.}}{=} y_i^2 y_j^2 \boldsymbol{S}_i \cdot \boldsymbol{S}_j \tag{2.51}$$

such that

$$\langle \boldsymbol{S}_i \cdot \boldsymbol{S}_j \rangle = \frac{y_i^2}{z_i} \frac{y_j^2}{z_j} \langle \psi_0 | \boldsymbol{S}_i \cdot \boldsymbol{S}_j | \psi_0 \rangle \tag{2.52}$$

This allows the identification of the Gutzwiller factors for the spin interaction term in the same manner as before such that we obtain the final result

$$g_i^J \equiv \begin{cases} \frac{y_{di}^2}{z_{di}} = \frac{2}{2-n_i} & \text{if} \quad n_i \leq 1 \\ \frac{y_{hi}^2}{z_{hi}} = \frac{2}{n_i} & \text{if} \quad n_i > 1 \end{cases} \tag{2.53}$$

and can write

$$\langle \boldsymbol{S}_i \cdot \boldsymbol{S}_j \rangle = g_i g_j \langle \psi_0 | \boldsymbol{S}_i \cdot \boldsymbol{S}_j | \psi_0 \rangle \tag{2.54}$$

To derive the renormalization of the hopping term, we have to work a bit harder. First we evaluate explicitly the expression for the fugacity starting from Eq. (2.48). As before we assume $n_{i\uparrow} = n_{i\downarrow} = \frac{n_i}{2}$:

$$y_{di}^2 = \left(1 - \frac{n_i}{2}\right)^2 \frac{1}{1-n_i} \tag{2.55a}$$

$$y_{hi}^2 = \frac{2(n_i - 1)}{n_i} \tag{2.55b}$$

[18] This discussion is summarized: solely the the x, y-component of the spin-operators are responsible for the spin-exchange process and therefore projective, but we manually set the same renormalization calculated for the x, y-components also for the z-component to obtain a rotational invariant result. For the z-component we have after inspection of Eq. (C.8)

$$\mathcal{P}_i \mathcal{P}_j (S_{ix} S_{jx} + S_{iy} S_{jy}) \mathcal{P}_i \mathcal{P}_j = y_i^2 y_j^2 (S_{ix} S_{jx} + S_{iy} S_{jy}) \tag{2.50}$$

as the operator $S_{ix} S_{jx} + S_{iy} S_{jy}$ is orthogonal to the empty site contributions in $\mathcal{P}_i$ and $\mathcal{P}_j$.

The derivation of the following operator identities from Eq. (2.34) is straight-forward

$$\mathcal{P}_{id} c_{is} \mathcal{P}_{id} = y_i (1 - n_{i\bar{s}}) c_{is} \qquad \text{and} \quad \text{h.c.} \tag{2.56a}$$

$$\mathcal{P}_{ih} c_{is} \mathcal{P}_{ih} = y_i^3 n_{i\bar{s}} c_{is} \qquad \text{and} \quad \text{h.c.} \tag{2.56b}$$

The probability for a hopping process can be given as

$$\langle c_{is}^\dagger c_{js} \rangle = \frac{1}{z_i z_j} \langle \mathcal{P}_i c_{is}^\dagger \mathcal{P}_i \mathcal{P}_j c_{js} \mathcal{P}_j \rangle_0 \tag{2.57}$$

Insertion of Eq. (2.56) into this equation[19] and using the already derived expressions for y and z we can immediately give the result for the Gutzwiller factor

$$g_i^t \equiv \begin{cases} \frac{y_{di}}{z_{di}} (1 - \frac{n_i}{2}) = \sqrt{\frac{2(1-n_i)}{(2-n_i)}} & \text{if} \quad n_i \leq 1 \\ \frac{y_{hi}^3}{z_{di}} \frac{n_i}{2} = \sqrt{\frac{2(n_i-1)}{n_i}} & \text{if} \quad n_i > 1 \end{cases} \tag{2.58a}$$

such that

$$\langle c_{is}^\dagger c_{js} \rangle = g_i^t g_j^t \langle c_{is}^\dagger c_{js} \rangle_0 \tag{2.59}$$

2.3.3. Conclusion

At this stage we have completed the derivation of the renormalization coefficients — the Gutzwiller factors — that allow to find an approximation of an expectation value in a projected state by a corresponding preprojected state.

We already see that this is only a first part of the work that has to be accomplished when one wants to calculate physical quantities in this formalism. This requires an explicit construction of the state $|\psi_0\rangle$ which is usually achieved using the Bogoliubov — de Gennes formalism introduced and discussed in the following.

We will also see that the "correspondence" between the two states $|\psi\rangle$ and $|\psi_0\rangle$ is not always obvious. This delicate question as well as several practical, technical difficulties concerning calculations with the Gutzwiller factors will as well be treated in the next section.

[19] For the case that $n_i \leq 1$ and $n_j > 1$ e.g. we have $\langle c_{is}^\dagger c_{js} \rangle = \frac{y_{di}}{z_{di}} \frac{y_{hj}^3}{z_{hj}} (1 - n_{i\bar{s}}) n_{j\bar{s}} \langle c_{is}^\dagger c_{js} \rangle_0$.

3. The BdG and the RMFT formalism

In this chapter first the Bogoliubov - de Gennes (BdG) equations are derived in a way that aims to clarify its physical interpretation. We follow Datta and Bagwell (2008) in several aspects. This is closed with a presentation of the self-consistency conditions and all necessary formulas. Then the so-called renormalized mean-field theory (RMFT) is introduced. It is based on a BdG evaluation of a renormalized hamiltonian that is constructed with the ideas of chapter 2. This is basically a recapitulation of the ideas of Zhang *et al.* (1988) and Wang *et al.* (2006). Finally results that concern the practical numerical solution of the BdG equations are presented.

3.1. Derivation and interpretation of the BdG equation

The task is to evaluate an effective one-particle hamiltonian that can be derived starting from the microscopic hamiltonian with a mean-field decoupling scheme and a variational calculation (see section C of the appendix). We assume that we already dispose of such a one-particle hamiltonian. In our case it will necessarily be of the following form

$$H = \sum_{ijs} H_{ij} c_{is}^{\dagger} c_{js} + \sum_{ij} (\Delta_{ij} c_{j\uparrow}^{\dagger} c_{i\downarrow}^{\dagger} + \text{h.c.}) \tag{3.1}$$

with H_{ij} and Δ_{ij} some coefficient functions that depend on expectation values of annihilation and creation operators. In particular

$$\Delta_{ij} \equiv \frac{J_{ij}}{2} \big(\langle c_{i\downarrow} c_{j\uparrow} \rangle + \langle c_{j\downarrow} c_{i\uparrow} \rangle \big) \tag{3.2}$$

is the spin-singlet order parameter for electron-pairing.[1] J_{ij} is a spin-coupling constant discussed later on.

To calculate the spectrum of this hamiltonian, we have to obtain a representation of the stationary Schroedinger equation. This will turn out to be the BdG equation and is derived in the following subsection.

3.1.1. Representation in a one-particle basis

A matrix representation in $\mathcal{C}^n$ of the hamiltonian Eq. (3.1) can easily be obtained by re-grouping the terms in the sums of Eq. (3.1)

[1] For basic information concerning unconventional superconductivity confer e.g. the lecture notes of Sigrist (2006) or the book by Mineev and Samokhin (1999).

$$
\begin{aligned}
H &= \sum_{ijs} H_{ij} c_{is}^\dagger c_{js} + \sum_{ij} (\Delta_{ij} c_{j\uparrow}^\dagger c_{i\downarrow}^\dagger + \text{h.c.}) \\
&= \sum_{ij} \left(H_{ij} c_{i\uparrow}^\dagger c_{j\uparrow} + \Delta_{ij} c_{j\uparrow}^\dagger c_{i\downarrow}^\dagger + \Delta_{ij}^* c_{i\downarrow} c_{j\uparrow} - H_{ij} c_{j\downarrow} c_{i\downarrow}^\dagger \right) \qquad (3.3) \\
&= \sum_{ij} \left(H_{ij} c_{i\uparrow}^\dagger c_{j\uparrow} + \Delta_{ij} c_{i\uparrow}^\dagger c_{j\downarrow}^\dagger + \Delta_{ij}^* c_{i\downarrow} c_{j\uparrow} - H_{ij}^* c_{i\downarrow} c_{j\downarrow}^\dagger \right) \qquad (3.4)
\end{aligned}
$$

where from the first to the second line we dropped the constant $\sum_i H_{ii}$ that results from anticommuting $c_{i\downarrow}^\dagger c_{i\downarrow}$ and from the second to the third we used the symmetry $\Delta_{ij} = \Delta_{ji}$ and the hermiticity $H_{ij} = H_{ji}^*$.

It is now possible to write this sum formally in matrix notation with the definitions $\boldsymbol{c}_s \equiv (c_{1s}\ c_{2s}\ \dots\ c_{Ls})^T$, $\boldsymbol{c}_s^\dagger \equiv (c_{1s}^\dagger\ c_{2s}^\dagger\ \dots\ c_{Ls}^\dagger)^T$, $\hat{H} = (H_{ij})_{ij=0}^{L-1}$ and $\hat{\Delta} = (\Delta_{ij})_{ij=0}^{L-1}$ the expression Eq. (3.4) is identical with

$$
H = \begin{pmatrix} \boldsymbol{c}_\uparrow^\dagger & \boldsymbol{c}_\downarrow \end{pmatrix} \begin{pmatrix} \hat{H} & \hat{\Delta} \\ \hat{\Delta}^* & -\hat{H}^* \end{pmatrix} \begin{pmatrix} \boldsymbol{c}_\uparrow \\ \boldsymbol{c}_\downarrow^\dagger \end{pmatrix} \quad , \qquad H_{\mathrm{C}} \equiv \begin{pmatrix} \hat{H} & \hat{\Delta} \\ \hat{\Delta}^* & -\hat{H}^* \end{pmatrix} \qquad (3.5)
$$

To derive a representation of H that is "diagonal" (in which only L instead of L^2 operator terms are involved) when expressed with certain operators we diagonalize the $\mathrm{C}^{2L} \times \mathrm{C}^{2L}$ matrix H_{C} by solving the eigenvalue problem

$$
\begin{pmatrix} \hat{H} & \hat{\Delta} \\ \hat{\Delta}^* & -\hat{H}^* \end{pmatrix} \begin{pmatrix} \boldsymbol{u} \\ \boldsymbol{v} \end{pmatrix} = \mathcal{E}_n \begin{pmatrix} \boldsymbol{u} \\ \boldsymbol{v} \end{pmatrix} \qquad (3.6)
$$

where we used the definitions $\boldsymbol{u} \equiv (u_1\ u_2\ \dots\ u_L)^T$ and $\boldsymbol{v} \equiv (v_1\ v_2\ \dots\ v_L)^T$. Eq. (3.6) is called "BdG equation".

This eigenvalue problem can be simplified by using the time-reversal invariance of the hamiltonian[2] that implies that for each pair of an eigenvalue and eigenvector $\{\mathcal{E}_n, (\boldsymbol{u}\ \boldsymbol{v})^T\}$ there exists another one $\{-\mathcal{E}_n, (-\boldsymbol{v}^*\ \boldsymbol{u}^*)^T\}$. A formal derivation for this is done by realizing that the matrix $\mathcal{T}$ acts on the hamiltonian in the following way

$$
\mathcal{T} \equiv \begin{pmatrix} 0 & 1 \\ -1 & 0 \end{pmatrix} \ , \quad \mathcal{T}^{-1} = -\mathcal{T} \qquad \Rightarrow\ \mathcal{T} H_{\mathrm{C}} \mathcal{T}^{-1} = -H_{\mathrm{C}}^* \qquad (3.7)
$$

This allows to transform the eigenvalue equation to yield

$$
\begin{aligned}
H_{\mathrm{C}} \begin{pmatrix} \boldsymbol{u} \\ \boldsymbol{v} \end{pmatrix} = \mathcal{E}_n \begin{pmatrix} \boldsymbol{u} \\ \boldsymbol{v} \end{pmatrix} &\Leftrightarrow \mathcal{T} H_{\mathrm{C}} \mathcal{T}^{-1} \mathcal{T} \begin{pmatrix} \boldsymbol{u} \\ \boldsymbol{v} \end{pmatrix} = \mathcal{T} \mathcal{E}_n \begin{pmatrix} \boldsymbol{u} \\ \boldsymbol{v} \end{pmatrix} \\
&\Leftrightarrow -H_{\mathrm{C}}^* \begin{pmatrix} -\boldsymbol{v} \\ \boldsymbol{u} \end{pmatrix} = \mathcal{E}_n \begin{pmatrix} -\boldsymbol{v} \\ \boldsymbol{u} \end{pmatrix} \Leftrightarrow H_{\mathrm{C}} \begin{pmatrix} -\boldsymbol{v}^* \\ \boldsymbol{u}^* \end{pmatrix} = -\mathcal{E}_n \begin{pmatrix} -\boldsymbol{v}^* \\ \boldsymbol{u}^* \end{pmatrix} \qquad (3.8)
\end{aligned}
$$

[2] It is spin-symmetric upon complex conjugation.

This proves the assertion.

Using time-reversal invariance one can now write down the explicit form of the unitary matrix that diagonalizes the matrix H_{C}

$$U \equiv \begin{pmatrix} \hat{\boldsymbol{u}} & -\hat{\boldsymbol{v}}^* \\ \hat{\boldsymbol{v}} & \hat{\boldsymbol{u}}^* \end{pmatrix} \Leftrightarrow U^\dagger \equiv \begin{pmatrix} \hat{\boldsymbol{u}}^\dagger & \hat{\boldsymbol{v}}^\dagger \\ -\hat{\boldsymbol{v}}^T & \hat{\boldsymbol{u}}^T \end{pmatrix} \tag{3.9}$$

where the $L \times L$ matrices $\hat{\boldsymbol{u}}$ and $\hat{\boldsymbol{v}}$ are defined through their columns, the vectors $\boldsymbol{u}$ and $\boldsymbol{v}$.[3]

Finally the diagonal operator form of H is derived by insertion of two identies $\mathrm{Id} = UU^\dagger$ left and right of H_{C} in Eq. (3.5)

$$H = \begin{pmatrix} \gamma_\uparrow^\dagger & \gamma_\downarrow \end{pmatrix} \begin{pmatrix} \mathcal{E} & \\ & -\mathcal{E} \end{pmatrix} \begin{pmatrix} \gamma_\uparrow \\ \gamma_\downarrow^\dagger \end{pmatrix} \tag{3.10}$$

where the definitions $\mathcal{E} \equiv \mathrm{diag}(\mathcal{E}_n)_{n=0}^{L-1}$ and

$$\begin{pmatrix} \gamma_\uparrow \\ \gamma_\downarrow^\dagger \end{pmatrix} \equiv U^\dagger \begin{pmatrix} \boldsymbol{c}_\uparrow \\ \boldsymbol{c}_\downarrow^\dagger \end{pmatrix} \tag{3.11}$$

were used. The result of the matrix multiplication in Eq. (3.10) reads

$$H = \sum_n \mathcal{E}_n (\gamma_{n\uparrow}^\dagger \gamma_{n\uparrow} + \gamma_{n\downarrow}^\dagger \gamma_{n\downarrow}) \tag{3.12}$$

Note that the anticommutation canceled the minus-sign that is still present in Eq. (3.10).

3.1.2. Two possibilities of interpreting the BdG equation

As the hamiltonian in Eq. (3.1) consists only of terms bilinear in the two operators c and $c^\dagger$ it can be evaluated in a one particle Hilbert space. Was this common knowledge already used in the preceding subsection? This is not evident. In order to understand the physical meaning of the BdG equation and later of its renormalized counterpart this lack of understanding should be overcome. This is achieved in the present subsection.

What is a one-particle Hilbert space that can be used (and that was implicitly used in the preceding section) to evaluate the hamiltonian of Eq. (3.1)? The practical requirement for its definition is that its basis vectors have to be able to provide a bijection from the operator H to a matrix representation. We see that this is not possible with a naive one-particle Hilbert space[4] consisting solely of states that correspond to a physical particle as then expectation

[3] As the group of unitary $2N \times 2N$ matrices $\mathcal{U}(2N)$ has dimension $(2N)^2$, one can always parametrize a matrix U belonging to this group with $(2N)^2 = 2N^2 + 2N^2$ parameters $\hat{\boldsymbol{u}}$, $\hat{\boldsymbol{v}}$ (each of them is a complex $N \times N$ matrix and therefore allows $2N^2$ free parameters). It is also possible if the matrix to diagonalize is not time-reversal invariant. But in this latter case there is no longer a simple correspondence between $\uparrow$- and $\downarrow$-spin eigenstates as given by the bijection "multiply with $\mathcal{T}$ and perform a complex conjugation". Then also the right column of U cannot be obtained from the left column with a simple mapping.

[4] The simplest one-particle Hilbert space that can describe two types of quantum particles on a lattice would consist of vectors $|\psi\rangle = \sum_i (\alpha_i |i\uparrow\rangle + \beta_i |i\downarrow\rangle)$ spanned by the basis vectors $|i\uparrow\rangle \equiv c_{i\uparrow}^\dagger |vac\rangle$ and $|i\downarrow\rangle \equiv c_{i\downarrow}^\dagger |vac\rangle$ where $|vac\rangle$ is the vacuum state defined as being devoid of particles. Normalization of $|\psi\rangle$ guarantees that the particle number in the state is one: $\langle\psi|\psi\rangle = \sum_i (|\alpha_i|^2 + |\beta_i|^2) = 1 = \langle \sum_i (n_{i\uparrow} + n_{i\downarrow}) \rangle$.

values as $\langle c^\dagger_{i\downarrow} c^\dagger_{j\uparrow}\rangle$ cannot be assigned a finite value. This leads to considering a basis that consists of particle and hole states. It will become clear that it is sufficient to consider only $\uparrow$-spin electron and $\downarrow$-spin hole states, such that the space has the same dimension $\dim = 2L$ as the naive guess that consists solely of electron states. The basis vectors for this space are given by

$$|e_{i\uparrow}\rangle \equiv c^\dagger_{i\uparrow}|0\rangle \ , \quad |h_{i\downarrow}\rangle \equiv c_{i\downarrow}|0\rangle \tag{3.13}$$

The state $|0\rangle$ does not describe the vacuum $|\mathrm{vac}\rangle$ devoid of particles (in which case the definition would be redundant as $c_{i\downarrow}|\mathrm{vac}\rangle = 0$) but a state filled with down-spin electrons:

$$|0\rangle \equiv \prod_{i<L} c^\dagger_{i\downarrow}|\mathrm{vac}\rangle \tag{3.14}$$

where i runs over all lattice sites. A vector in this Hilbert space has the form

$$|\psi\rangle \equiv |\psi(\tilde{\boldsymbol{u}}, \tilde{\boldsymbol{v}})\rangle \equiv \sum_i (\tilde{u}_i|e_{i\uparrow}\rangle + \tilde{v}_i|h_{i\downarrow}\rangle) \tag{3.15}$$

It is a normalized superposition of the basis vectors $\{|e_{i\uparrow}\rangle, |h_{i\downarrow}\rangle\}$, $\langle\psi|\psi\rangle = \sum_i |\tilde{u}_i|^2 + |\tilde{v}_i|^2 = 1$. We can imagine the state $|\psi\rangle$ in Eq. (3.15) as a configuration of up-spin particles and down-spin holes (vacancies) on a lattice.

With these states it is now possible to give a representation of H[5]

$$H_{e,h} \equiv \begin{pmatrix} |e_\uparrow\rangle & |h_\downarrow\rangle \end{pmatrix} \begin{pmatrix} \hat{H} & \hat{\Delta} \\ \hat{\Delta}^* & -\hat{H}^* \end{pmatrix} \begin{pmatrix} \langle e_\uparrow| \\ \langle h_\downarrow| \end{pmatrix} \tag{3.17}$$

where $|e_\uparrow\rangle \equiv (|e_{1\uparrow}\rangle\ |e_{2\uparrow}\rangle\ \ldots\ |e_{L\uparrow}\rangle)^T$ and analogously for $|h_\downarrow\rangle$, $\langle e_\uparrow|$ and $\langle h_\downarrow|$. This is nothing more than returning from the second quantization to the first quantization language. But still it helps to clarify the viewpoint that is taken when calculating with the expression Eq. (3.5) and the BdG equation. This viewpoint is not obvious as the physical states of Eq. (3.13) are not the usual electron tight-binding states assigned to each lattice site and identified with the electron creation operators of the second quantization language. It can be traced back to the fact that H is an effective hamiltonian that assumes the underlying ground state of the many-body hamiltonian in order to be a meaningful definition. To conclude, here the

[5] This is done by a calculation of the matrix elements in the basis $\{|e_{i\uparrow}\rangle, |h_{i\downarrow}\rangle\}$.

$$\langle e_{i\uparrow}|H|e_{j\uparrow}\rangle = \sum_{kl} H_{kl}\langle 0|c_{i\uparrow}c^\dagger_{k\uparrow}c_{l\uparrow}c^\dagger_{j\uparrow}|0\rangle = H_{ij} \tag{3.16a}$$

$$\langle h_{i\downarrow}|H|h_{j\downarrow}\rangle = \sum_{kl} (-H_{kl})\langle 0|c^\dagger_{i\downarrow}c_{l\downarrow}c^\dagger_{k\downarrow}c_{j\downarrow}|0\rangle = -H_{ji} \tag{3.16b}$$

$$\langle e_{i\uparrow}|H|h_{j\downarrow}\rangle = \sum_{kl} \Delta_{kl}\langle 0|c_{i\uparrow}c^\dagger_{l\uparrow}c^\dagger_{k\downarrow}c_{j\downarrow}|0\rangle = \Delta_{ji} \tag{3.16c}$$

$$\langle h_{i\downarrow}|H|e_{j\uparrow}\rangle = \sum_{kl} \Delta^*_{kl}\langle 0|c^\dagger_{i\downarrow}c_{k\downarrow}c_{l\uparrow}c^\dagger_{j\uparrow}|0\rangle = \Delta^*_{ij} \tag{3.16d}$$

The representation is then derived by insertion of identities $\mathrm{Id} = \sum_j (|e_{j\uparrow}\rangle\langle e_{j\uparrow}| + |h_{j\downarrow}\rangle\langle h_{j\downarrow}|)$ left and right of the operator terms in Eq. (3.4) and employing the just calculated matrix elements.

notation in terms of the physical states Eq. (3.13) with the reference state $|0\rangle$ is more clear than the second quantized picture as the latter obscurely suggests that H can be interpreted as an ordinary hamiltonian that already gives a complete description of the system.

When transforming to the diagonal form as in Eq. (3.10) we obtain the represenation

$$H_{\gamma_\uparrow,\gamma_\downarrow} \equiv \begin{pmatrix} |\gamma_\uparrow\rangle & |\gamma_\downarrow\rangle \end{pmatrix} \begin{pmatrix} \mathcal{E} & \\ & -\mathcal{E} \end{pmatrix} \begin{pmatrix} \langle\gamma_\uparrow| \\ \langle\gamma_\downarrow| \end{pmatrix} \tag{3.18}$$

which uses states of the form $|\gamma_{i\uparrow}\rangle \equiv \sum_i u_i|e_{i\uparrow}\rangle + v_i|h_{i\downarrow}\rangle = \psi(\boldsymbol{u},\boldsymbol{v})$ and is equivalent to the operator based notation Eq. (3.21). The spin index s here serves now as a mere distinction between the two blocks in the matrix Eq. (3.18) which do no longer correspond to physical spins but rather to a new band index.

In the following the consequences for the interpretation of the BdG equation, Eq. (3.6), are discussed. Now it is obvious that the BdG equation is a representation of the stationary Schroedinger equation for the hamiltonian Eq. (3.1) in its generic basis $\{|e_{i\uparrow}\rangle, |h_{i\downarrow}\rangle\}$. Take the hamiltonian in its form Eq. (3.17) and act on an arbitrary one-particle state also represented in this basis

$$\langle e_{i\uparrow}|H|\psi(\boldsymbol{u},\boldsymbol{v})\rangle = \mathcal{E}_n\langle e_{i\uparrow}|H|\psi(\boldsymbol{u},\boldsymbol{v})\rangle \quad \Leftrightarrow \quad \text{Eq. (3.6)} \tag{3.19}$$

for the rows in the physical spin-up blocks. The same is obtained by multiplication with $\langle h_{i\downarrow}|$ from the left for the spin-down blocks. By solving the BdG equation we solve the eigenvalue problem for the operator H in the "amplitude space" C^{2L} that leads to single-particle eigenstates $|\gamma_{i\uparrow}\rangle \equiv \gamma^\dagger_{i\uparrow}|0\rangle \equiv \psi(\boldsymbol{u},\boldsymbol{v})$ and $|\gamma_{i\downarrow}\rangle \equiv \gamma_{i\downarrow}|0\rangle \equiv \psi(-\boldsymbol{v}^*,\boldsymbol{u}^*)$ that have opposite energy eigenvalues $\{\mathcal{E}_n, -\mathcal{E}_n\}$.[6]

When employing the operator based notation one sees that the states created by $\gamma^\dagger_{i\uparrow}$ and $\gamma^\dagger_{i\downarrow}$ do not have opposite energy but are rather energetically degenerate $\{\mathcal{E}_n, \mathcal{E}_n\}$ as seen in Eq. (3.12). Reminding the derivation of the effective one-particle hamiltonian it is also clear that $\gamma^\dagger_{i\uparrow}$ and $\gamma^\dagger_{i\downarrow}$ describe one-particle excitations that make only sense when acting on the ground-state of the full many-body hamiltonian. This ground-state is much too complicated to be even numerically calculated but has been very successfully approximated by the BCS variational wave function and generalizations of it.

If we do not assume the excitation viewpoint associated with the operator based notation we can as well derive a physical picture of the system in terms of solely one-particle states — following Datta and Bagwell (2008) we call it "one-particle picture". This second possibility hinges on the fact that also in the case of the excitation picture we do not use the full ground-state but a variational wave function being equivalent to a description in terms of a mean-field hamiltonian. But only the excitation picture can be connected to the many-body hamiltonian by means of perturbation theory and is therefore justified on a fundamental level. This cannot a priori be claimed for the one-particle picture. Clearly, showing the equivalence of both pictures overcomes this lack of justification. If this is the case, we can

[6] Note that the state labeled by $\downarrow$ still is a "hole-state" in the sense that it is associated with an annihilation operator although it is a superposition of physical electrons and holes. Analogously for the $\uparrow$-state.

in good conscience interpret e.g. the negative energy states of the BdG equation as physical states, this being solely possible in the one-particle picture.

The equivalence can formally be expressed by the mathematical identity that the generalized BCS variational ground-state $|\mathrm{gBCS}\rangle$, known to be the basis for the definition of the excitation picture, can be constructed as (Datta and Bagwell 2008)

$$|\mathrm{gBCS}\rangle = \prod_{n<L} \gamma^{\dagger}_{n\downarrow}|0\rangle \tag{3.20}$$

that is, as a product of all one-particle eigen states of the BdG equation that have a negative eigen value. Here $|0\rangle$ is the product of $\downarrow$-electrons, as defined in Eq. (3.14). In Eq. (3.20) we consider $\mathcal{E}_n$ not only as an eigenvalue of H_{C} that artificially assumes negative values, but use it as a classification to denote $|\gamma_{i\uparrow}\rangle \equiv \gamma^{\dagger}_{i\uparrow}|0\rangle$ as positive energy eigenstates of H_{C} and $|\gamma_{i\downarrow}\rangle \equiv \gamma_{i\downarrow}|0\rangle$ as negative energy eigenstates. When analyzed from this, the one-particle point of view, $|\mathrm{gBCS}\rangle$ does not correspond to a variational wave function that approximates the ground state of the full hamiltonian, but rather to a "full" band of quasi-particles described by the operator $\gamma^{\dagger}_{n\downarrow}$, i.e. a direct product of the one particle state $|\mathrm{gBCS}\rangle = |\gamma_{1\downarrow}\rangle \otimes \cdots \otimes |\gamma_{L\downarrow}\rangle$. This band is always filled at $T = 0$[7] and orthogonal to the second band described by quasi-particles $\gamma^{\dagger}_{n\uparrow}$. The system is excited by annihilation of a particle in the lower band and simultaneous creation of a particle in the upper one with $\gamma^{\dagger}_{i\uparrow}\gamma_{i\downarrow}$. It can thus be understood in which sense the "spin" index is considered a quantum number that distinguishes two effective bands.

To finally discuss two physical observations in the one-particle picture we note that, for example, here it is immediately clear that the lowest lying excitation has energy $2\mathcal{E}_0$ as the two effective bands have opposite energy eigenvalues. Considering as a second example the phenomenon of current transport one states that it can be classified as two effects: the supercurrent that is due to transport in the lower effective band[8] and corresponds in the excitation picture to the pair tunneling of the fraction of condensed electrons in the ground-state. And the normal current that is due to processes in the upper effective band which corresponds to ordinary electron tunneling which is only possible at $T > 0$.

3.2. Self consistency relations and summary of formulas

The eigenstates of Eq. (3.1) can be interpreted as quasi-particle excitations that have been derived in the previous section and already partly been given in vector form in Eq. (3.11).

[7] The construction of the BdG incorporating the chemical potential μ implies that the filling of the "band" described by $\downarrow$ is independent of the physical particle density in the system.

[8] If it were a physical band, due to its full filling, it would be a band insulator at $T = 0$. This is not the case for the effective band.

The scalar expressions which are much easier to handle are the following

$$\gamma_{n\uparrow} = \sum_{i<L}(u_{in}c_{i\uparrow} + v^*_{in}c^\dagger_{i\downarrow}) \qquad \gamma^\dagger_{n\uparrow} = \sum_{i<L}(u^*_{in}c^\dagger_{i\uparrow} + v_{in}c_{i\downarrow}) \tag{3.21}$$

$$\gamma_{n\downarrow} = \sum_{i<L}(-v^*_{in}c^\dagger_{i\uparrow} + u_{in}c_{i\downarrow}) \qquad \gamma^\dagger_{n\downarrow} = \sum_{i<L}(-v_{in}c_{i\uparrow} + u^*_{in}c^\dagger_{i\downarrow}) \tag{3.22}$$

The inverse transformation is

$$c_{i\uparrow} = \sum_{n<L}(u_{in}\gamma_{n\uparrow} - v^*_{in}\gamma^\dagger_{n\downarrow}) \qquad c^\dagger_{i\uparrow} = \sum_{n<L}(u^*_{in}\gamma^\dagger_{n\uparrow} - v_{in}\gamma_{n\downarrow}) \tag{3.23}$$

$$c_{i\downarrow} = \sum_{n<L}(v^*_{in}\gamma^\dagger_{n\uparrow} + u_{in}\gamma_{n\downarrow}) \qquad c^\dagger_{i\downarrow} = \sum_{n<L}(v_{in}\gamma_{n\uparrow} + u^*_{in}\gamma^\dagger_{n\downarrow}) \tag{3.24}$$

The effective hamiltonian of Eq. (3.1) when expressed with the quasi-particle operators above is diagonal as in Eq. (3.12). It is therefore of the form of a gas of free fermionic particles that obey Fermi-Dirac statistics.[9] In the ground state of the gas of free particles, an antisymmetric product state, it therefore holds

$$\langle\gamma^\dagger_{ns}\gamma_{ms'}\rangle = \delta_{nm}\delta_{ss'}f(\mathcal{E}_n) \tag{3.25}$$

$$\langle\gamma_{ns}\gamma^\dagger_{ms'}\rangle = \delta_{nm}\delta_{ss'}(1 - f(\mathcal{E})) = \delta_{nm}\delta_{ss'}f(-\mathcal{E}) \tag{3.26}$$

The second expression follows by using the fermionic anticommutation relation of the quasi-particles $\{\gamma, \gamma^\dagger\} = 1$ and the property of the fermi function:

$$f(\mathcal{E}) \equiv \frac{1}{e^{\beta\mathcal{E}} + 1} \quad \Rightarrow \quad 1 - f(\mathcal{E}) = f(-\mathcal{E}) \tag{3.27}$$

With this one can evaluate all expectation values of interest. If the derived expressions appear explicitly as (mean-)fields in the hamiltonian H_C they are also called self-consistency relations, as the solution of the eigenvalue problem requires a simultaneous, consistent evaluation of the expressions for the expectation values.

The local spin-dependent occupation numbers are

$$\begin{aligned} n_{i\uparrow} \equiv \langle c^\dagger_{i\uparrow}c_{i\uparrow}\rangle &= \sum_{nm<L}\langle(u^*_{in}\gamma^\dagger_{n\uparrow} - v_{in}\gamma_{n\downarrow})(u_{im}\gamma_{m\uparrow} - v^*_{im}\gamma^\dagger_{m\downarrow})\rangle \\ &= \sum_{n<L}|u_{in}|^2 f(\mathcal{E}_n) + |v_{in}|^2 f(-\mathcal{E}_n) \end{aligned} \tag{3.28}$$

$$\begin{aligned} n_{i\downarrow} \equiv \langle c^\dagger_{i\downarrow}c_{i\downarrow}\rangle &= \sum_{nm<L}\langle(v_{in}\gamma_{n\uparrow} + u^*_{in}\gamma^\dagger_{n\downarrow})(v^*_{im}\gamma^\dagger_{m\uparrow} + u_{im}\gamma_{m\downarrow})\rangle \\ &= \sum_{n<L}|u_{in}|^2 f(\mathcal{E}_n) + |v_{in}|^2 f(-\mathcal{E}_n) = n_{i\uparrow} \end{aligned} \tag{3.29}$$

We find $n_{i\uparrow} = n_{i\downarrow} = \frac{n_i}{2}$ as the hamiltonian is parametrized in a way that made exactly this assumption.

[9] This is consistent with the full one-particle picture described in the preceding section.

For the pairing order parameter in Eq. (3.2) we need the expectation value

$$\begin{aligned}
\langle c_{j\downarrow} c_{i\uparrow}\rangle &= \sum_{nm<L} \langle (v_{jn}^* \gamma_{n\uparrow}^\dagger + u_{jn}\gamma_{n\downarrow})(u_{in}\gamma_{n\uparrow} - v_{in}^*\gamma_{n\downarrow}^\dagger)\rangle \\
&= \sum_{n<L} v_{jn}^* u_{in} f(\mathcal{E}_n) - v_{in}^* u_{jn}(1-f(\mathcal{E}_n)) \\
&= \sum_{n<L} v_{jn}^* u_{in}(f(\mathcal{E}_n) - \tfrac{1}{2}) - v_{in}^* u_{jn}(\tfrac{1}{2} - f(\mathcal{E}_n))) \qquad (3.30) \\
&= -\tfrac{1}{2}\sum_{n<L} (v_{jn}^* u_{in} + v_{in}^* u_{jn}) \tanh(\tfrac{\beta}{2}\mathcal{E}_n) \qquad (3.31) \\
&= \langle c_{i\downarrow} c_{j\uparrow}\rangle
\end{aligned}$$

where from the second to the third line, $\frac{1}{2}\langle\{c_{i\downarrow}, c_{j\uparrow}\}\rangle \equiv 0$ was subtracted, from the third to the fourth line $\tanh(\frac{\beta}{2}\mathcal{E}_n) = 1 - 2f(\mathcal{E}_n)$[10] was employed and in the last step the apparent symmetry in i, j was used.

Due to the symmetry $\langle c_{j\downarrow} c_{i\uparrow}\rangle = \langle c_{i\downarrow} c_{j\uparrow}\rangle$ the pairing order parameter of Eq. (3.2) can be written as

$$\begin{aligned}
\Delta_{ij} &\equiv J_{ij}\langle c_{j\downarrow} c_{i\uparrow}\rangle \qquad (3.32) \\
&= -\tfrac{J_{ij}}{2}\sum_{n<L} (v_{jn}^* u_{in} + v_{in}^* u_{jn}) \tanh(\tfrac{\beta}{2}\mathcal{E}_n) \qquad (3.33)
\end{aligned}$$

This is called the self-consistency relation for the pairing field Δ_{ij}. For a homogeneous system it is equivalent to an extended form of the so-called gap equation of BCS theory.

For the expectation value of the hopping process, one finds

$$\begin{aligned}
\widetilde{\chi}_{ij\uparrow} \equiv \langle c_{i\uparrow}^\dagger c_{j\uparrow}\rangle &= \sum_{nm<L} \langle (u_{in}^* \gamma_{n\uparrow}^\dagger - v_{in}\gamma_{n\downarrow})(u_{jm}\gamma_{m\uparrow} - v_{jm}^*\gamma_{m\downarrow}^\dagger)\rangle \\
&= \sum_{n<L} u_{in}^* u_{jn} f(\mathcal{E}_n) + v_{in} v_{jn}^* f(-\mathcal{E}_n) \qquad (3.34) \\
\widetilde{\chi}_{ij\downarrow} \equiv \langle c_{i\downarrow}^\dagger c_{j\downarrow}\rangle &= \sum_{nm<L} \langle (v_{in}\gamma_{n\uparrow} + u_{in}^* \gamma_{n\downarrow}^\dagger)(v_{jm}^*\gamma_{m\uparrow}^\dagger + u_{jm}\gamma_{m\downarrow})\rangle \\
&= \sum_{n<L} u_{in}^* u_{jn} f(\mathcal{E}_n) + v_{in} v_{jn}^* f(-\mathcal{E}_n) = \chi_{ij\uparrow} \qquad (3.35)
\end{aligned}$$

This allows the definition of $\chi_{ij} \equiv \chi_{ij\uparrow} = \chi_{ij\downarrow}$.

Note that for a numerical evaluation on a computer one uses a different form for the expressions of the preceding expectation values.[11]

[10] $1 - 2f(x) = 1 - 2\frac{1}{e^{\beta x}+1} = \frac{e^{\beta x}+1-2}{e^{\beta x}+1} = \frac{e^{\beta x}-1}{e^{\beta x}+1} = \frac{e^{\beta x/2}-e^{-\beta x/2}}{e^{\beta x/2}+e^{-\beta x/2}} = \tanh(\frac{\beta x}{2})$

[11] For the implementation on a computer one does not use the parametrization in terms of $\boldsymbol{u}_n$ and $\boldsymbol{v}_n$ and the explicit structure of the unitary matrix U (this allows in addition to incorporate magnetic systems). We give the expressions for all order parameters in terms of the different notation in which the eigenvectors of the BdG equation are $\boldsymbol{w}_n = (\boldsymbol{u}_n, \boldsymbol{v}_n)^T$ with $2L$ eigenvalues $\{\mathcal{E}_n\}$ and the unitary matrix U has the $\boldsymbol{w}_n$ as colums. With this notation we have the relations

$$\langle \gamma_{ns}^\dagger \gamma_{ms'}\rangle = \begin{cases} \delta_{nm}\delta_{ss'} f(\mathcal{E}_n) & \text{if} \quad s = \uparrow \\ \delta_{nm}\delta_{ss'} f(-\mathcal{E}_{n+L}) & \text{if} \quad s = \downarrow \end{cases} \qquad (3.36)$$

In this work only the $T = 0$ case is considered. The above expressions then read:

$$n_{i\uparrow} = \sum_{n<L} |v_{in}|^2 = n_{i\downarrow} = \tfrac{1}{2} n_i \tag{3.39}$$

$$\Delta_{ij} = -\tfrac{J_{ij}}{2} \sum_{n<L} (v^*_{jn} u_{in} + v^*_{in} u_{jn}) \tag{3.40}$$

$$\widetilde{\chi}_{ij\uparrow} = \sum_{n<L} v_{in} v^*_{jn} = \chi_{ij\downarrow} \tag{3.41}$$

Finally it is noted that a solution of the BdG equation Eq. (3.6) amounts to a solution of the explicit eigenvalue problem while fulfilling the above self-consistency relations. How this is done in practice is described in the last section of this chapter, Sec. 3.4.

Then the evaluated expectation values are the following

$$\begin{aligned}
\widetilde{\chi}_{ij\uparrow} &= \sum_{nm<L} \langle (w^*_{in}\gamma^\dagger_{n\uparrow} - w_{i(n+L)}\gamma_{n\downarrow})(w_{jm}\gamma_{m\uparrow} - w^*_{j(m+L)}\gamma^\dagger_{m\downarrow}) \rangle \\
&= \sum_{n<L} w^*_{in} w_{jn} f(\mathcal{E}_n) + w^*_{i(n+L)} w_{j(n+L)} f(\mathcal{E}_{n+L}) \\
&= \sum_{n<2L} w^*_{in} w_{jn} f(\mathcal{E}_n) \qquad (3.37a) \\
\widetilde{\chi}_{ij\downarrow} &= \sum_{nm<L} \langle (w^*_{i(n+L)}\gamma^\dagger_{n\uparrow} - w_{(i+L)(n+L)}\gamma_{n\downarrow})(w_{(j+L)m}\gamma_{m\uparrow} - w^*_{(j+L)(m+L)}\gamma^\dagger_{m\downarrow}) \rangle \\
&= \sum_{n<L} w^*_{(i+L)n} w_{(j+L)n} f(-\mathcal{E}_n) + w^*_{(i+L)(n+L)} w_{(j+L)(n+L)} f(-\mathcal{E}_{n+L}) \\
&= \sum_{n<2L} w^*_{(i+L)n} w_{(j+L)n} f(-\mathcal{E}_n) \qquad (3.37b) \\
\langle c_{j\downarrow} c_{i\uparrow} \rangle &= \sum_{nm<L} \langle (w^*_{(j+L)n}\gamma^\dagger_{n\uparrow} - w_{(j+L)(n+L)}\gamma_{n\downarrow})(w_{im}\gamma_{m\uparrow} - w^*_{i(m+L)}\gamma^\dagger_{m\downarrow}) \rangle \\
&= \sum_{n<L} w^*_{(j+L)n} w_{in} f(\mathcal{E}_n) + w^*_{(j+L)(n+L)} w_{(i+L)(n+L)} f(\mathcal{E}_{n+L}) \\
&= \sum_{n<2L} w^*_{(j+L)n} w_{in} f(\mathcal{E}_n) \qquad (3.37c)
\end{aligned}$$

The occupation numbers can be obtain with $n_{is} = \chi_{iis}$. All these expressions are valid also for a magnetized system.

For zero temperature $T = 0$ they reduce to (as $\mathcal{E}_n > 0$ for $n < L$ and $\mathcal{E}_n < 0$ for $n > L$)

$$\widetilde{\chi}_{ij\uparrow} = \sum_{n<L} w^*_{i(n+L)} w_{j(n+L)} \tag{3.38a}$$

$$\widetilde{\chi}_{ij\downarrow} = \sum_{n<L} w^*_{(i+L)n} w_{(j+L)n} \tag{3.38b}$$

$$\langle c_{j\downarrow} c_{i\uparrow} \rangle = \sum_{n<L} w^*_{(j+L)(n+L)} w_{(i+L)(n+L)} \tag{3.38c}$$

3.3. Renormalized mean-field theory (RMFT)

In this section the Gutzwiller approximation introduced in Sec. 2 is used to derive a renormalized mean-field theory (RMFT) that takes into account combinatorial correlations due to a strong Coulomb repulsion. The idea is to employ the Gutzwiller approximation for the evaluation of expectation values when deriving the effective one-particle hamiltonian from the full microscopic many-body hamiltonian. The effective hamiltonian which then has a renormalized form is eventually solved within the BdG framework.

3.3.1. Derivation of a renormalized hamiltonian

To be concrete and due to the application of interest in Sec. 4 the derivation is performed for a specific decomposition of the t-J-model hamiltonian Eq. (2.20). To begin, the spin interaction term of the t-J-model is decomposed with Hartree-Fock mean-field arguments as justified and derived in Sec. C. From here on it is necessary, as was already done in Sec. 2, to distinguish expectation values in a non-correlated, preprojected state $\langle\cdot\rangle_0$ and a correlated, projected state $\langle\cdot\rangle$. It holds with $\widetilde{\chi}_{ij} \equiv \widetilde{\chi}_{ij\uparrow} = \widetilde{\chi}_{ij\downarrow}$ and $\widetilde{\Delta}_{ij} \equiv \langle c_{j\downarrow} c_{i\uparrow}\rangle$ [12]

$$\langle \boldsymbol{S}_i \cdot \boldsymbol{S}_j\rangle_0 = -\frac{3}{4}(\widetilde{\chi}^*_{ij}\widetilde{\chi}_{ij} + \widetilde{\Delta}^*_{ij}\widetilde{\Delta}_{ij}) \quad , \qquad \frac{1}{4}\langle \hat{n}_i\hat{n}_j\rangle_0 = \frac{1}{4}(-\widetilde{\chi}^*_{ij}\widetilde{\chi}_{ij} + \widetilde{\Delta}^*_{ij}\widetilde{\Delta}_{ij}) \tag{3.42}$$

For the expectation value of the spin-interaction term an approximation in terms of a renormalized expectation value in the non-correlated system was derived in Sec. 2 in Eq. (2.54).[13] It was further shown in Sec. 2 that the charge density interaction is not renormalized, such that

$$\langle \boldsymbol{S}_i \cdot \boldsymbol{S}_j\rangle \overset{\text{Gutzw.}}{=} g^J_{ij}\langle \boldsymbol{S}_i \cdot \boldsymbol{S}_j\rangle_0 \quad , \qquad \frac{1}{4}\langle \hat{n}_i\hat{n}_j\rangle \overset{\text{Gutzw.}}{=} \frac{1}{4}\langle \hat{n}_i\hat{n}_j\rangle_0 \tag{3.43}$$

It then follows

$$\langle \boldsymbol{S}_i \cdot \boldsymbol{S}_j - \hat{n}_i\hat{n}_j\rangle \overset{\text{Gutzw.}}{=} -(\tfrac{3}{4}g^J_{ij} - \tfrac{1}{4})\widetilde{\chi}^*_{ij}\widetilde{\chi}_{ij} - (\tfrac{3}{4}g^J_{ij} + \tfrac{1}{4})\widetilde{\Delta}^*_{ij}\widetilde{\Delta}_{ij} \tag{3.44}$$

The approximation of the expectation value for the hopping process was aready given in Eq. (2.59)

$$\langle c_{is}c_{js}\rangle \overset{\text{Gutzw.}}{=} g^t_{ij}\langle c_{is}c_{js}\rangle_0 = g^t_{ij}\widetilde{\chi}_{ijs} \tag{3.45}$$

With this and by mean-field (MF) decoupling the t-J-hamiltonian, we can finally evaluate

[12] See the appendix Sec. C for a derivation and reference for this decomposition.

[13] Remember that for a system that is persistently below half filling the expression for g^J derived in Eq. (2.53) is equivalent with that of Wang *et al.* (2006). The same is true for g^t.

its expectation value in order to obtain an approximation E_{RMFT} for the energy $E \equiv \langle H \rangle$.

$$\begin{aligned}\langle H \rangle \overset{\text{Gutzw.+MF}}{\simeq} E_{\mathrm{RMFT}} \equiv & -\sum_{(ij)s} g_{ij}^t t_{ij} (\widetilde{\chi}_{ijs}^* + \mathrm{h.c.}) \\ & -\sum_{\langle ij \rangle} (\tfrac{3}{4} g_{ij}^J - \tfrac{1}{4}) J_{ij} \widetilde{\chi}_{ij}^* \widetilde{\chi}_{ij} - \sum_{\langle ij \rangle} (\tfrac{3}{4} g_{ij}^J + \tfrac{1}{4}) J_{ij} \widetilde{\Delta}_{ij}^* \widetilde{\Delta}_{ij} \\ & -\sum_i (\mu - \epsilon_i) \hat{n}_i \end{aligned} \tag{3.46}$$

where summations are over pairs of nearest $\langle ij \rangle$ or over nearest and next nearest neighbors (ij), respectively.

A variational calculation with respect to all self-consistent parameters as explained in Sec. C yields the effective hamiltonian[14]

$$\begin{aligned} H_{\mathrm{RMFT}} = & -\sum_{(ij)s} g_{ij}^t t_{ij} c_{is}^\dagger c_{js} + \mathrm{h.c.} \\ & -\sum_{\langle ij \rangle} \Big((\tfrac{3}{4} g_{ij}^J - \tfrac{1}{4}) J_{ij} \widetilde{\chi}_{ij}^* c_{i\uparrow}^\dagger c_{j\uparrow} + \mathrm{h.c.} \Big) - \sum_{\langle ij \rangle} \Big((\tfrac{3}{4} g_{ij}^J + \tfrac{1}{4}) J_{ij} \widetilde{\Delta}_{ij} c_{j\uparrow}^\dagger c_{i\downarrow}^\dagger + \mathrm{h.c.} \Big) \\ & -\sum_i (\mu - \epsilon_i) \hat{n}_i \end{aligned} \tag{3.47}$$

From here the convention that t_{ij} is a $L \times L$ matrix that has non-zero entries only for nearest and next-nearest neighbors and that J_{ij} is a $L \times L$ matrix that has non-zero entries only for nearest neighbors is assumed. With the redefinition $\frac{1}{2} J_{ij} \to J_{ij}$ the hamiltonian can be written as[15]

$$\begin{aligned} H_{\mathrm{RMFT}} = & -\sum_{ijs} \big(g_{ij}^t t_{ij} + (\tfrac{3}{4} g_{ij}^J - \tfrac{1}{4}) J_{ij} \widetilde{\chi}_{ij}^* \big) c_{is}^\dagger c_{js} \\ & -\sum_{ij} \Big((\tfrac{3}{4} g_{ij}^J + \tfrac{1}{4}) J_{ij} \widetilde{\Delta}_{ij} c_{j\uparrow}^\dagger c_{i\downarrow}^\dagger + \mathrm{h.c.} \Big) - \sum_i (\mu - \epsilon_i) \hat{n}_i \end{aligned} \tag{3.49}$$

[14] The variation with respect to the Gutzwiller factors $g^t \equiv g^t(n_i, n_j)$ and $g^J \equiv g^J(n_i, n_j)$ is not performed here due to reasons explained in the following section. Further note that a formal spin-asymmetry is introduced in the χ_{ij}-term of the hamiltonian Eq. (3.47) because we defined $\chi_{ij} \equiv \langle c_{i\uparrow}^\dagger c_{j\uparrow} \rangle$.

[15] An intermediate step yields the following hamiltonian

$$\begin{aligned} H_{\mathrm{RMFT}} = & -\sum_{ijs} \big(g_{ij}^t t_{ij} + (\tfrac{3}{4} g_{ij}^J - \tfrac{1}{4}) J_{ij} \tfrac{1}{2} \widetilde{\chi}_{ij}^* \big) c_{is}^\dagger c_{js} \\ & -\sum_{ij} \Big((\tfrac{3}{4} g_{ij}^J + \tfrac{1}{4}) J_{ij} \tfrac{1}{2} \widetilde{\Delta}_{ij} c_{j\uparrow}^\dagger c_{i\downarrow}^\dagger + \mathrm{h.c.} \Big) - \sum_i (\mu - \epsilon_i) \hat{n}_i \end{aligned} \tag{3.48}$$

Here the factors $\frac{1}{2}$ in front of the $\widetilde{\chi}_{ij}$- and the $\widetilde{\Delta}_{ij}$-term are due to different reasons. For the kinetic term and the χ_{ij} term one can write $\sum_{\langle ij \rangle} \ldots c_{i\uparrow}^\dagger c_{j\uparrow} + \mathrm{h.c.} = \sum_{i \langle j \rangle_i} \ldots c_{i\uparrow}^\dagger c_{j\uparrow}$ where $\langle j \rangle_i$ denotes summation over all sites j that are nearest neighbors of i. But still one has to account for the spin summation that now also affects χ_{ij} with a factor $\frac{1}{2}$. For the $\widetilde{\Delta}_{ij}$-term the evaluation of the sum over pairs is not possible, but due to the symmetry $\widetilde{\Delta}_{ij} = \widetilde{\Delta}_{ji}$ one can nevertheless write $\sum_{\langle ij \rangle} \widetilde{\Delta}_{ij} (c_{j\uparrow}^\dagger c_{i\downarrow}^\dagger + \mathrm{h.c.}) = \frac{1}{2} \sum_{i \langle j \rangle_i} \widetilde{\Delta}_{ij} (c_{j\uparrow}^\dagger c_{i\downarrow}^\dagger + \mathrm{h.c.})$. Finally a summation $\sum_{i \langle j \rangle_i}$ is the same as $\sum_{ij}$ if the preceding convention for the entries of t_{ij} and J_{ij} is employed.

Following the convention used in Garg *et al.* (2008), we drop the factor $\frac{1}{2}$ in the hamiltonian corresponding to a replacement $\frac{1}{2} J_{ij} \to J_{ij}$ and obtain Eq. (3.49).

Finally the following definitions are employed

$$H_{ij} \equiv -\, g_{ij}^t t_{ij} - (\tfrac{3}{4} g_{ij}^J - \tfrac{1}{4}) J_{ij} \widetilde{\chi}_{ij}^* - \delta_{ij}(\mu - \epsilon_i) \tag{3.50}$$

$$\Delta_{ij} \equiv (\tfrac{3}{4} g_{ij}^J + \tfrac{1}{4}) J_{ij} \widetilde{\Delta}_{ij} \tag{3.51}$$

to obtain the corresponding BdG equation

$$\sum_j \begin{pmatrix} H_{ij} & \Delta_{ij} \\ \Delta_{ij}^* & -H_{ij}^* \end{pmatrix} \begin{pmatrix} u_j \\ v_j \end{pmatrix} = \mathcal{E}_n \begin{pmatrix} u_i \\ v_i \end{pmatrix} \tag{3.52}$$

which is of the form of Eq. (3.6).

From this one calculates $\widetilde{\Delta}_{ij}$, $\widetilde{\chi}_{ij}$ and n_i as described in Sec. 3.2.

3.3.2. Interpretation of the renormalized BdG equation

Which physical meaning do the quantities Δ_{ij}, χ_{ij}, n_i, $\widetilde{\Delta}_{ij}$ and $\widetilde{\chi}_{ij}$, the hamiltonian H_{RMFT} and the corresponding variational ground state

$$|\psi_{\mathrm{RMFT}}\rangle \equiv \prod_{n<L} \gamma_{n\downarrow}^\dagger \prod_{i<L} c_{i\downarrow}^\dagger |\mathrm{vac}\rangle \tag{3.53}$$

have? All of them are obtained by solving the renormalized BdG equation Eq. (3.52).

The straightforward interpretation already used by Zhang *et al.* (1988) and by most authors today is to make the identification $|\psi_0\rangle \equiv |\psi_{\mathrm{RMFT}}\rangle$.[16] Thus the pre-projected state $|\psi_0\rangle$ — employed throughout in Sec. 2 when deriving the Gutzwiller factors — is thought to be equal to the state $|\psi_{\mathrm{RMFT}}\rangle$ which is determined by H_{RMFT}. One argument for this identification is that $|\psi_{\mathrm{RMFT}}\rangle$ has the same functional form as $|\psi_0\rangle$. Both have the form of a generalized BCS state which is far from being as complicated as the form of an exactly projected state $|\psi\rangle \equiv \mathcal{P}|\psi_0\rangle$.[17] Having made this identification, all physical quantities can be obtained with the arguments of Sec. 2 by properly rescaling the expectation value in the state $|\psi_0\rangle \equiv |\psi_{\mathrm{RMFT}}\rangle$. Then it holds for the physical expectation values $\langle\cdot\rangle$ in the correlated system $|\psi\rangle$ with the definition of the Gutzwiller factor for a hopping process g_{ij}^t in Eq. (2.58)

$$\langle c_{is}^\dagger c_{js} \rangle = g_{ij}^t \langle \psi_{\mathrm{RMFT}} | c_{is}^\dagger c_{js} | \psi_{\mathrm{RMFT}} \rangle = g_{ij}^t \widetilde{\chi}_{ij} \tag{3.54a}$$

$$\langle c_{is}^\dagger c_{is} \rangle = \langle \psi_{\mathrm{RMFT}} | c_{is}^\dagger c_{is} | \psi_{\mathrm{RMFT}} \rangle = n_{is} \tag{3.54b}$$

$$\mathrm{OP}_{ij}^{\Delta} \equiv \langle c_{i\downarrow} c_{j\uparrow} \rangle = g_{ij}^t \langle \psi_{\mathrm{RMFT}} | c_{i\downarrow} c_{j\uparrow} | \psi_{\mathrm{RMFT}} \rangle = g_{ij}^t \widetilde{\Delta}_{ij} \tag{3.54c}$$

Here the renormalization of the anomalous expectation value $\langle c_{i\downarrow} c_{j\uparrow} \rangle$ is derived with similar arguments and an analogous calculation as compared to the renormalization of the hopping process.

[16] For example, Wang *et al.* (2006) states "$|\psi_0\rangle$ is determined by H_{RMFT}, so are the variational order parameters."

[17] Another argument for the identification $|\psi_0\rangle \equiv |\psi_{\mathrm{RMFT}}\rangle$ will be presented in the following but is much more subtle.

The author doubts that this straightforward interpretation which builds on the identification of $|\psi_0\rangle \equiv |\psi_{\mathrm{RMFT}}\rangle$, is completely sound. A first criticsm is based on an inspection of the distribution of different energies among the different physical processes in the system. Such an inspection is in the spirit of the Gutzwiller approximation.[18] As $|\psi_{\mathrm{RMFT}}\rangle$ is the variational ground-state corresponding to E_{RMFT} or equivalently H_{RMFT}, it is fully governed by the renormalized energy scales. One can therefore state that, e.g. $|\psi_{\mathrm{RMFT}}\rangle$ incorporates the fact that hopping is unfavorable in areas of density $n_i \sim 1$. In the renormalized system it is not possible to gain much energy in these areas such that electrons will e.g. rather be localized to augment their potential energy. This is a direct consequence of a small effective hopping parameter $g_{ij}^t t_{ij} \leq t_{ij}$. One can therefore state that the ground state $|\psi_{\mathrm{RMFT}}\rangle$ incorporates already much of the energetic aspects of the physics of a projected state $|\psi\rangle$ making it questionable if $|\psi_{\mathrm{RMFT}}\rangle$ can nevertheless be identified with $|\psi_0\rangle$. To be precise, the just described reduction of kinetic energy that mirrors a feature of a correlated system, has to be understood as a relative statement made in comparison with the variational ground-state $|\psi_0'\rangle$ of a non-renormalized hamiltonian with bare parameters t_{ij}, J_{ij}. Only the relative statement: $g_{ij}t_{ij}$ is smaller than t_{ij} is meaningful. Therefore here the ground-state $|\psi_0'\rangle$ leading to the uncorrelated energy scales is proposed as a much more intuitive choice for $|\psi_0\rangle$ as compared to $|\psi_{\mathrm{RMFT}}\rangle$. The interpretation of $|\psi_{\mathrm{RMFT}}\rangle$ on the other hand cannot be fully clarified. But although its interpretation as a physical state is questionable, there is no doubt that in the combination with the renormalized hamiltonian H_{RMFT} one is still able to obtain a good approximation for certain quantities of an exactly projected system.

The inspection of these quantities leads to further aspects of the argumentation. The first question one can pose concerns the kinetic energy:[19] Is $E_{\mathrm{kin}} = \sum_{ij} g_{ij}^t t_{ij} \widetilde{\chi}_{ij}$ a meaningful approximation for the kinetic energy in the projected wave function $|\psi\rangle$? Yes, it is without doubt and independent of the interpretation of $|\psi_{\mathrm{RMFT}}\rangle$. The energy quantity $g_{ij}^t t_{ij}\chi_{ij} \equiv g_{ij}^t t_{ij} \langle\psi_{\mathrm{RMFT}}|c_{is}^\dagger c_{js}|\psi_{\mathrm{RMFT}}\rangle$ is explicitly present in H_{RMFT}. Its resemblance to the energy $t_{ij}\langle\psi|c_{is}^\dagger c_{js}|\psi\rangle$ is the basis of the Gutzwiller approximation and therefore for the derivation of H_{RMFT}. This resemblance is at least qualitatively correct as it is the outcome of a variational calculation with the variational wave function $|\psi_{\mathrm{RMFT}}\rangle$ subject to certain physical constraints. That it is even quantitatively close is astonishing and was checked with variational Monte Carlo methods already by Zhang *et al.* (1988).

From the way it was just argued that the energy quantity $g_{ij}^t t_{ij} \langle\psi_{\mathrm{RMFT}}|c_{is}^\dagger c_{js}|\psi_{\mathrm{RMFT}}\rangle$ resembles $t_{ij}\langle\psi|c_{is}^\dagger c_{js}|\psi\rangle$ one could now conlcude that $|\psi_0\rangle$ resembles $|\psi_{\mathrm{RMFT}}\rangle$.[20] But this conclusion is not obvious in the authors mind. Consider a hypothetical calculation with an exactly projected state $|\psi\rangle = \mathcal{P}|\psi_0\rangle$. After projection of $|\psi_0\rangle$ one must minimize the energy

[18] We can formulate the assumption of the "Gutzwiller approximation" in this way: a crude adaption of the energies for different processes leading to a renormalized hamiltonian is an approximate description of its physical behavior. In this light the "Gutzwiller approximation" states that the physical behavior is mainly due to energetical questions and not much influenced by the quantum correlations induced by the explicit structure of the true state $|\psi\rangle$ of the system. To be consistent with the original assumption one should therefore judge the argument which follows in the text above, more important than the preceding argument referring to the structure of the state.

[19] The Fock-shift contribution $|\chi_{ij}|^2$ is not considered here. We discuss the simplest case of a hamiltonian that is governed only by hopping, pairing and local potentials.

[20] This refers to the second argument mentioned in footnote 17.

respecting the functional form of $|\psi\rangle$ but in dependence of the variational parameters that are as well present in $|\psi_0\rangle$. This variation is clearly subject to the effect of projection such that on a qualitative level one can, for example, say that it will assign much fewer energy to hopping processes and more to spin exchange processes as without projection. This characteristic feature is consistent with the Gutzwiller projection and reflected in the approximation of the "exactly projected variation" via the renormalized terms in E_{RMFT}. As already stated in the preceding paragraph, the result of the approximated variational calculus for the value of the kinetic energy should therefore qualitatively resemble the result of the exact variation. But the interpretation of the optimized set of variational parameters is a different question, as it is a much more detailed result related to the microscopic structure of the states. Imagine to take this set of exactly calculated variational parameters and plug it into the functional form of $|\psi_0\rangle$. Then, one faces a state the parameters of which were optimized with respect to a completely different functional form, namely $\mathcal{P}|\psi_0\rangle$. The physical behavior of the system $|\psi_0\rangle$ is then the one of an uncorrelated system,[21] which means e.g. that it will have the energy scales of an uncorrelated system. But still one has to be careful. The state $|\psi_0\rangle$ is in the following sense not a physical, uncorrelated state, as its parameters, optimized to the correlated case, will in general not fulfill the self-consistency equations of the uncorrelated system.

In the case of the derivation of $|\psi_{\mathrm{RMFT}}\rangle$ there is a substantially different aspect. Also in this case the variational parameters are adjusted in order to respect the energetics of the correlated system due to the renormalization which leads to a meaningful value of the variational energy. But after the process of variation is completed, in this case it is not possible to obtain a corresponding un-correlated state $|\psi_0\rangle$ by plugging in the just optimized variational parameters in a completely different functional form. Already from the beginning one assumed the form of $|\psi_0\rangle$ for the variational wave function $|\psi_{\mathrm{RMFT}}\rangle$. This form is a much worse ansatz for the variational wave function than the projected form, such that $|\psi_{\mathrm{RMFT}}\rangle$ can neither be identified with an approximation for $|\psi\rangle$ but even less with an uncorrelated state $|\psi_0\rangle$.

Having made this argumentation, the result for the order parameter $\mathrm{OP}_{ij}^{\Delta}$ in Eq. (3.54c) is not to be justified as it completely relies on the identification $|\psi_0\rangle = |\psi_{\mathrm{RMFT}}\rangle$. The author thinks that a clear statement about the order parameter cannot be made. Only the energy gap Δ_{ij} of H_{RMFT} is a meaningful quantity in terms of the Gutzwiller approximation considered here. The gap Δ_{ij} is self-consistently determined and incorporates the effects of locally augmented spin-correlations and reduced hopping parameters. This is consistent with the scenario of an experiment that measures the gap of a strongly correlated system approximately described by H_{RMFT}. There one would clearly measure the value Δ_{ij}, neither $\widetilde{\Delta}_{ij}$ nor $\mathrm{OP}_{ij}^{\Delta}$.

Comparison of a correlated with an uncorrelated system In Sec. 4 we aim to compare a correlated with an uncorrelated system. There, we will proceed in the way that

[21] Insertion of the variational parameters obtained with $\mathcal{P}|\psi_0\rangle$ in $|\psi_0\rangle$ corresponds to "reversing" the projection.

was also used by Garg *et al.* (2008). They compare two systems, one of which described by a bare and the other by a renormalized hamiltonian. Both are taken with the same hopping parameters t_{ij} and impurity potentials ε_i, but with spin correlations J_{ij} that are scaled with a constant factor in order to have $\Delta_{ij}^{\text{bare}} = \Delta_{ij}^{\text{renorm.}}$ [22] in the homogeneous regions of the system, far away from impurities. Having in mind the argumentation just made, this fixing of the value of the gap Δ_{ij} is the only transparent way in order to make a meaningful comparison between the value for a supercurrent in a correlated and an uncorrelated system, also because the supercurrent is approximately proportional to Δ_{ij}.[23] Doing the same calculation for two systems where one fixed $\text{OP}_{ij}^{\Delta\text{bare}} = \text{OP}_{ij}^{\Delta\text{renorm.}}$ or as a third possibility $\widetilde{\Delta}_{ij}^{\text{bare}} = \widetilde{\Delta}_{ij}^{\text{renorm.}}$ is obscure. To confirm this, we analyze these situations numerically in Sec. 4.7.

Impurity potential renormalization To conclude this section about the interpretation of the renormalized BdG equation we briefly address the possibility to incorporate a renormalization term of the impurity potential in H_{RMFT}. As mentioned in footnote 14, in the renormalized hamiltonian of Eq. (3.49), we did not account for the variation of the Gutzwiller factors with respect to the local densities n_i. With this we proceed in the way as authors like Tsuchiura *et al.* (2001), Raczkowski and Poilblanc (2009) and Garg *et al.* (2008) do. Other authors like Fukushima *et al.* (2009), Zhang *et al.* (1988) and Li *et al.* (2006) include it in their calculations. There is no doubt that a straightforward variational calculation respecting n_i as a parameter must do so, also mentioned in the theoretical work of Wang *et al.* (2006). Nevertheless, this is not done here for a consistency reason independent of the variational calculus. The incorporation of renormalization terms for the potential leads to completely different effective impurity potentials. This fact makes a meaningful comparison with an uncorrelated state impossible as this is of course subject to the bare potentials.[24] We decided therefore not to take into account the impurity potential renormalization and regret that due to numerical reasons, we cannot provide any comparisons with calculations which include it, in order to support our assertion considering a consistent comparison.

3.4. Convergence of the iterative solution to the BdG equation

In this section results that concern the numerical evaluation of the BdG equation Eq. (3.6) and its renormalized counterpart Eq. (3.52) are presented. These are results relevant to the practical work making it unnecessary to read this section if one is only interested in

[22] $\Delta_{ij}^{\text{bare}}$ denotes the self-consistent value of the gap in the bare, non-renormalized, uncorrelated system, obtained with a standard BdG evaluation. $\Delta_{ij}^{\text{renorm.}}$ denotes the self-consistent value of the gap in the renormalized, correlated system, obtained in a RMFT calculation.

[23] Confer Sec. A.

[24] Another aspect is the following. Impurity potential renormalization ensures that the density in the system is always below $n_i < 1$. This has the effect that $|\psi_{\text{RMFT}}\rangle$ gets much closer to a veritable projected state $\mathcal{P}|\psi_0\rangle$. But if this is the case the whole ansatz of the renormalized BdG equation is contradictory as it is based on the fact that $g_{ij}^t t_{ij} \langle\psi_{\text{RMFT}}|c_{is}^\dagger c_{js}|\psi_{\text{RMFT}}\rangle$ is a meaningful value for the kinetic energy in the correlated system. If $|\psi_{\text{RMFT}}\rangle$ has all features of $\mathcal{P}|\psi_0\rangle$, than the renormalization is meaningless and contradicts the original idea of the ansatz.

understanding Sec. 4.

3.4.1. General convergence criteria

Usually, the BdG-equations Eq. (3.6) are solved iteratively on a computer. One initializes the hitherto unknown matrix H_{C}[25] with an initial guess for Δ_{ij}, χ_{ij}, n_i and μ. This is usually not a very good one: e.g. in the case of inhomogeneous systems it does not take into account a spatial variation of the parameters.

Then a sequential procedure of diagonalizing H_{C} and a following calculation of $\widetilde{\Delta}_{ij}$, $\widetilde{\chi}_{ij}$, n_i and μ from the eigenvectors $(\boldsymbol{u}\ \boldsymbol{v})^T$ is carried out. If the procedure works, at each step of the iteration, the mean-field approximation of energy expectation value $\langle H\rangle$ decreases and the values of the self-consistent parameters approach a unique solution. We can already now state that when working without a renormalized hamiltonian, this method will almost always work. Why is this so? And why are there considerable problems when working with a renormalized hamiltonian?

We assume that the following system of equations has a unique solution

$$H_{\mathrm{C}}(\widetilde{\Delta}_{ij},\widetilde{\chi}_{ij},n_i,\mu)w_n = \mathcal{E}_n w_n \tag{3.55a}$$

with

$$\widetilde{\chi}_{ij} = \sum_{n<L} w^*_{i(n+L)} w_{j(n+L)} f(\mathcal{E}_{n+L}) \tag{3.55b}$$

$$n_i = \chi_{ii} \tag{3.55c}$$

$$\widetilde{\Delta}_{ij} = \sum_{n<L} w^*_{(j+L)(n+L)} w_{(i+L)(n+L)} f(\mathcal{E}_{n+L}) \tag{3.55d}$$

Here we adopted the notation of Eq. (3.38). It was already stated that this is an equivalent formulation of a variation of the mean-field approximation of $\langle H\rangle$, the direct representation of which in an operator space that has been mapped to C by application of the Fermi function in Eq. (3.25).

To obtain this unique solution with iterations one proceeds, using the index ν to denote an iteration, as

$$H_{\mathrm{C}}(\widetilde{\Delta}^{\nu-1}_{ij},\widetilde{\chi}^{\nu-1}_{ij},n^{\nu-1}_i,\mu^{\nu-1})w^\nu_n = \mathcal{E}^\nu_n w^\nu_n \tag{3.56a}$$

with

$$\widetilde{\chi}^\nu_{ij} = \sum_{n<L} w^{\nu*}_{i(n+L)} w^\nu_{j(n+L)} f(\mathcal{E}^\nu_{n+L}) \tag{3.56b}$$

$$n^\nu_i = \chi^\nu_{ii} \tag{3.56c}$$

$$\widetilde{\Delta}^\nu_{ij} = \sum_{n<L} w^{\nu*}_{(j+L)(n+L)} w^\nu_{(i+L)(n+L)} f(\mathcal{E}^\nu_{n+L}) \tag{3.56d}$$

These equations are too complicated to be analyzed in a meaningful way. We consider therefore an easier example — the spatially homogeneous case that can be solved in $\boldsymbol{k}$-space.

[25] See Eq. (3.5) to check that this is the l.h.s. of the BdG equation.

We rename n to $\boldsymbol{k}$ to signify that the unitary transformation that diagonalizes H_{C} is a discrete Fourier transform. We set $|\widetilde{\Delta}_{ij}| \equiv \Delta$ and $n_i \equiv n$ and perform an evaluation.[26]

Momentum space Consider the case without χ. In $\boldsymbol{k}$-space, the form of the self-consistency relation for the order parameter is commonly known as the gap equation of an extended BCS theory. For a pure d-wave order parameter it reads

$$\Delta = \frac{1}{L} \sum_{\boldsymbol{k} \in \mathcal{BZ}} \frac{J_{\mathrm{eff}}}{2} (\cos k_x - \cos k_y) \frac{\Delta_{\boldsymbol{k}}}{2E_k} \tag{3.57}$$

where

$$\Delta_{\boldsymbol{k}} = -2\Delta(\cos k_x - \cos k_y) \tag{3.58}$$

$$\xi_{\boldsymbol{k}} = -2t(\cos k_x + \cos k_y) - \mu \tag{3.59}$$

$$E_k = \sqrt{\xi_k^2 + \Delta_k^2} \tag{3.60}$$

where J_{eff} is a coupling constant that will later contain a renormalization.

If we do not consider the Gutzwiller case, an iterative solution can be done only by solving this equation. Again with an initial guess for Δ, Δ^0 and then iteratively calculating $\Delta^{\nu+1}$ by plugging in Δ^ν on the r.h.s. of Eq. (3.57). This equation can be analyzed using the Banach fixed point theorem. For this we define the map

$$G(\Delta) \equiv \frac{1}{L} \sum_{\boldsymbol{k} \in \mathcal{BZ}} \frac{J_{\mathrm{eff}}}{2} (\cos k_x - \cos k_y) \frac{\Delta_{\boldsymbol{k}}}{2E_k} \tag{3.61}$$

The Banach fixed point theorem states that if a function $F(x)$ is a contraction for all $x \in D \subset X$ (X a vector space which provides a norm, here just the euclidian norm), i.e. if

$$|F(x_1) - F(x_2)| \leq q|x_1 - x_2| \tag{3.62}$$

for a $q < 1$, then there exists a unique fixed point x^f for which $F(x^f) = x^f$ holds. This fixed point can be obtained by calculating the sequence $x^{\nu+1} = F(x^\nu)$ for an arbitrary starting point x^0. Convergence is exponential.[27] For a one-dimensional problem, i.e. $x \in D \subset \mathrm{R}$, the weaker condition $F(x)' \leq q$ is already sufficient. But also for $x \in D \subset \mathrm{R}^2$ or a higher dimensional space, it is useful to consder $\partial_{x_i} F(x)$: If $F(x)$ is a contraction in any small subset of D, the iteration procedure will at least converge if we start close enough to the solution.[28] For two values of x very close to each other $|x_1 - x_2| < \epsilon$ we see that Eq. (3.62) is equivalent to the condition for the partial derivatives

$$\partial_{x_i} F(x) \leq q \quad \forall \quad x_i \tag{3.63}$$

[26] In this chapter, there is no need to make the rigorous distinction between $\widetilde{\Delta}_{ij}$ and Δ_{ij} such that in the following, we drop the tilde $|\widetilde{\Delta}_{ij}| \equiv \Delta$ for notational simplicity.

[27] See e.g. Forster (2008, Chap. 8, p. 88).

[28] This investigation is rather an inspection of the stability of the procedure, i.e. of the attractiveness of the fixed point.

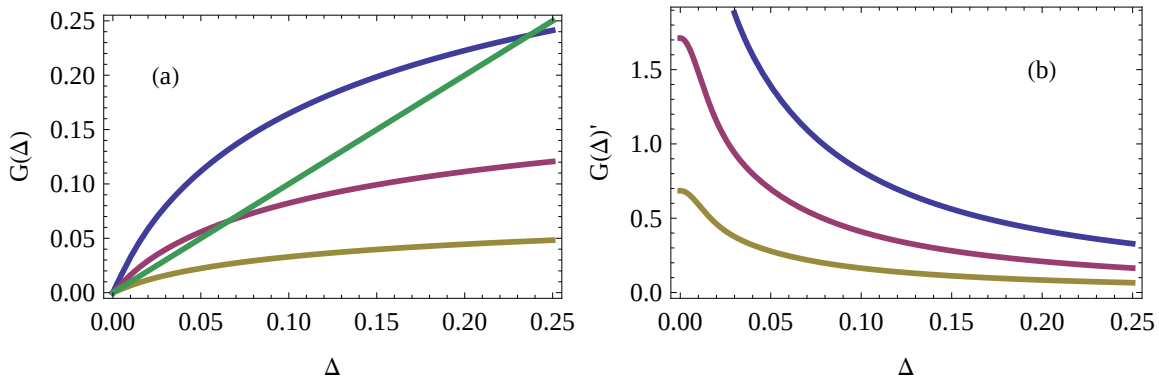

Figure 3.1.: Plot of $G(\Delta)$ and $G'(\Delta)$ as given in Eqs. (3.64) for $J_{\text{eff}} = 2$ (blue), $J_{\text{eff}} = 1$ (red) and $J_{\text{eff}} = 0.4$ (yellow). This is for a square 2D system of $L = 121$ lattice sites, hopping $t = 1$ and $\mu = 0$. Note that the fixed point values for Δ are given by the intersections of the green line (corresponding to Δ) with the other lines. This is for a square 2D system of $L = 121$ lattice sites and hopping $t = 1$.

for a $q < 1$. Knowing this, we inspect the derivatives of the gap equation Eq. (3.57).

3.4.2. Convergence of a standard BdG calculation

In the case of a standard BdG calculation, i.e. Eq. (3.61) and J_{eff} is a simple constant, it is sufficient to analyze the ordinary derivative. We rewrite Eq. (3.61) and obtain for the derivative

$$G(\Delta) = \frac{J_{\text{eff}}}{2}\frac{1}{L}\sum_{\boldsymbol{k}\in\mathcal{BZ}} \frac{\Delta(\cos k_x - \cos k_y)^2}{(4\Delta^2(\cos k_x - \cos k_y)^2 + (2t(\cos k_x + \cos k_y) + \mu)^2)^{1/2}} \tag{3.64a}$$

$$G(\Delta)' = \frac{J_{\text{eff}}}{2}\frac{1}{L}\sum_{\boldsymbol{k}\in\mathcal{BZ}} \frac{(\cos k_x - \cos k_y)^2(2t(\cos k_x + \cos k_y) + \mu)^2}{(4\Delta^2(\cos k_x - \cos k_y)^2 + (2t(\cos k_x + \cos k_y) + \mu)^2)^{3/2}} \tag{3.64b}$$

In Fig. 3.1 the two functions of Eqs. (3.64) are plotted for an exemplary set of parameters. It is obvious that $G(\Delta)'$ is smaller than one in the whole range of interest. For a conventional BdG calculation without renormalization this shows that convergence is guaranteed. In the case of an RMFT calculation this is different.

3.4.3. Convergence of a RMFT calculation

For the solution of a renormalized hamiltonian, we have to solve simultaneously

$$\Delta = g^J(n)\frac{J}{2}\frac{1}{L}\sum_{k\in\mathcal{BZ}}(\cos k_x - \cos k_y)\frac{\Delta_{\boldsymbol{k}}}{2E_k} \tag{3.65}$$

$$n = \frac{2}{L}\sum_{k\in\mathcal{BZ}}\frac{\Delta_{\boldsymbol{k}}^2}{(\xi_{\boldsymbol{k}} + E_k)^2 + \Delta_{\boldsymbol{k}}^2} \tag{3.66}$$

where now

$$\xi_{\boldsymbol{k}} = -2g^t(n)t(\cos k_x + \cos k_y) - \mu \tag{3.67}$$

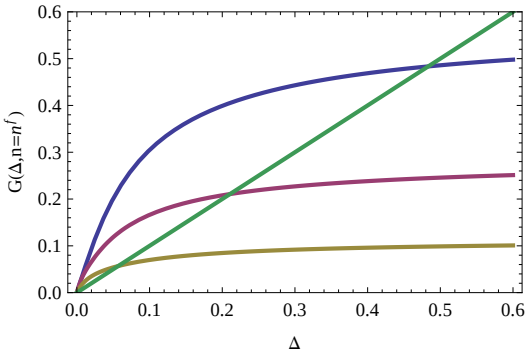

Figure 3.2.: Plot of $G(\Delta, n^f = 0.8)$ for $J = 1$ (blue), for $J = 0.5$ (red) and for $J = 0.2$ (yellow) together with Δ (green) versus Δ. All other parameters in Eq. (3.69) are fixed to their value in a selfconsistent solution.

with renormalized spin interaction constant $g^J(n)J$ and hopping $g^t(n)t$. This is solved with two initial guesses Δ^0 and n^0, and then iteratively calculating Δ^1, from this then n^1, from this again Δ^2 and so on.

To apply the Banach fixed point theorem again we define

$$G(\Delta, n) \equiv g^J(n)\frac{J}{2}\frac{1}{L}\sum_{\boldsymbol{k}\in\mathcal{BZ}}(\cos k_x - \cos k_y)\frac{\Delta_{\boldsymbol{k}}}{2E_k} \tag{3.68}$$

$$N(\Delta, n) \equiv \frac{2}{L}\sum_{k\in\mathcal{BZ}}\frac{\Delta_{\boldsymbol{k}}^2}{(\xi_{\boldsymbol{k}} + E_k)^2 + \Delta_{\boldsymbol{k}}^2} \tag{3.69}$$

Now we have a two-dimensional map which should fulfill $|\sqrt{G(\Delta_1, n_1)^2 + N(\Delta_1, n_1)^2} - \sqrt{G(\Delta_1, n_1)^2 + N(\Delta_1, n_1)^2}| \leq q|\sqrt{{\Delta_1}^2 + {n_1}^2} - \sqrt{{\Delta_2}^2 + {n_2}^2}|$. Rewriting this in infinitesimal form leads to an analyzation of the partial derivatives in order to make a statement about stability and convergence of the iteration.

In Fig. 3.2 $G(\Delta, n = 0.8)$ is plotted together with Δ, the intersection of which gives the selfconsistent value Δ^f for different values of J. The picture differs only quantitatively from the case without Gutzwiller factors. Obviously, a calculation that fixes the density will converge as good as a standard BdG solution.

In Fig. 3.3 now we plot the derivatives $\partial_\Delta G(\Delta, n)$, $\partial_n G(\Delta, n)$, $\partial_n N(\Delta, n)$ and $\partial_\Delta N(\Delta, n)$. While panels (c), (d), (e) and (f) are only given for completeness, panels (a), (b), (g) and (h) describe the hypothetical situation, that the iteration has already converged with respect to one parameter. Even in this case, a very positive assumption, the stability of the iteration with respect to n is delicate: clearly, in panels (g) and (h) the derivatives very rapidly assume values above 1 in the region of interest, i.e. around half filling. Still one can make the following statement. In panel (g) the highest value of the spin interaction $J = 1$, corresponding to the blue line, yields a much more stable iteration than the lower values. In panel (f) this is also true, except for one narrow peak of the blue line at $n \approx 0.89$ below half filling, and two other peaks for $n > 1$. The smaller values for the spin interaction yield broader peaks, and

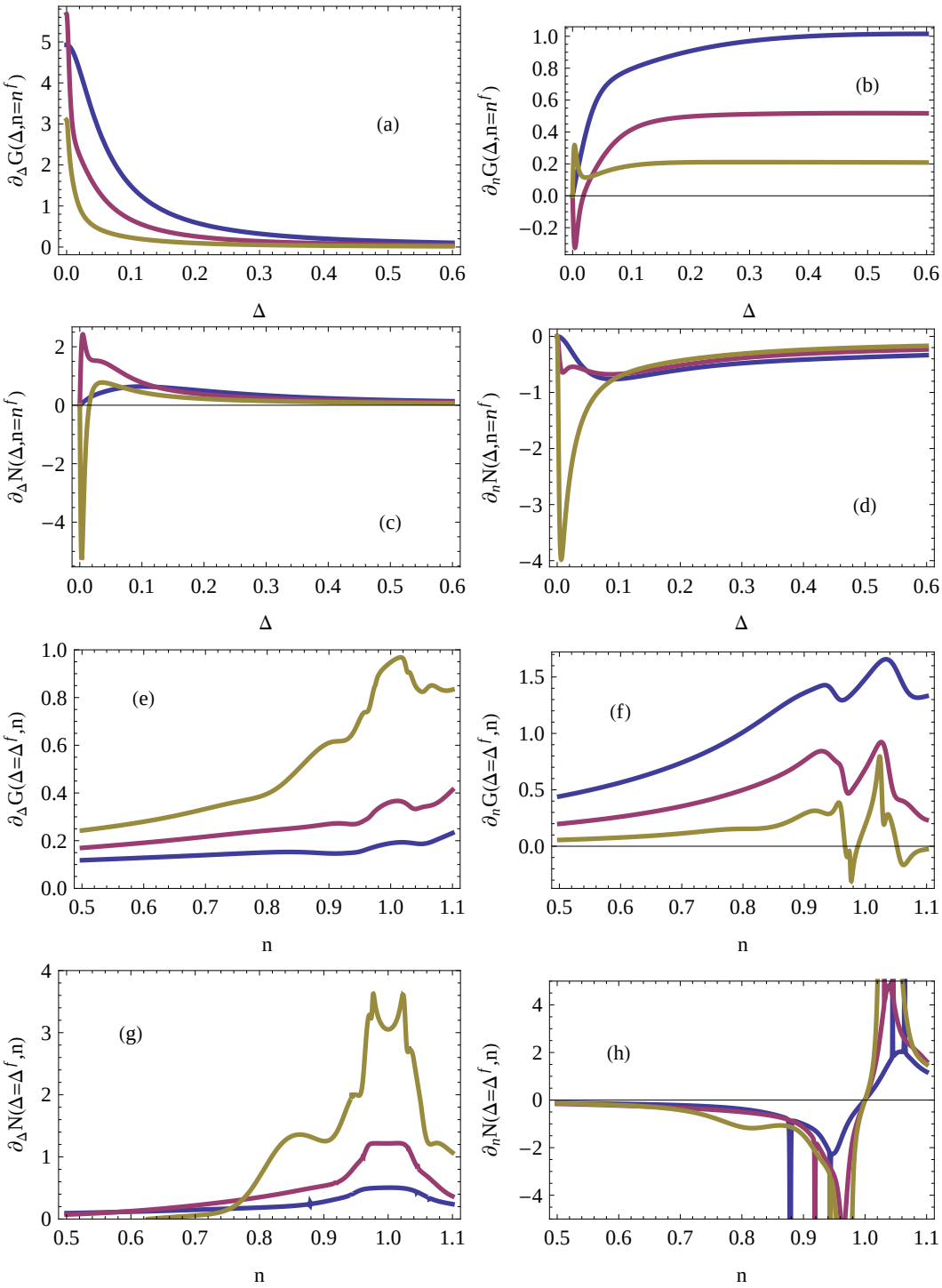

Figure 3.3.: Plots of $\partial_\Delta G(\Delta, n)$, $\partial_n N(\Delta, n)$, $\partial_n N(\Delta, n)$ and $\partial_\Delta G(\Delta, n)$ for $J = 1$ (blue), $J = 0.5$ (red) and $J = 0.2$ (yellow) versus Δ and n. All other parameters are fixed to their value in a selfconsistent solution, in particular the explicit parameters $n^f = 0.8$ and $\Delta^f = 0.48$, $\mu^f = -0.36$ for $J = 1$, $\Delta^f = 0.21$, $\mu^f = -0.25$ for $J = 0.5$ and $\Delta^f = 0.057$, $\mu^f = -0.177$ for $J^f = 0.2$. This is for a square 2D system of $L = 121$ lattice sites and hopping $t = 1$.

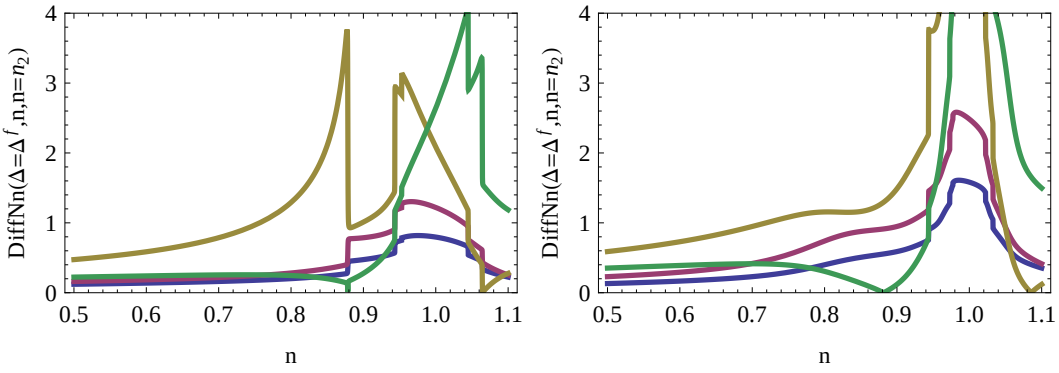

Figure 3.4.: Plot of the function DiffN. Left for $J = 1$ and right for $J = 0.2$. The different colors refer to different arguments n_2" $n_2 = 0.5$ (blue), $n_2 = 0.7$ (red), $n_2 = 0.9$ (yellow) and $n_2 = 1.1$ (green).

therefore a more unstable behavior. In contrast to panel (g) and (h), the convergence in (a) and (b) that depict the situation for Δ, is stable.

To inspect the case of Fig. 3.3(g) and (h) further, we finally define the function $\mathrm{DiffN}(\Delta, n)$

$$\mathrm{DiffN}(\Delta, n_1, n_2) \equiv |N(\Delta, n_1) - N(\Delta, n_2)| \tag{3.70}$$

which allows to analyze the condition for the fixed point theorem in its finite version. In Fig. 3.4 we plot $\mathrm{DiffN}(\Delta, n_1, n_2)$ for two values of J. In this figure, the preceding statement is confirmed. Around half filling, convergence becomes unstable, while far away from half filling it is not problematic. The left panel of Fig. 3.4 is for $J = 1$ while the right is for $J = 0.2$. In the right panel a much stronger increase around half filling is visible, such that again we conclude, that iterations are more stable for higher values of J.

To summarize: A RMFT calculation is best done for considerable hole doping, that is for a density $n \leq 0.8$ and with a sufficiently large spin interaction constant J. Otherwise, it is not possible to obtain convergent solutions. A fact not discussed in this chapter that turned out to be generic for inhomogeneous systems, is the destabilizing action of a too large value of J. Then, due to reasons that could not be clarified, the system tends away from a d-wave towards an unstructured solution. This leads to the conclusion that only in a small interval for J and for low densities, one obtains physical, convergent solutions for RMFT calculations. This severely restricts the RMFT method.

Luckily, for the results of Sec. 4, we were able to choose physical parameters in the narrow convergent regime in order to obtain selfconsistent solutions. Being aware of the convergence problem, in all calculations, we checked convergence for a large number of single lattice sites with great care.

4. Supercurrent through GBs in the presence of strong correlations

In this chapter we apply the techniques discussed in the previous parts of the thesis to the problem of the determination of the critical current through grain boundaries (GBs). The first four sections of this chapter are similar to the reference Wolf *et al.* (2012) except for several additional remarks and extensions. The sections beyond provide further results.

4.1. Introduction

The model system of a GB is, in a certain respect, a particularly inhomogeneous system that deals with very strong impurities that to our knowledge have not yet been described within the Gutzwiller approach. The energy scale of the system is set by the hopping parameter t_{bulk} in the homogeneous bulk regions far away from the GB. In cuprates we typically expect a Coulomb repulsion of $U \sim 20\, t_{\text{bulk}}$ and a spin exchange interaction $J_{ij} \sim t_{ij}$, where t_{ij} is the hopping matrix element for nearest and next-nearest neighbor sites. It has been shown that charge barriers at the GB lead to local impurity potentials[1] of the order of

[1] In this thesis, we start with the results of Graser *et al.* (2010). In this publication a molecular dynamics algorithm that allows to obtain the lattice structure at a GB is described. Using Slater-Koster tables, the algorithm calculates hopping amplitudes and spin-exchange couplings, and as a second outcome, the charge inhomogenities at single lattice sites resulting from the imperfection of the lattice.

In order to determine the absolute value of the impurity potentials which model the charge inhomogenities in the theoretically reconstructed GB, one has to make an assumption about the screening length in the CuO_2 planes. Experimentally, it is only known that the screening length l is smaller than the inter-atomic distance (the lattice spacing) $a \approx 4$Å. In order to take into account this uncertainty, we perform calculations for two values $l = 1.2$Å and $l = 2$Å.

Furthermore, it is instructive to see how the absolute value of the impurity potential is obtained by the lattice-defect induced charging q of each lattice site. This charging q is positive or zero for almost all lattice sites. To obtain the absolute value of the local impurity potential ε for one given site, one explicitily integrates over the screened Coulomb interaction energy (a Yukawa potential). The result is a quantity in units [energy $\times$ area]

$$\tilde{\varepsilon} = -\int_0^\infty d^2r \frac{eq}{4\pi\epsilon_0}\frac{e^{-r/l}}{r} = \frac{2\pi l}{4\pi\epsilon_0} qe = 2\pi\bar{q} l a_0 \frac{e^2}{4\pi\epsilon_0 a_0} = 2\pi\bar{q} l a_0 2\text{Ryd} \tag{4.1}$$

where $\epsilon_0 \sim 8.8510^{-12}$As/Vm, $\bar{q}$ the local charging in units of e, $a_0 \sim 0.53$Å and 1Ryd ~ 13.6eV. The impurity potential ε (in units eV) is then obtained by reintroducing the fact that q is the charging for one site, i.e. for a unit cell. We thus normalize using $\varepsilon = \tilde{\varepsilon}/a^2$ for the lattice constant $a \approx 4$Å such that

$$\varepsilon = \frac{l a_0}{a^2} 4\pi\bar{q}\text{Ryd} \tag{4.2}$$

With $a_0 \simeq a/8$ and assuming $l \approx 2\text{Å} \approx a/2$ one obtains

$$\varepsilon \approx \bar{q}\, 10.7\text{eV} \tag{4.3}$$

and for $l \approx 1.2$Å, $\varepsilon \approx \bar{q}\, 6.4$eV.

$\varepsilon_i \sim -20\,t_{\text{bulk}}$ (Graser *et al.* 2010) or more, therefore close to the GB, the estimate $\varepsilon_i \sim -U$ applies. Although in the bulk regions of a hole-doped system, the local charge densities n_i are below half filling, the positive charges in the vicinity of the GB can induce sites with n_i well above half filling, even in the presence of strong Coulomb repulsion. As an example, in Fig. 4.2(c), (d) and (e) local charge densities, impurity potentials and hopping amplitudes are shown as a function of the distance from a GB with misalignment angle $\alpha = 44°$.

Such systems with strongly positively charged regions cannot be described by the standard Gutzwiller approximation. We thus employ the implementation presented in this thesis in Sec. 2.3. In Sec. 4.2, the formalism is justified for the particular case of a GB model and in Sec. 4.3, technical details are given. In the sections starting from Sec. 4.4, we analyze our results for the critical current and other quantities, calculated with the new method.

4.2. Model of a grain-boundary

Crystals as they appear in nature are never the mathematically well defined Bravais lattices usually employed in solid state physics. A sample in the laboratory, for example, is never perfectly clean. Moreover the crystal growth does not proceed in a globally uniform way but starts at spatially separated grains. After the preparation of the sample is completed, to each of these grains an area of perfect crystal orientation can be assigned. In two neighboring grains, the perfect crystals will in general have a different orientation and the boundary region in between is called a grain boundary. For a two dimensional CuO_2-plane this situation is schematically depicted in Fig. 4.1.

For the description of the GB system we use the Gutzwiller projected t-J-model. Within

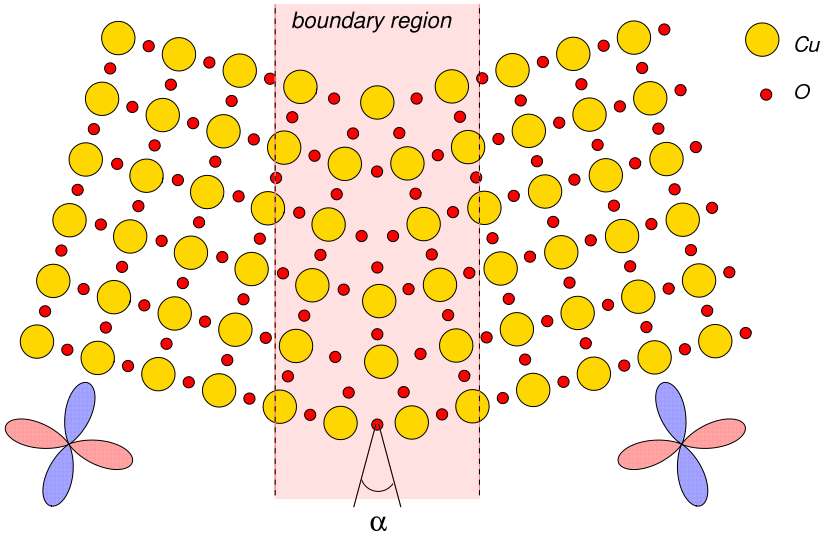

Figure 4.1.: Schematic view of a two dimensional grain boundary in a CuO_2 plane. Here the misalignement angle α is defined. This figure is taken with permission from Graser *et al.* (2010).

the Hartree-Fock decoupling scheme it is given by the hamiltonian[2]

$$\begin{aligned} H = &- \sum_{ijs} (g_{ij}^t t_{ij} + \chi_{ij}^*) c_{is}^\dagger c_{js} \\ &- \sum_{ij} (\Delta_{ij} c_{j\uparrow}^\dagger c_{i\downarrow}^\dagger + \text{h.c.}) - \sum_i \mu_i \hat{n}_i \end{aligned} \tag{4.4}$$

$$\text{with} \quad \Delta_{ij} \equiv (\tfrac{3}{4} g_{ij}^J + \tfrac{1}{4}) J_{ij} \widetilde{\Delta}_{ij}, \tag{4.5}$$

$$\chi_{ij} \equiv (\tfrac{3}{4} g_{ij}^J - \tfrac{1}{4}) J_{ij} \widetilde{\chi}_{ij}, \tag{4.6}$$

where $\widetilde{\Delta}_{ij} \equiv \frac{1}{2}(\langle c_{i\downarrow} c_{j\uparrow} \rangle + \langle c_{j\downarrow} c_{i\uparrow} \rangle)$, $\widetilde{\chi}_{ij} \equiv \frac{1}{2}(\langle c_{i\uparrow}^\dagger c_{j\uparrow} \rangle + \langle c_{i\downarrow}^\dagger c_{j\downarrow} \rangle)$, $\hat{n}_i = \sum_s c_{is}^\dagger c_{is}$, and $\mu_i \equiv \mu - \varepsilon_i$. The matrix for the tunneling amplitudes t_{ij} has non-zero entries for nearest and next-nearest neighbor hopping which have been calculated jointly with the matrices for the spin-coupling J_{ij} and the local potentials ε_i in a molecular dynamics algorithm by Graser *et al.* (2010) in order to incorporate the charge barriers and defects of the lattice at the GB.

The Gutzwiller factors in (4.4) are defined as derived in Sec. 2.3: $g_{ij}^t \equiv g_i^t g_j^t$ and $g_{ij}^J \equiv g_i^J g_j^J$, where

$$g_i^t \equiv \sqrt{\frac{2|1 - n_i|}{|1 - n_i| + 1}}, \tag{4.7a}$$

$$g_i^J \equiv \frac{2}{|1 - n_i| + 1}. \tag{4.7b}$$

For local densities $n_i \leq 1$ these expressions coincide with the commonly employed definitions of Wang *et al.* (2006). By introducing the absolute values in their definitions we obtain a renormalization that is symmetric with respect to half filling $n_i = 1$. This is equivalent to a local particle-hole transformation for sites where $n_i > 1$. Due to the particle-hole invariance of the Hubbard model[3] from which the t-J-model is derived, this treatment is obviously correct for a homogeneous system with $n_i \equiv n > 1$.

The rigorous derivation was presented in Sec. 2.3. To summarize it: The basis is the definition of a projection operator $\mathcal{P} \equiv \prod_i \mathcal{P}_i$ that locally projects either doubly occupied sites or holes out of a BCS type wave function $|\psi\rangle_0$ depending on the local density:

$$\mathcal{P}_i \equiv \begin{cases} y_i^{\hat{n}_i}(1 - D_i) & \text{if } n_i \leq 1 \\ y_i^{\hat{n}_i}(1 - E_i) & \text{if } n_i > 1 \end{cases} \tag{4.8}$$

Here, $D_i = \hat{n}_{i\uparrow}\hat{n}_{i\downarrow}$ and $E_i = (1 - \hat{n}_{i\uparrow})(1 - \hat{n}_{i\downarrow})$ denote the projection on doubly occupied and empty sites, respectively. Note that the selection of different projectors depending on the local density is a natural extension of the operator $y_i^{\hat{n}_i}$: this operator assigns different weights to contributions from empty and singly occupied sites and thus ensures a projected state $|\psi\rangle$ that can be transparently compared with the pre-projected state $|\psi_0\rangle$ due to its common set[4] of local densities (Wang *et al.* 2006). The comparison of expectation values

[2] For the derivation see the calculations preceding Eq. (3.49).

[3] We only refer to the particle-invariance of the interaction term, confer the argumentation made in Sec. 2.

[4] It should be noted here, that the comparison we employ is not between the pre-projected state $|\psi_0\rangle$ and $|\psi\rangle$ but based on the considerations given in Sec. 3.3. This gives an answer to the question one might ask,

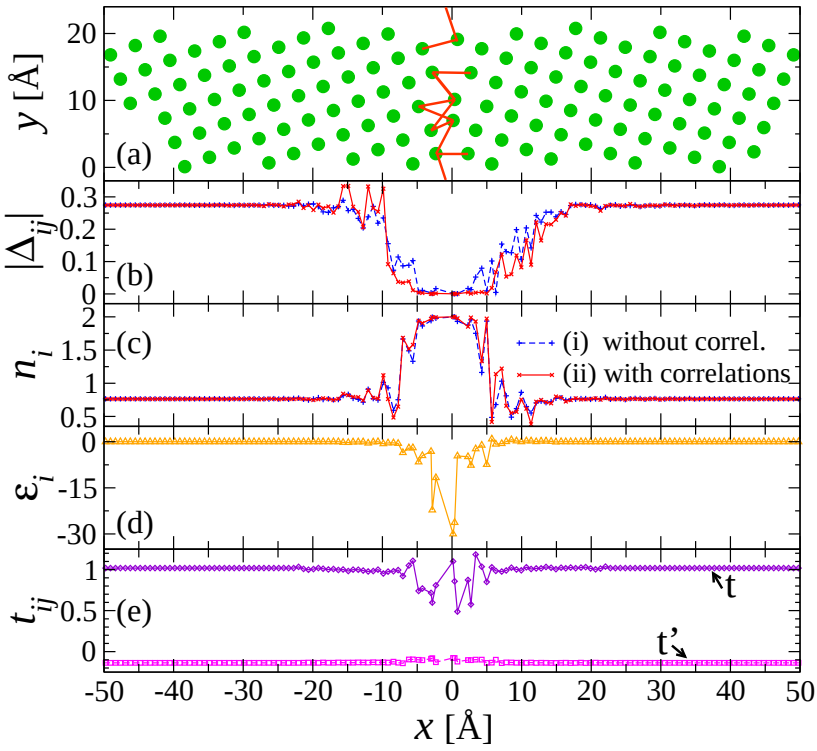

Figure 4.2.: The lattice structure for a (520) GB with misalignment angle $\alpha_{(520)} = 44°$ in the x,y-plane (a). Orange lines mark the bonds defining the "channels" through the GB that explicitly appear in the sum of Eq. 4.10. Results of a self-consistent calculation for the (520) GB at a bulk filling of $n = 0.8$ without (i) and with (ii) Gutzwiller factors include the d-wave projection of the order parameter Δ_{ij} (b) and the local density n_i (c). In addition the local impurity potentials ε_i (d) and the averages over all nearest neighbor (t) and next-nearest neighbor (t') hopping parameters of single sites i (e) are shown. Energies are measured in units of $t_{\text{bulk}} = 1$. The spin-interaction is calculated from the nearest-neighbor entries of t_{ij} for (i) as $J_{ij} = 2.38 t_{ij}$ and for (ii) as $J_{ij} = 0.9 t_{ij}$ so that $\Delta_{\text{bulk}} = 0.275 t_{\text{bulk}}$ has the same value for both calculations. The precise values of the impurity potentials ε_i are obtained from the charge fluctuations assuming a screening length $l = 2$Å.

evaluated with the wave functions $|\psi_0\rangle$ and $|\psi\rangle = \mathcal{P}|\psi_0\rangle$ presented in Sec. 2.3, yields the results of Eq. (4.7).

It remains to be justified that the implementation of a symmetric renormalization around half filling, or equivalently, projecting out empty and doubly occupied sites in the free wave function, is physically meaningful. The argumentation here is very similar to the original idea of Gutzwiller, to project doublons out of the wave function due to their energy cost. Our extension is obviously justified for bulk regions: In an environment where μ_i is large enough to yield $n_i > 1$, a local particle-hole transformation leads to the removal of empty

why in Fig. 4.2(c) the densities of the correlated (i) and the uncorrelated (ii) system are not *exactly* on top of each other. Going back further, we trace the reason to the fact that in Sec. 2.3 we approximately evaluated the constraint $\langle \hat{n}_i \rangle = \langle \hat{n}_i \rangle_0$ by using the Gutzwiller approximation, not exactly. Already at that stage, exact correspondence is lost. But obviously, the current through the GB should not depend on the details of the density distribution at the GB, only on its generic features. In Sec. 4.5 the generic feature is identified as the large fluctuations also visible in Fig. 4.2(c) for both calculations (i) and (ii), leading to a region close to half filling.

sites from the wave function. Also at the boundary of such a region the definition of Eq. (4.8) is consistent since on a site with $\mu_i \sim U$, the gain of potential energy cancels the cost of double occupancy, independent of the situation on neighboring sites. Thus the energy cost to create a holon at site i is of the size of U and consequently it is projected out.

Note that this procedure is possible in the Gutzwiller approximation only due to its fundamental assumption that inter-site correlations can be neglected. In the framework of the Gutzwiller approach it is a consistent improvement of the wave function modeling in the spirit of assigning different weights to different sites with the fugacity factor $y_i^{\hat{n}_i}$. It is a heuristic, very detailed and sophisticated method of minimizing the energy of a system described in a phenomenological mean-field picture. Below we will show that this picture is sufficiently realistic to accurately describe the physics of superconducting charge transport through a GB.

4.3. Technical Proceeding

The renormalized model hamiltonian of Eq. (4.4) is evaluated within the Bogoliubov–de Gennes (BdG) framework as discussed in Sec. 3.

To obtain a current carrying system we enforce constant phases with a difference $\phi = \pi/2$ on the order-parameters Δ_{ij} on either end of the sample, in the center of which the GB is situated.[5] The corresponding phase gradient induces finite currents[6] given by

$$j_{ij} = -2g_{ij}^t t_{ij} \sum_s \mathrm{Im}(\langle c_{is}^\dagger c_{js} \rangle). \tag{4.9}$$

The normalized total current through the GB is

$$j_\mathrm{c} = \frac{\sin(\alpha/2)}{M_y} \sum_{x_i<0, x_j>0} j_{ij}, \tag{4.10}$$

where x_i and x_j are the x-coordinates of sites on either side of the GB, α is the misalignment angle and M_y the second Miller index of the $(M_x M_y M_z)$ GB.[7] The factor $\sin(\alpha/2)/M_y$ normalizes the current to a unit length in y-direction.

To be able to compare with experimental results we employ the following relation (Graser *et al.* 2010) between the current $j_\mathrm{c}^\mathrm{abs}$ in absolute units A/cm^2 and the current in units $[t_\mathrm{bulk}] = \mathrm{eV}$

$$j_\mathrm{c}^\mathrm{abs} = \frac{\Delta^\mathrm{exp}}{\Delta^\mathrm{theo}} \frac{N_\mathrm{Cu}}{ac} \frac{e}{\hbar} j_\mathrm{c}\,, \tag{4.11}$$

[5] We performed calculations that imposed a Peierls phase on the boundaries of a GB model together with periodic boundary conditions, in contrast to the calculations leading to the results that are presented here. For these open boundary conditions were employed. The calculations using a Peierls phase yield very similar results but convergence takes much longer (5000 instead of 1000 BdG iterations for an ordinary (non-RMFT) calculation).

[6] The evaluation of Eq. (4.9) within the BdG framework is possible with the equations for $\widetilde{\chi}_{ij}$, cf. Eq. (3.34). The expression Eq. (4.9) can be easily derived using the continuity equation. One starts with a calculation of the time evolution of the density operator $\hat{n}_i$.

[7] The misalignment angle α can be given as $\alpha = 2\arctan(\frac{aM_x}{bM_y})$, where $a = 3.82$Å and $b = 3.89$Å are the lattice spacings in x- and z-direction, respectively. We note that the only sample with $M_y \neq 1$ we employ is the (520) GB with $M_y = 2$.

where $N_{\mathrm{Cu}} = 2$ is the number of CuO_2 planes per unit cell, α the misalignment angle and $a = 3.82$Å and $c = 11.7$Å the lattice spacing in x- and z-direction, respectively. The values $\Delta^{\mathrm{exp}} \sim 0.025$eV and $\Delta^{\mathrm{theo}} = 0.275$eV are valid for the bulk regions. In order to compensate the smaller magnitude of the experimental quantities we employ the factor $\Delta^{\mathrm{exp}}/\Delta^{\mathrm{theo}} \simeq 0.09$ where we make use of the fact that j_{c} scales approximately linearly w.r.t. Δ. Due to numerical reasons a calculation with the exact experimental quantities is not possible.[8]

Considering the system size, we note that calculations were performed in systems with several supercells in y-direction in order to obtain samples with $L \sim 1500$ lattice sites.[9] For this purpose one may imagine the pattern shown in Fig. 4.2(a) to be continued to the top in a periodical way.

We also tried to calculate results for angles smaller than $\alpha_{710} \approx 16°$, i.e. we checked samples for a (810) GB and a (910) GB. Calculations with those samples take even more computational time and lead to currents that are about one or two orders of magntiude too small. This observation should be related to the fact that it is questionable in which sense the limit $\alpha \to 0$ can be meaningfully described by the BdG formalism (for the ordinary as well as for the RMFT calculation). For large angles it can be argued that the physics is almost exclusively influenced by impurities breaking Cooper pairs at the GB. This is the main effect that determines the maximum strength of the current, i.e. of j_c. It is known that this type of behavior can be well described on the Hartree-Fock mean-field level. But the strength of the global current in the sample without impurities is a different question.

Finally we note that the codes employed to obtain the following results were checked by successfully reproducing the data of Garg *et al.* (2008) and Graser *et al.* (2010).

4.4. Angle dependence of the supercurrent

In Fig. 4.3(a) and (b) we show on a logarithmic scale the dependence of the zero-temperature supercurrent on the GB misalignment angle for a hole-doped system ($n = 0.8$). We compare two types of calculations with experimental data taken from Hilgenkamp and Mannhart (2002): (i) a standard evaluation of the GB-hamiltonian within the BdG framework (i.e. $g^t_{ij} = g^J_{ij} = 1$) and (ii) an evaluation with the local Gutzwiller factors as defined in Eq. (4.7). In order to provide a meaningful comparison of (i) and (ii) we employ the same hopping matrices t_{ij} and impurity potentials ε_i for all calculations, but globally scale J_{ij} to obtain identical values for the d-wave order parameter in the bulk: $\Delta_{\mathrm{bulk}} = 0.275\, t_{\mathrm{bulk}}$. Note that the d-wave projection of the order parameter Δ_{ij} shown in Fig. 4.2(a) does not differ qualitatively for the evaluation without (i) and with (ii) Gutzwiller factors, even at the GB.

As can be seen from Fig. 4.3 the supercurrent decays in both cases (i) and (ii) exponentially with the GB angle. We also find that the current in the correlated system (ii) is almost one order of magnitude smaller than in the system without correlations (i). As the screening length l in the CuO_2 planes is only approximately known we performed two calculations

[8] For a discussion of the scaling relation Eq. (4.11) see the appendix Sec. A.

[9] In Sec. A we show that this is sufficient to eliminate finite-size effects. In Sec. D we give an explanation of the super-cell method.

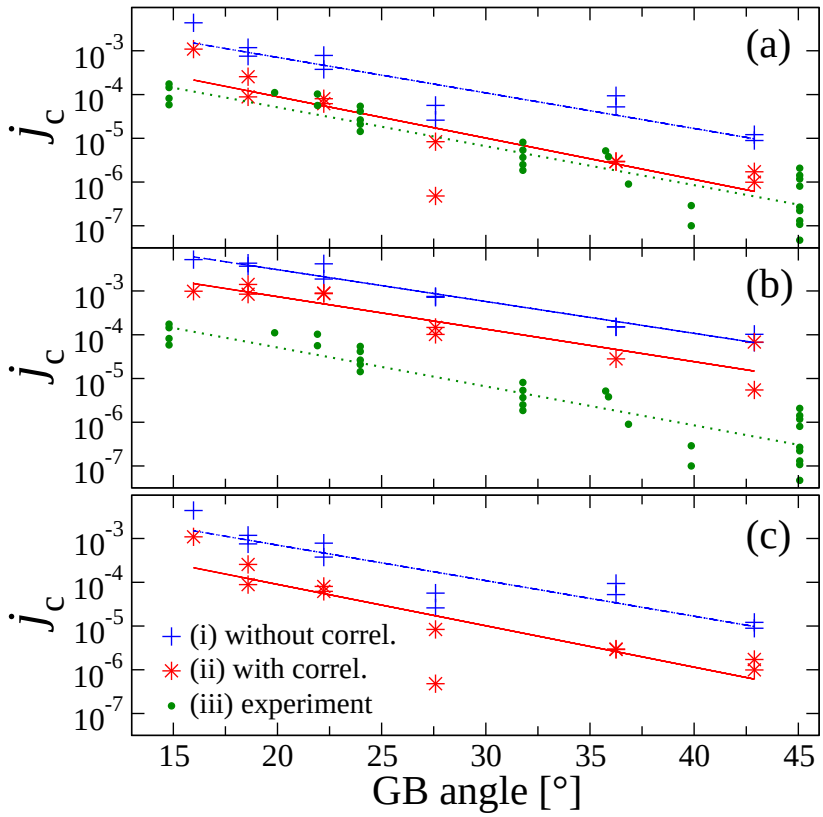

Figure 4.3.: Angular dependence of the critical current for GB samples with electron density $n = 0.8$ (a,b) and $n = 1.2$ (c). The impurity potentials have been calculated from the charge fluctuations assuming a screening length of $l = 2$Å (a) and $l = 1.2$Å (b,c). The current is given in units of t_{bulk}. Depicted are calculations using the BdG hamiltonian of Eq. (4.4) where for (i) all Gutzwiller factors are set to 1 and for (ii) all Gutzwiller factors are taken as defined in Eq. (4.7). The theoretical values in (a) and (b) are compared to the same experimental data (iii) taken from Hilgenkamp and Mannhart (2002). For the calculation without correlations (i) we set $J_{\text{bulk}} = 2.38$ whereas for (ii) we set $J_{\text{bulk}} = 0.9$ in order to obtain the same self-consistent d-wave gap $\Delta_{\text{bulk}} = 0.275$ in both cases. Lines serve as a guide to the eye and are calculated as linear fits to the logarithm of the data points.

assuming different values of l, with $l = 2$Å for Fig. 4.3(a) and $l = 1.2$Å for Fig. 4.3(b). For the choice of $l = 2$Å we obtain excellent agreement with the experimentally determined critical currents over a wide range of GB angles.

In Fig. 4.3(c) we show the angle dependence of the current for an electron-doped system with $n = 1.2$. Comparing panels (b) and (c) of Fig. 4.3, we find that the current is approximately symmetric with respect to hole- and electron-doping. Correlation effects are known to be strongest at half filling where a Mott insulator is obtained in the Gutzwiller approximation. The dominant reduction of the current due to correlations should therefore be caused by areas in the system where $n_i \sim 1$. These areas are equally present in the hole- and electron-doped system in the transition region to the bulk (see Sec. 4.5). In the hole-doped case such a region is already implied by the fact that, directly at the GB, the system is always well above half filling. In the electron-doped case it is caused by large density fluctuations.

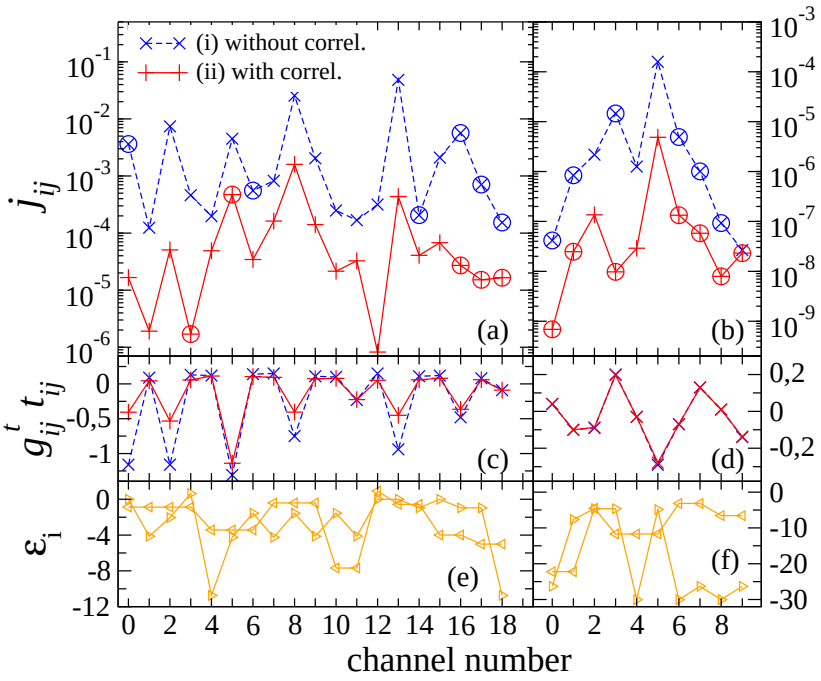

Figure 4.4.: Left column (a,c,e): (710) GB with angle $\alpha_{(710)} \sim 16°$ and right column (b,d,f): (520) GB with angle $\alpha_{(520)} \sim 44°$. In the first row (a,b) we show the value for the current through each channel on a logarithmic scale. Channels through the GB are depicted for the example of the (520) GB in Fig. 4.2(a) as orange lines. Negative currents are marked with a circle around the data point. In the second row (c, d) the effective tunneling parameter $g^t_{ij}t_{ij}$ is plotted where for the standard BdG calculation (i) $g^t_{ij} = 1$. In the third row (e, f) we show the local impurity potentials of the two sites connected by the corresponding channel.

These appear due to the charge fluctuations with the same magnitude in the electron- and the hole-doped case. For a hole-doped example, Fig. 4.2(c) shows values for the density with $0.5 \leq n_i \leq 2$. Obviously, these arguments imply that the correlation effects are controlled by the charge fluctuations. Furthermore, the fact that the narrow transition regions have a similar extension for all angles explains that the exponential behavior w.r.t. the GB angle appears in both calculations (i) and (ii): only the break-up of pairs by impurities (present in (i) and (ii)) causes the exponential behavior while the correlation induced reduction of the supercurrent is constant for all angles.

Fig. 4.4 allows further insight into the mechanism of charge transport at the GB. For large angles, charge transport through the GB is carried almost entirely by few channels. The GB region is governed by several bonds with black flowing currents (marked with circles in Fig. 4.4) leading to circular current patterns. For a qualitative picture of these patterns in two dimensions see Fig. 4.5. Our calculations show that the presence of strong correlations leads to an almost homogeneous reduction of the current by one order of magnitude in all channels. In addition one finds that the channels carrying the main current are exposed only to weak impurity potential fluctuations, as seen by comparing the first (a,b) and the third (e,f) row of Fig. 4.4. In the second row (c,d) of Fig. 4.4 we depict the effective, renormalized hopping parameters $g^t_{ij}t_{ij}$ for the two cases (i) and (ii). Since they differ only slightly, it is clear that

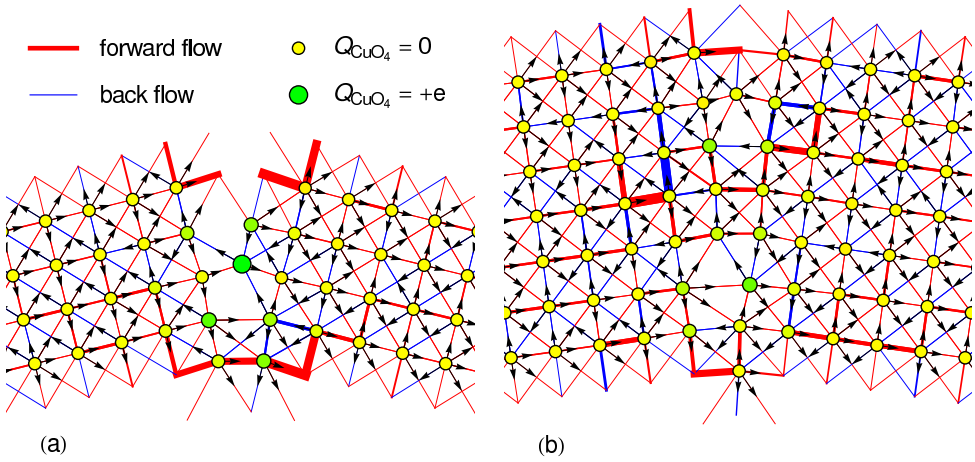

Figure 4.5.: The current pattern in the vicinity of a (410) GB (a) and a (710) GB (b) for a standard BdG calculation. The evaluation for a RMFT calculation yields the same pattern on a qualitative level. For a quantitative comparison see Fig. 4.4. The arrows in this figure display the direction of the current, the red lines denote current flowing forwar, the blue lines denote current flowing backward. The line thickness shows the current strength, while the point size and color of the Cu sites correspond to the on-site potential. This figure is taken with permission from Graser *et al.* (2010).

the current reduction is not due to a simple suppression of the hopping parameters by g^t_{ij} as they appear in Eq. (4.9). This observation confirms that correlations induce a significant suppression of j_c in the regions which are close to half filling, i.e. in regions at some distance to the GB, and not directly at the GB where the system is well above half filling.

4.5. The density distribution

In the preceding sections we explained how to theoretically determine the supercurrent through GBs in its dependence on the misalignment angle. This can also be found in the reference Wolf *et al.* (2012). The following sections are dedicated to supplementary remarks and answers to open questions that may still exist, not present in this reference.

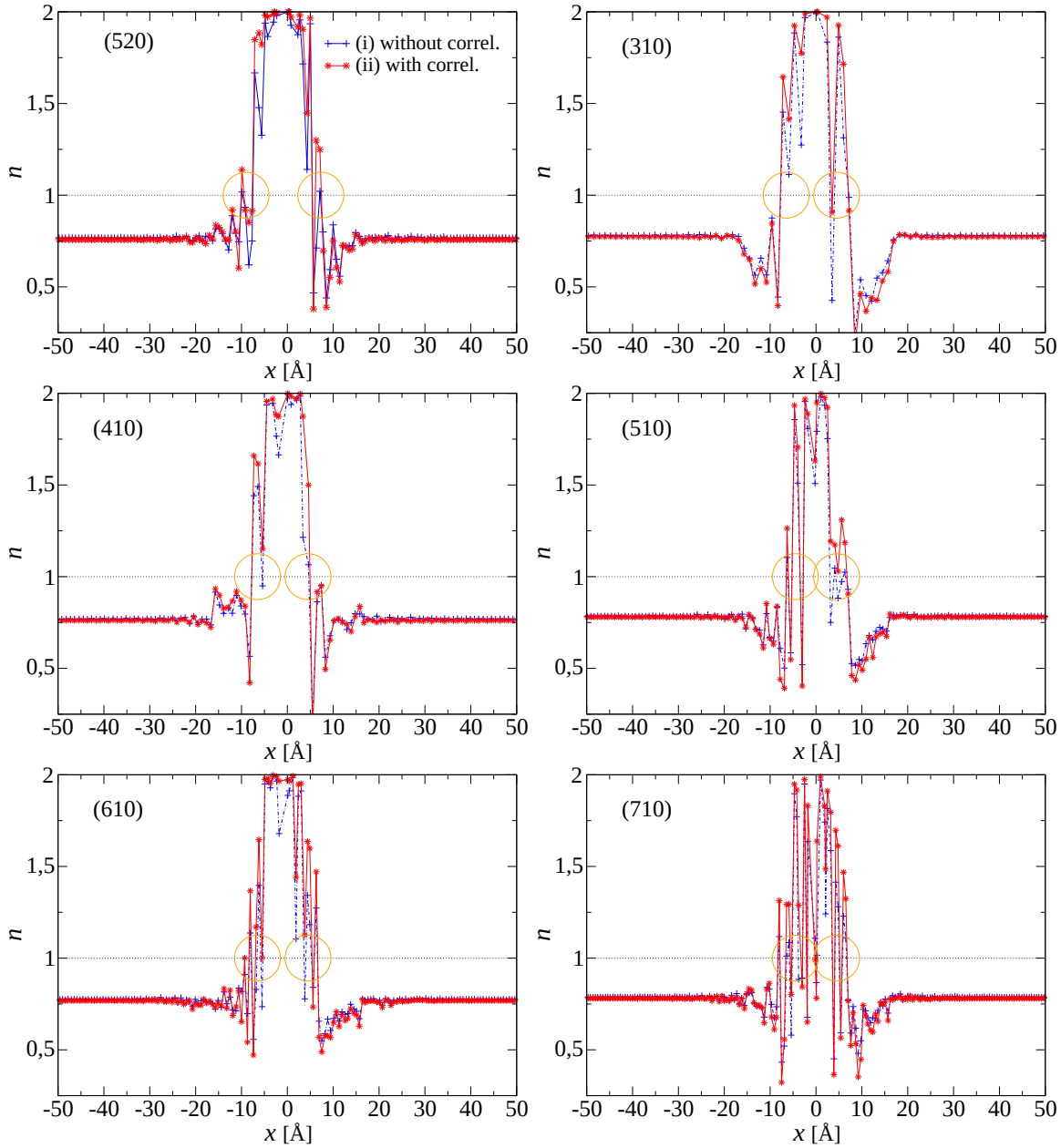

Figure 4.6.: Density profiles for different GBs. These are calculations for one of the two samples for each angle α, used in this thesis. The system is at $n = 0.8$ filling and calculations without (i) and with (ii) Gutzwiller factors are shown. All other parameters are used as in Fig. 4.3(a). Orange circles mark the transition region to the bulk which is close to half filling.

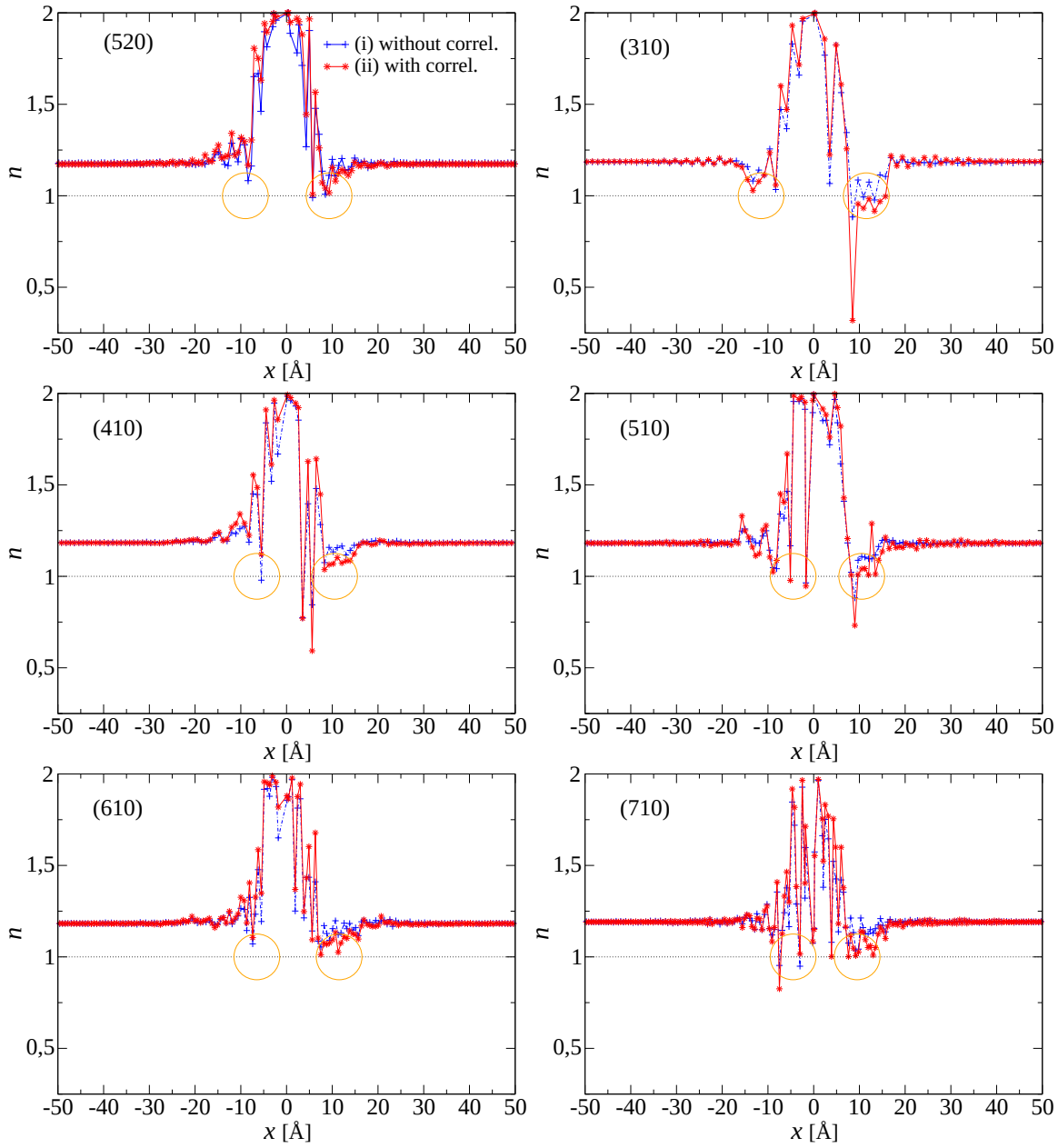

Figure 4.7.: Density profiles for different GBs for the same systems as in Fig. 4.7 but for electron-doping, $n = 1.2$.

In a RMFT calculation the density distribution is of fundamental importance as it directly influences the renormalization of the hopping and spin-interaction constants t_{ij} and J_{ij}. Clearly, the renormalization factors g_{ij}^t and g_{ij}^J are smooth functions of the local densities n_i, i.e. the density distribution.

In Sec. 4.4 it was argued, that density fluctuations in the transition regions from the GB to the bulk are responsible for the correlation driven reduction of j_c as they lead to areas where the system is close to half filling. For the renormlized system this implies small effective hopping constants $g_{ij}^t t_{ij}$. In Figs. 4.6 and 4.7 we depict the density distribution for hole- and electron-doped systems, respectively. In these figures, orange circles mark the transition

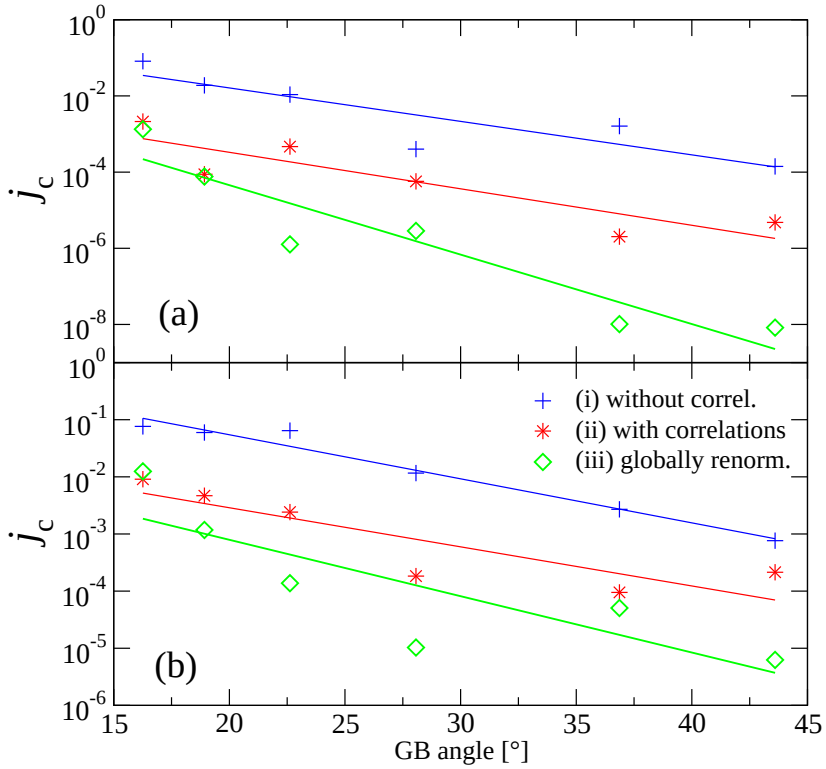

Figure 4.8.: Angle dependence of the critical current. The impurity potentials have been calculated from the charge fluctuations assuming a screening length of $l = 2$Å (a) and $l = 1.2$Å (b). The current is given in units of t_{bulk}. Depicted are calculations for three setups with different implementations of the Gutzwiller factors: (i) the plain BdG hamiltonian (4.4) with all Gutzwiller factors set to 1 (ii) Gutzwiller factors as defined in (4.7) and (iii) constant Gutzwiller factors calculated from the average density in the system. For the calculation without correlations (i) we set $J_{\text{bulk}} = 2.38$ whereas for (ii) and (iii) we set $J_{\text{bulk}} = 0.9$ in order to obtain the same self-consistent d-wave gap $\Delta_{\text{bulk}} = 0.275$ in both cases. Lines serve as a guide to the eye and are calculated as linear fits to the logarithm of the data points.

regions that are close to half filling. Although regions close to half filling were not expected for electron-doped systems, the figures show that these regions appear with approximately the same extension in the hole- and the electron-doped systems. Clearly, the strong impurity potentials induce fluctuations of the same magnitude independent of the doping.

4.6. Comparison with a globally renormalized system

In this section we consider the current in a globally renormalized system. For a global renormalization, constant Gutzwiller factors are employed. These are calculated with the average charge density n instead of the local densities n_i. The globally renormalized system is a third case (iii) interesting to compare[10] with the two cases discussed in the preceding section: (i) a standard evaluation of the GB-hamiltonian within the BdG framework, (ii) an evaluation with the local Gutzwiller factors as defined in Eq. (4.7).

[10]For example, Tsuchiura *et al.* (2001) considered such a comparison.

The globally renormalized system is controled by the same effective hopping amplitude $g_{\mathrm{bulk}} t_{\mathrm{bulk}}$ in the large bulk regions as the correlated system (ii). In Fig. 4.8 the resulting current is seen to be one order of magnitude smaller as the result for calculation (ii) and clearly shows a different exponent for the exponential decrease: In panel (a) of Fig. 4.8 this is obvious from an inspection of the fitting curve, while in panel (b) only the first four data points show a clearly different behavior. We suppose that due to the extreme current reduction in case (iii), that the last two data points in (b) are not reliable.

The figure shows that a mere reduction of the hopping amplitude by a global Gutzwiller factor $g_{ij}^t \equiv g^t < 1$ leads to a completely different result than taking the local Gutzwiller factors. Thus the effects described in the preceding sections cannot be obtained by a simple change of parameters, to which the global renormalization amounts. It furthermore confirms that the conductivity of the whole sample is governed by the effects in the vicinity of the GB region, otherwise the globally and the locally renormalized curves would coincide.

4.7. Different possibilities to compare uncorrelated and correlated systems

To supplement the discussion about the interpretation of RMFT calculations made in Sec. 3.3 with numerical data we discuss results for different schemes to obtain a comparable uncorrelated system. Although we already concluded in Sec. 3.3 that the scheme that we employed to obtain the results for j_{c} in Sec. 4.4 is the only meaningful one, it is worthwhile to consider other cases which are potentially relevant. This is important also to stress once again the subtlety and care that has to be taken when working with an RMFT calculation.

4.7.1. Effects on the critical current

In Sec. 3.3, several possibilities (henceforth denoted (I), (II) and (III)) were considered to obtain the physical d-wave order parameter Δ^{exp}

$$\Delta_{ij}^{\mathrm{exp}} \overset{\mathrm{(I)}}{=} \Delta_{ij} = (\tfrac{3}{4} g_{ij}^J + \tfrac{1}{4}) J_{ij} \widetilde{\Delta}_{ij} \tag{4.12a}$$

$$\Delta_{ij}^{\mathrm{exp}} \overset{\mathrm{(II)}}{=} g_{ij}^t \widetilde{\Delta}_{ij} \equiv \mathrm{OP}_{ij}^{\Delta} \tag{4.12b}$$

$$\Delta_{ij}^{\mathrm{exp}} \overset{\mathrm{(III)}}{=} \widetilde{\Delta}_{ij} \tag{4.12c}$$

where $\widetilde{\Delta}_{ij} \equiv \frac{1}{2}(\langle c_{i\downarrow} c_{j\uparrow} \rangle_0 + \langle c_{j\downarrow} c_{i\uparrow} \rangle_0)$.

We argued that possibility (I) is the only meaningful one if the aim is to make a transparent comparison between the current carrying properties of a correlated and an uncorrelated system. This applies because only if (I) is used, i.e. one fixes $\Delta_{\mathrm{bulk}}^{\mathrm{uncorrelated}} = \Delta_{\mathrm{bulk}}^{\mathrm{correlated}}$, one compares two systems with the same gap in the spectrum — we argued further that in particular this energetic quantity is a reliable outcome of the Gutzwiller calculation in contrast to a veritable order parameter $\mathrm{OP}_{ij}^{\Delta}$, that aims to describe the fraction of condensed electrons (we do not claim that the condensate fraction in our Gutzwiller calculation is given

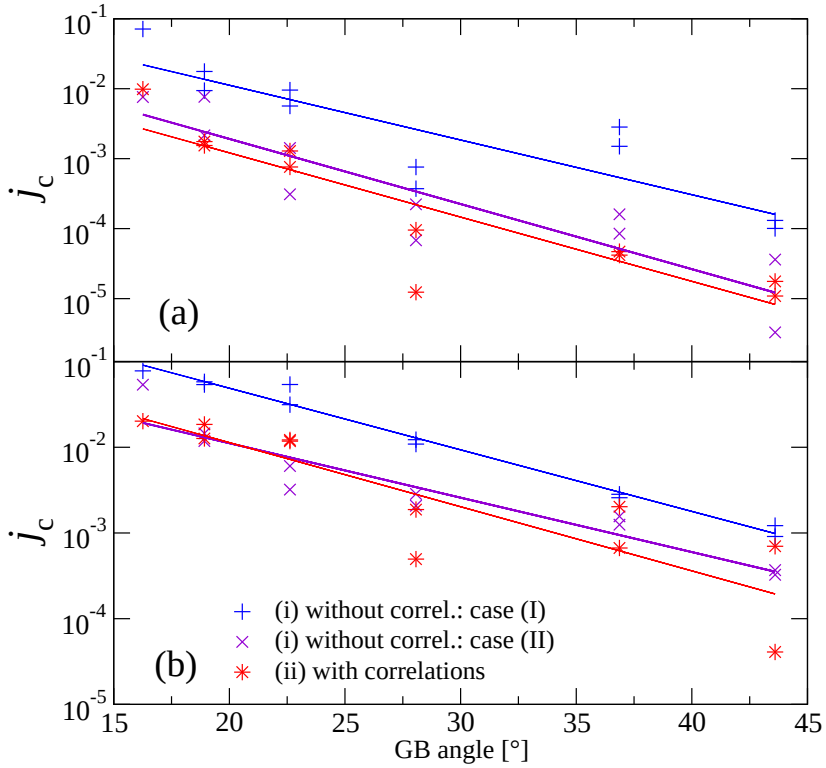

Figure 4.9.: Angular dependence of the critical current. The impurity potentials have been calculated from the charge fluctuations assuming a screening length of $l = 2$Å (a) and $l = 1.2$Å (b). The current is given in units of t_{bulk}. Depicted are calculations for two setups with different implementations of the Gutzwiller factors: (i) the plain BdG hamiltonian (4.4) with all Gutzwiller factors set to 1 (ii) Gutzwiller factors as defined in (4.7). For the calculations without correlations (i) we set $J_{\text{bulk}} = 2.4$ in case I and $J_{\text{bulk}} = 1$ in case II. For (ii) we set $J^{\text{gutz}}_{\text{bulk}} = 0.9$.

by Δ_{ij}). Finally it can be shown in a simple numerical check, that j_c scales approximately linearly with the energy gap Δ_{ij} and not with OP^{Δ}_{ij} or $\widetilde{\Delta}_{ij}$. This check was done in Sec. A.

If nevertheless a comparison is based on fixing the gap in the corresponding uncorrelated system in accordance with possibility (II), then a strongly reduced current in the uncorrelated system is the consequence.[11] This is clear as then $\Delta^{\text{uncorrelated}}_{\text{bulk}} < \Delta^{\text{correlated}}_{\text{bulk}}$ which stills controls the magnitude of j_c. In Fig. 4.9 the cases (I) and (II) are plotted jointly with the corresponding Gutzwiller calculation, used to fix the respective values of the order parameter for the standard BdG calculations. It can be seen that if (II) is employed, the ordinary BdG calculation yields almost the same result as the RMFT calculation (ii) — from this calculation one would have to conclude, that correlations do not have any reducing effect on the current. As this is a completely unphysical result it confirms that (II) is not a meaningul choice to set up the determination of j_c.

Finally, in accordance with possibility (III), one can fix the parameter $\widetilde{\Delta}^{\text{uncorrelated}}_{\text{bulk}} =$

[11] In this case one fixes the order parameter of the uncorrelated system $g^t_{ij}\widetilde{\Delta}^{\text{correlated}}_{ij} = \widetilde{\Delta}^{\text{uncorrelated}}_{ij}$ to the much smaller value (by reduction of $g^t_{ij} < 1$) of the correlated system. We remind, that in the uncorrelated case $g^t_{ij} \equiv 1$.

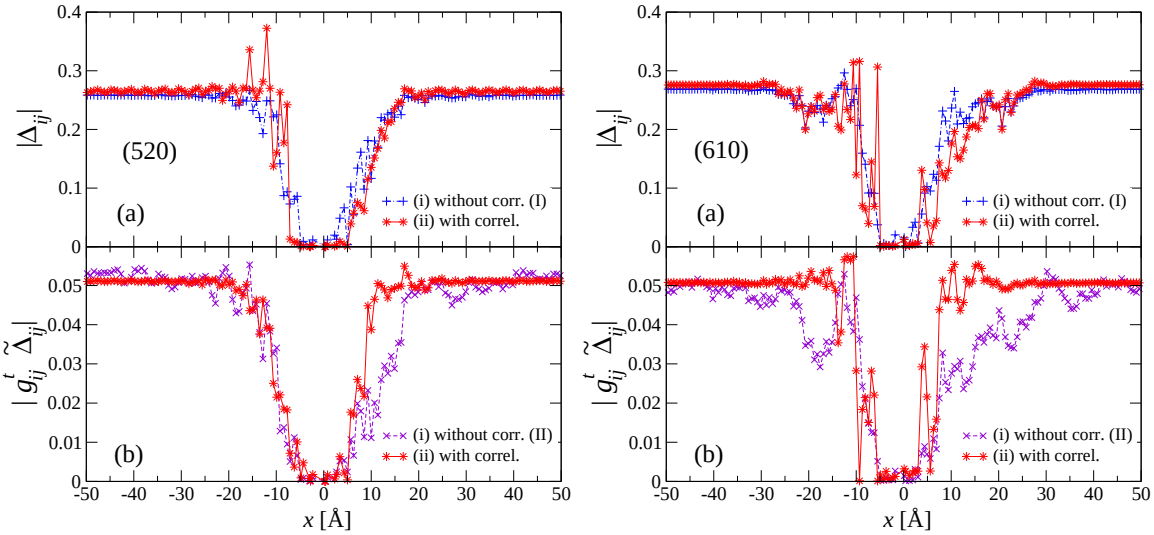

Figure 4.10.: For a (520) GB and a (610) GB, the spatial variation of $|\Delta_{ij}|$ in panels (a) and of $|g_{ij}^t \widetilde{\Delta}_{ij}|$ in panels (b) is depicted. For these calculations the same parameters as in Fig. 4.2 were used. In the case of (i), in panels (a) and (b) the same calculation was used. In the case of (ii), in panels (a) and (b) the results of two different calculations fixing the value of Δ_{ij} (I) or of $\mathrm{OP}_{ij}^{\Delta} = g_{ij}^t \widetilde{\Delta}_{ij}$ (II) are depicted. For the calculation without correlations (i) we set $J_{\mathrm{bulk}} = 2.38$ in case (I) whereas for case (II) we set $J_{\mathrm{bulk}} = 1$. For (ii) we set $J_{\mathrm{bulk}} = 0.9$ throughout.

$\widetilde{\Delta}_{\mathrm{bulk}}^{\mathrm{correlated}}$. The resulting current of the standard BdG calculation is about two orders of magnitude larger than the Gutzwiller calculation.

4.7.2. Effects on the spatial variation of the gap

Although, possibility (II) fails to set up a comparison for the critical current j_c the arguments to derive it are nevertheless sufficiently good to consider it an interesting quantity that might be the right way to approach the veritable condensate fraction in a truely correlated system.

In Fig. 4.10(a) and (b) we plot the spatial variation for the cases (I) and (II), respectively. In both cases the RMFT and the standard BdG calculation yield a similar result, except for one generic feature that can be identified. When employing (I) one does not perceive any different length scale for the healing of the gap when comparing (i) and (ii). In contrast, comparison (II) in panels (b) of Fig. 4.10 shows a shorter healing length for the order parameter $\mathrm{OP}_{ij}^{\Delta}$.

With these observations we cannot confirm the results of Garg *et al.* (2008) concerning the healing length of $|\Delta_{ij}|$. In this reference, a comparison of type (I) was made for the behavior of $|\Delta_{ij}|$ in the vicinity of single impurities. They claimed that correlations lead to a shorter healing length of the gap amplitude which is clearly not present in panels (a) of Fig. 4.10. That we find a shorter healing length for comparison type (II) can rather be traced back to the simple fact, that the spin-coupling is reduced by more than a factor of one half in the calculation (II) as compared to (I).[12] This reduced spin-coupling hampers

[12] And with that the gap $\Delta_{ij} \approx 0.14$ for case (II) instead of $\Delta_{ij} \approx 0.275$ for case (I).

electron condensation and therefore the healing of the gap leading to a longer healing length in the uncorrelated case (II). For the comparison to a single impurity, confer Sec. B.

5. Conclusion

In Sec. 2 the derivation of an extended Gutzwiller approximation was presented as a straightforward extension of the ansatz introduced by Wang *et al.* (2006) to treat inhomogeneous systems. The derivation relies on the identification of an extended projection operator that poses the new, symmetrized form of the Gutzwiller factors on mathematically save grounds. Apart from the characterization of the supercurrent through grain boundaries, we expect that our extension of the Gutzwiller projection approach is also instrumental for other strongly inhomogeneous systems with intrinsic impurities or artificial structures (heterostructures).

In Sec. 3 the subtleties of standard BdG and RMFT calculations were discussed in detail. In particular, the open questions regarding RMFT calculations do not seem to be much addressed in the literature. Furthermore, we made several statements concerning the practical solution of renormalized BdG equations, identifying useful hints in order to enhance the unstable numerical solution. Also regarding this topic, the standard literature lacks examples. A more detailed discussion would help to make a priori statements about the existence and feasibility of numerical solutions.

In Sec. 4, using the new Gutzwiller setup and the theoretically reconstructed GB samples of Graser *et al.* (2010), we found a reduction of the critical current of about one order of magnitude as compared to the current determined within an uncorrelated model calculation. These findings allowed to reproduce experimental results for the critical current over a large range of GB angles. The reduction of the current was shown to be due to the intertwining effects of large charge fluctuations and strong correlations. It can thus be understood that experimental doping of the GB in order to moderate these fluctuations significantly improves the current carrying properties which has already been observed for Ca-doped interfaces (Hammerl *et al.* 2000; 2002).

We finally note that the effect of pinned vortices in the GB region or the influence of macroscopic facetting extend over length scales larger than the ones considered in the present model and should be subject to further study.

A. Error analysis

In this chapter the assumptions made in Sec. 4 are justified with numerical results.

A.1. Scaling of the critical current with respect to the gap

In order to be able to make comparisons with experimental data, we employed the relation Eq. (4.11) where it was assumed that the current scales approximately linearly with respect to the gap $|\Delta_{\text{bulk}}|$.

In order to confirm this assumption we first make a change of the energy scale in our calculations. In an experiment one would usually expect a value of $t^{\text{exp}} \approx 0.4\text{eV}$ in the bulk regions while we calculated with $t^{\text{theo}} = 1\text{eV}$ in Sec. 4. This was done for numerical reasons and the convention in most theoretical work to set $t = 1$.

Changing the energy scale in our calculations by replacing $t^{\text{theo}} = 1\text{eV}$ with $t^{\text{exp}} = 0.4\text{eV}$ in order to calculate with the experimental value also implies scaling all other quantities with the same factor 0.4. If finite size effects do not play a role, i.e. the spectrum obtained by the numerical diagonalization procedure is sufficiently narrow, the change of the energy scale in the hamiltonian is exactly reproduced in all observables that are given in units of t_{bulk}. See Fig. A.1 for a standard BdG evalution.

We furthermore evaluated the angle dependence of the supercurrent for a calculation that uses the experimental energy scale $t_{\text{bulk}} = 0.4$. The main result of this thesis, Fig. 4.3 in

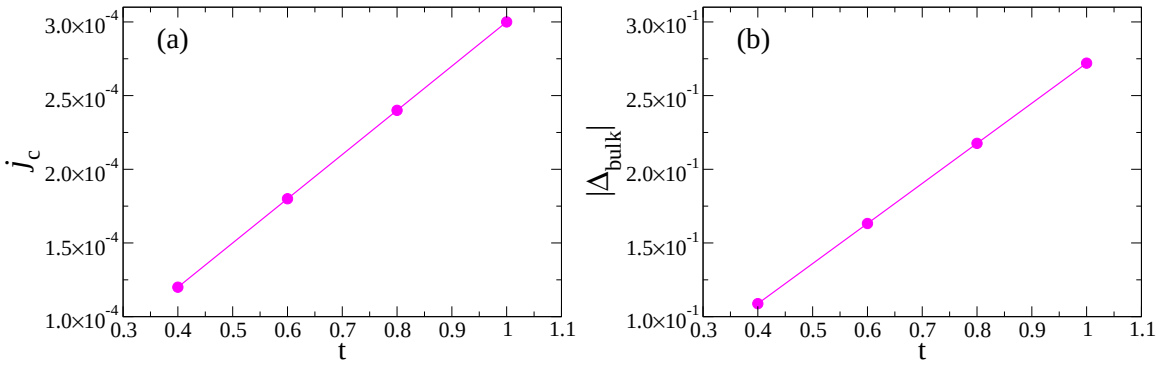

Figure A.1.: Changing the whole energy scale means scaling t_{bulk} together with J_{bulk} and the impurity potentials ε_i. Then the current (a) scales *exactly* linearly as it is given in units of t_{bulk}. To confirm this, the figure shows the standard BdG evaluation for a (310) GB with $N_s = 2$ supercells. The abcsissa therefore depicts the changing of all energy quantities, not only t_{bulk}. Also the absolute value of the gap (b) $\Delta_{\text{bulk}} = J_{\text{bulk}}\widetilde{\Delta}_{\text{bulk}}$ scales exactly linearly while $\widetilde{\Delta}_{\text{bulk}} = 0.11$ remains exactly constant, being a quantity without dimension.

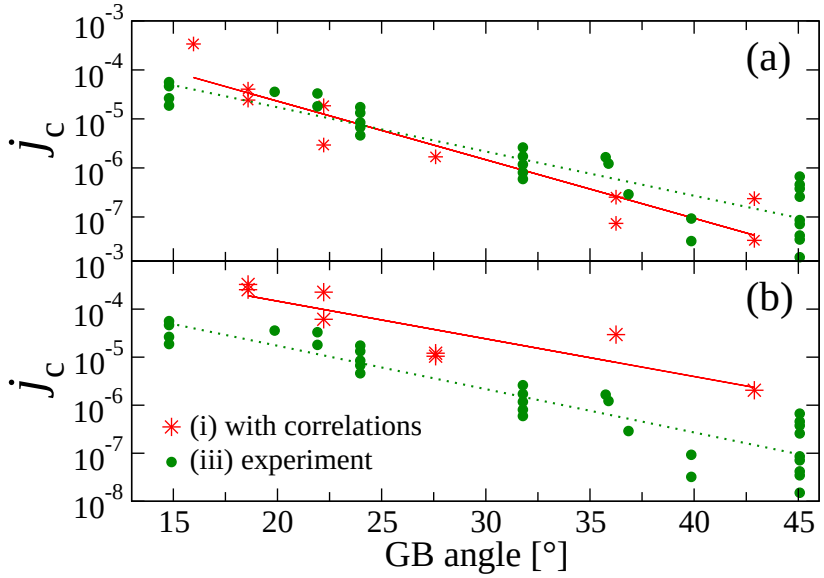

Figure A.2.: Angle dependence of the critical current for GB samples with electron density $n = 0.8$. The impurity potentials have been calculated from the charge fluctuations assuming a screening length of $l \sim 2.2$Å (a) and $l \sim 1.45$Å (b). The current is given in units of $t_{\text{bulk}} = 0.4$ in contrast to all results in Sec. 4 where the value $t_{\text{bulk}} = 1$ was employed. Depicted is a RMFT calculation using the BdG hamiltonian of Eq. (4.4) and the Gutzwiller factors as defined in Eq. (4.7). The theoretical values in (a) and (b) are compared to the same experimental data (iii) taken from Hilgenkamp and Mannhart (2002). This experimental data is obtained via Eq. (4.11) where the $\Delta_{\text{bulk}} = 0.11$ is used for the theoretical value Δ^{theo}. We set $J_{\text{bulk}} = 0.8t_{\text{bulk}}$ in order to obtain $\Delta_{\text{bulk}} = 0.11$. Lines serve as a guide to the eye and are calculated as linear fits to the logarithm of the data points. Missing data points are due to non-convergent solutions.

Sec. 4.4, can be exactly reproduced with such a calculation, except for missing data points due to a numerically more unstable behavior. In order to provide an example calculated with the different energy scale and a different outcome, in Fig. A.2(a) and (b) we present results for changed assumptions of the screening length $l \sim 2.2$Å and $l \sim 1.45$Å, respectively. The results can be seen to be very similar to those depicted in Fig. 4.3 except for a constant shift that is caused by the changed energy scale. Due to the stronger impurity potentials, for $l \sim 2.2$Å the theoretical curve is slightly below the experimental data while for $l \sim 2$Å in Fig. 4.3 it was slightly above. This suggests that the experimental value for the screening length is close to these values.

For Fig. A.2 we had to use Eq. (4.11) for the value $\Delta_{\text{bulk}} = 0.11 = \Delta^{\text{theo}}$, which is the lowest possible value that yields a convergent solution of the RMFT calculation. Although we are able to make a calculation with the experimental value for the hopping, it is not possible to obtain a self-consistent solution with $\Delta^{\text{exp}} = 0.025$. In Eq. (4.11) we made the assumption, that the separation of the experimental and the theoretical value of the gap can be approximately accounted for by linearly scaling j_c. In the case of $t_{\text{bulk}} = 0.4$ with a factor $\frac{\Delta^{\text{exp}}}{\Delta^{\text{theo}}} \approx 0.25$ and in the case of $t_{\text{bulk}} = 1$ used in Sec. 4 by a factor of $\frac{\Delta^{\text{exp}}}{\Delta^{\text{theo}}} \approx 0.09$. Obviously, the effective error is only the one related to the case with $\frac{\Delta^{\text{exp}}}{\Delta^{\text{theo}}} \approx 0.25$ as the

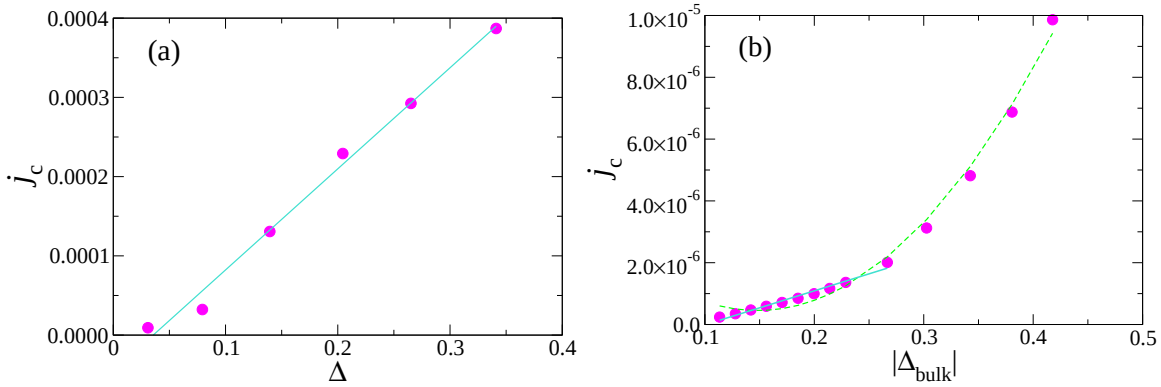

Figure A.3.: Scaling of the current w.r.t. Δ for constant t_{ij} and ε_i showing a calculation without (a) and (b) with Gutzwiller factors. This is for a (520) GB with $N_s = 3$ supercells at $n = 0.8$. All other parameters are chosen as in Fig. 4.3, in particular the energy scale $t_{\text{bulk}} = 1$. Turquoise fitting curves are linear fits, green fitting curves are quadratic fits.

remaining reduction of the gap is due to an exact change of the energy scale which does not add to the error.

In Fig. A.3(a) an almost exact linear dependence of j_c on Δ_{ij} can be observed for the standard BdG evaluation. For the RMFT calculation in Fig. A.3(b) a quadratic dependence is observed. In the region we are interested in, i.e. the interval in between $\Delta = 0.025$ and $\Delta = 0.11$, we can not calculate any data points due to numerical limitations. On the one hand, we could speculate, that the most left data points in Fig. A.3(b) already assume an almost linear behavior which then justifies our proceeding. On the other hand, if one extrapolates the quadratic fit, in the interval in between $\Delta = 0.025$ and $\Delta = 0.11$, a linear approximation of the parabola will produce an error, i.e. a wrong estimation of the corresponding experimental value, of $(0.11 - 0.025)^2 \simeq 0.007$, i.e. of about 24%. Given the fact, that we do not claim to obtain precise quantitative agreement, this error is completely acceptable.

A.2. Phase of the OP

To manually fix the phase of the d-wave gap on either side of the GB yields a physical phase gradient, as can be seen in Fig. A.4. This does not produce any error, although the implementation via Peierls phases, mentioned in Sec. 4.3 is a more elegant alternative.

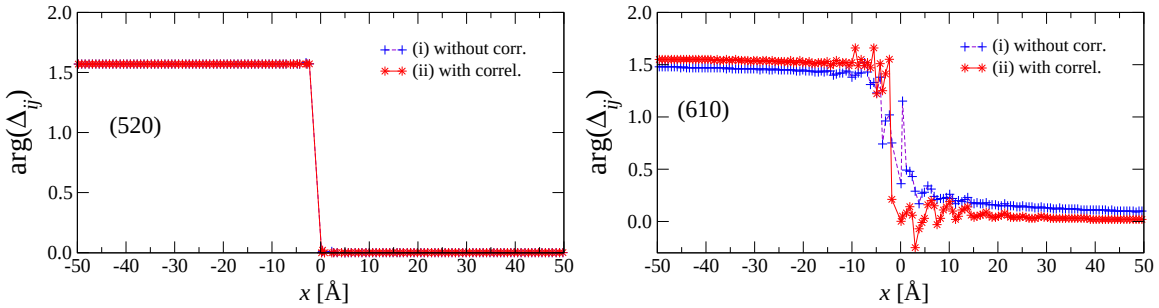

Figure A.4.: The phase of the order parameter for a (520) and a (610) GB. All parameters are chosen as in Fig. 4.2.

A.3. Influence of the system size

Finally we briefly show Fig. A.5 in order to demonstrate that the number of $N_s = 3$ supercells for a (520) sample is sufficient to eliminate finite size effects. For all samples the number of super cells is chosen in order to obtain $L \approx 1500$ lattice sites leading to similar pictures. Finite size effects enter an RMFT calculation in the same way as a standard BdG calculation. Thus, in Fig. A.5, we only present results for a standard BdG calculation.

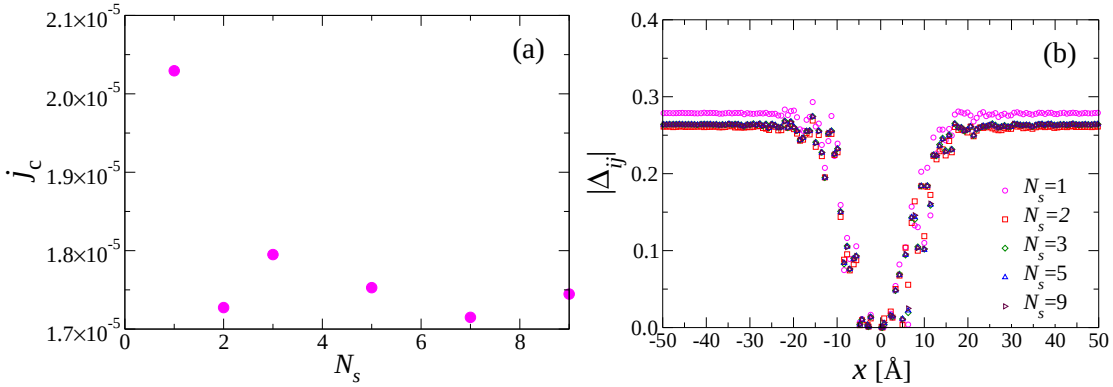

Figure A.5.: The dependence of the supercurrent (a) and the absolute value of the gap (b) on the number of supercells in the calculation. This is for a standard BdG calculation.

B. Comparison to a single impurity

In this chapter, the result of a Gutzwiller evaluation is compared to a standard BdG calculation for a single impurity.

In Fig. B.1 the d-wave gap Δ_{ij} is plotted for a $L = 11 \times 11$ system at $n = 0.8$ filling. The panels on the left depict the result of a standard BdG calculation while on the right the result of a RMFT calculation is shown. Clearly, a comparison of the behavior of Δ_{ij} reveals a shorter "healing length" in the RMFT case as compared to the uncorrelated simulation. This was first stated by Garg *et al.* (2008).

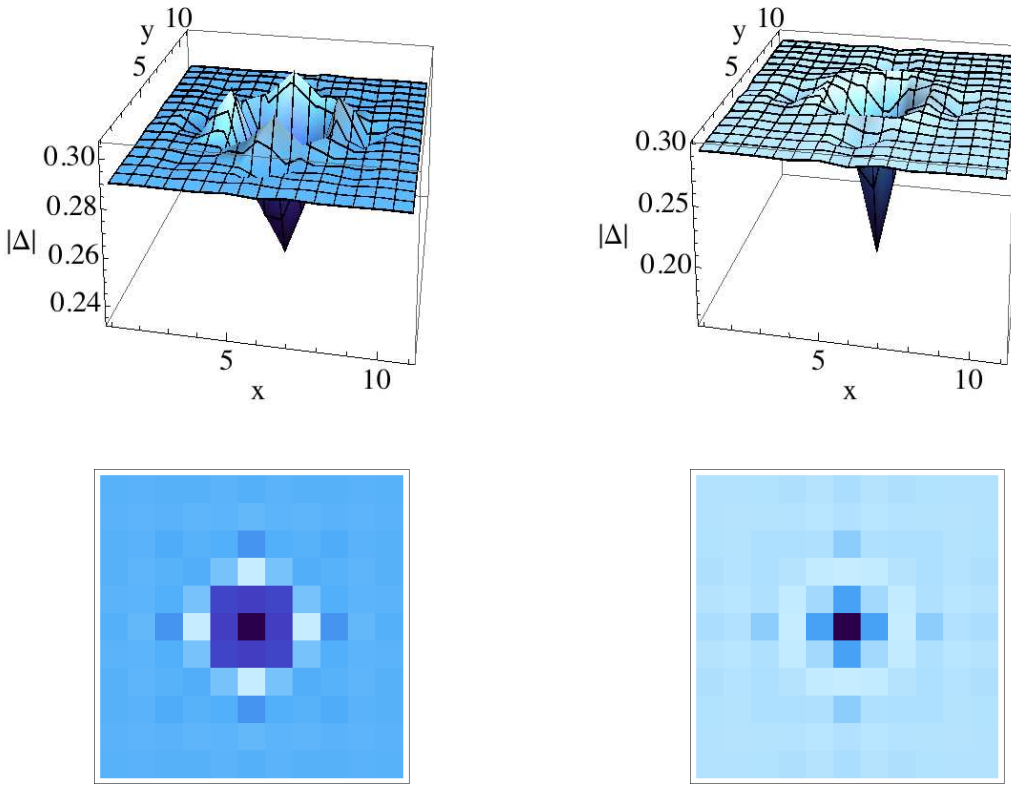

Figure B.1.: The d-wave gap Δ_{ij} for a $L = 11 \times 11$ system at $n = 0.8$ filling. The panels on the left show a calculation of type (i), i.e. a standard BdG evaluation, while the panels on the right show results of an RMFT calculation (ii). The hamiltonian for this system is given by Eq. (4.4), with $\varepsilon_i = 1\delta_{i\iota}$ and ι the index of a single impurity site in the center of the array. All other parameters are as follows: $t = 1$ sets the energy scale, $J = 1$ and $t' = 0.3$. This calculation was done for $N_s = 10 \times 10$ supercells. For the standard BdG calculation (i) a global renormalization as in Sec. 4.6 was employed.

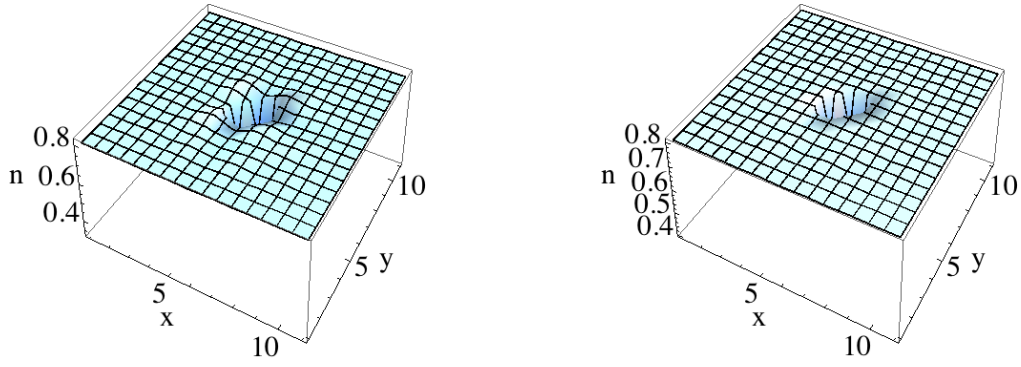

Figure B.2.: The density distribution n_i for the calculation depicted in Fig. B.1. Left panel: A standard BdG evaluation. Right panel: A RMFT evaluation. As can be seen from the figure, both calculations yield almost the same density distribution. can be

In Fig. B.2 we plot the density distribution for the cases of Fig. B.1. Here, in accordance with the discussions in Sec. 3.3 and Sec. 4.5, we do not observe any qualitative difference.

We already stated that in the GB system, we do not observe the shorter healing length for the gap Δ_{ij}. We also note that we could not reproduce the phenomenon for negative impurity potentials (in Fig. B.1 a positive potential on a single site with value $\varepsilon_i = t = 1$ was used). All calculations found in the literature considering the healing length have up to now only been performed for positive impurity potentials at which the electron density is reduced. A single negative impurity potential will increase the electron density and yields a completely different picture.

In order to analyze the common features of the single impurity and the GB system, we constructed a GB for which we gradually added more and more generic features: few impurity potentials, random lattice defects, ordered misalignment and strong impurity potentials. We clearly obtained a qualitatively different result when studying many strong impurity potentials, as compared to the artificial case of a single site. We conclude that the study of single impurities cannot be simply generalized to a strong impurity concentration in extended areas, such as GBs, and stress that the result of Garg *et al.* (2008) is to be investigated for more general situations. This was not achieved in the thesis and remains to be investigated in future research — the current chapter is only meant to draw attention to it.

C. An effective one-particle hamiltonian for the t-J-model

First a general mean-field decomposition is motivated and introduced. Then using the variational principle, an effective one-particle hamiltonian for the t-J-model is derived.

C.1. General Hartree-Fock mean-field decomposition

The notion "mean-field" decomposition refers to a certain approximative evaluation of expectation values of operators that include more than two c or $c^\dagger$ operators (two-particle observables) — the interaction terms. For the t-J-model, the interaction term is the spin interaction $\langle \boldsymbol{S}_i \cdot \boldsymbol{S}_j - \frac{1}{4} n_i n_j \rangle$.

Let us proceed in the following way: rewrite two c or $c^\dagger$ operators[1]

$$c_1 c_2 = \langle c_1 c_2 \rangle + (c_1 c_2 - \langle c_1 c_2 \rangle) \tag{C.1}$$

where $\langle c_1 c_2 \rangle$ is called a mean-field — this is just a complex number and can later serve as a variational parameter. Then one makes the following assumption

$$\begin{aligned} \langle c_1 c_2 c_3 c_4 \rangle &= \big\langle \big(\langle c_1 c_2 \rangle + (c_1 c_2 - \langle c_1 c_2 \rangle) \big) \big((\langle c_3 c_4 \rangle + (c_3 c_4 - \langle c_3 c_4 \rangle) \big) \big\rangle \\ &= \big\langle - \langle c_1 c_2 \rangle \langle c_3 c_4 \rangle + \langle c_1 c_2 \rangle c_3 c_4 + c_1 c_2 \langle c_3 c_4 \rangle + \overbrace{(c_1 c_2 - \langle c_3 c_4 \rangle)(c_3 c_4 - \langle c_3 c_4 \rangle)}^{= \text{small}} \big\rangle \qquad \text{(C.2)} \\ &\sim \langle c_1 c_2 \rangle \langle c_3 c_4 \rangle \qquad \text{(C.3)} \end{aligned}$$

The product of the deviations of the operators pairs from their mean values is supposed to make only a small contribution to the expectation value. Clearly this approximation can only be justified by calculating the actual contribution of the fluctuation term. This is in general not possible such that the approximation is an uncontrolled one. It is nevertheless employed here. We do this in a heuristic spirit knowing that Hartree-Fock mean-field theory is very successful in some cases[2] and for certain observables.

[1] From here c_1, c_2, ... can be either creation or annihilation operators.

[2] Already note here that successful theories like BCS make this assumption. This implies that the corresponding mean-field state $|\text{BCS}\rangle = \prod_{\boldsymbol{k}} (u_{\boldsymbol{k}} + v_{\boldsymbol{k}} c^\dagger_{\boldsymbol{k}\uparrow} c^\dagger_{-\boldsymbol{k}\downarrow}) |\text{vac}\rangle$ a priori neglects the fluctuation term. As $\langle c^\dagger_{\boldsymbol{k}\uparrow} c^\dagger_{-\boldsymbol{k}\downarrow} c_{-\boldsymbol{k}'\uparrow} c_{\boldsymbol{k}'\downarrow} \rangle_{\text{BCS}} = \langle c^\dagger_{\boldsymbol{k}\uparrow} c^\dagger_{-\boldsymbol{k}\downarrow} \rangle_{\text{BCS}} \langle c_{-\boldsymbol{k}'\uparrow} c_{\boldsymbol{k}'\downarrow} \rangle_{\text{BCS}}$ is an exact identity the fluctuation term is exactly zero in the BCS state.

The decomposition of Eq. (C.3) can be done in all three ways of pairing the four operators:

$$\langle c_1 c_2 c_3 c_4\rangle \sim \frac{1}{3}\big(\langle c_1 c_2\rangle\langle c_3 c_4\rangle - \langle c_1 c_3\rangle\langle c_2 c_4\rangle + \langle c_1 c_4\rangle\langle c_2 c_3\rangle\big) \tag{C.4}$$

where for the second term anti-commutation was used to employ the notation of Eq. (C.1).

Depending on how many possible pairings of operators one includes when evaluating expectation values of interaction terms, one obtains expressions depending on different numbers of mean-fields. It was already mentioned that the mean-fields serve as a variational parameter. Thus, the best approximation is obtained if all pairing possibilities are employed in order to work with the maximal number of variational parameters and with that attain the lowest possible energy expectation value.

C.2. The BdG equations derived from the variational principle

To explicitly refer to what is needed in this thesis, we solely consider the t-J-model

$$H = -\sum_{(ij)s} t_{ij}(c^\dagger_{is}c_{js} + \text{h.c.}) + J\sum_{\langle ij\rangle}(\boldsymbol{S}_i\cdot\boldsymbol{S}_j - \frac{1}{4}\hat{n}_i\hat{n}_j) \tag{C.5}$$

where $\boldsymbol{S}_i = \frac{1}{2}c^\dagger_{is}\boldsymbol{\sigma}_{ss'}c_{is'}$. Here the no double occupancy condition is not accounted for, as in our calculations, it is either implemented via the Gutzwiller projection operator or completely neglected.

C.2.1. Energy expectation value

The interaction contributions can be written as

$$\boldsymbol{S}_i\cdot\boldsymbol{S}_j = S_{ix}S_{jx} + S_{iy}S_{jy} + S_{iz}S_{jz} \tag{C.6}$$

$$= S_{i+}S_{j-} + S_{i-}S_{j+} + S_{iz}S_{jz} \tag{C.7}$$

where the single terms are evaluated as

$$S_{ix}S_{jx} + S_{iy}S_{jy} = \frac{1}{2}(c^\dagger_{i\uparrow}c_{i\downarrow}c^\dagger_{j\downarrow}c_{j\uparrow} + c^\dagger_{i\downarrow}c_{i\uparrow}c^\dagger_{j\uparrow}c_{j\downarrow}) \tag{C.8a}$$

$$S_{iz}S_{jz} = \frac{1}{4}\big((n_{i\uparrow}n_{j\uparrow} + n_{i\downarrow}n_{j\downarrow}) - (n_{i\uparrow}n_{j\downarrow} + n_{i\downarrow}n_{j\uparrow})\big) \tag{C.8b}$$

Here and in the following we drop the hat on the operators $\hat{n}_{is}$ for notational simplicity. The charge density interaction is

$$\frac{1}{4}n_i n_j = (n_{i\uparrow}n_{j\downarrow} + n_{i\downarrow}n_{j\uparrow}) + (n_{i\uparrow}n_{j\uparrow} + n_{i\downarrow}n_{j\downarrow}) \tag{C.9}$$

such that

$$\boldsymbol{S}_i \cdot \boldsymbol{S}_j - \frac{1}{4} n_i n_j = \frac{1}{2}[(c^\dagger_{i\uparrow} c_{i\downarrow} c^\dagger_{j\downarrow} c_{j\uparrow} + c^\dagger_{i\downarrow} c_{i\uparrow} c^\dagger_{j\uparrow} c_{j\downarrow}) - (n_{i\uparrow} n_{j\downarrow} + n_{i\downarrow} n_{j\uparrow})] \tag{C.10}$$

Employ now the Hartree-Fock mean-field decoupling scheme introduced in Eq. (C.3). Here we decouple the expectation value of the spin interaction solely in the one "relevant" field $\langle c_{i\downarrow} c_{j\uparrow} \rangle$[3] which then reads

$$\begin{aligned}
\langle \boldsymbol{S}_i \cdot \boldsymbol{S}_j - \frac{1}{4} n_i n_j \rangle &= \frac{1}{2} \Big\langle (c^\dagger_{i\uparrow} c_{i\downarrow} c^\dagger_{j\downarrow} c_{j\uparrow} + c^\dagger_{i\downarrow} c_{i\uparrow} c^\dagger_{j\uparrow} c_{j\downarrow}) - (c^\dagger_{i\uparrow} c_{i\uparrow} c^\dagger_{j\downarrow} c_{j\downarrow} + c^\dagger_{i\downarrow} c_{i\downarrow} c^\dagger_{j\uparrow} c_{j\uparrow}) \Big\rangle \\
&= \frac{1}{2} \Big\langle (c^\dagger_{j\downarrow} c^\dagger_{i\uparrow} c_{i\downarrow} c_{j\uparrow} + c^\dagger_{j\uparrow} c^\dagger_{i\downarrow} c_{i\uparrow} c_{j\downarrow}) - (c^\dagger_{j\downarrow} c^\dagger_{i\uparrow} c_{i\uparrow} c_{j\downarrow} + c^\dagger_{j\uparrow} c^\dagger_{i\downarrow} c_{i\downarrow} c_{j\uparrow}) \Big\rangle \\
&\sim \frac{1}{2} (\langle c^\dagger_{j\downarrow} c^\dagger_{i\uparrow} \rangle \langle c_{i\downarrow} c_{j\uparrow} \rangle + \langle c^\dagger_{j\uparrow} c^\dagger_{i\downarrow} \rangle \langle c_{i\uparrow} c_{j\downarrow} \rangle) - (\langle c^\dagger_{j\downarrow} c^\dagger_{i\uparrow} \rangle \langle c_{i\uparrow} c_{j\downarrow} \rangle + \langle c^\dagger_{j\uparrow} c^\dagger_{i\downarrow} \rangle \langle c_{i\downarrow} c_{j\uparrow} \rangle)
\end{aligned} \tag{C.11}$$

At this point it is meaningful to define the pair wave function as the symmetrized sum of the mean-field $\langle c_{i\downarrow} c_{j\uparrow} \rangle$

$$\widetilde{\Delta}_{ij} \equiv \frac{1}{2} (\langle c_{i\downarrow} c_{j\uparrow} \rangle + \langle c_{j\downarrow} c_{i\uparrow} \rangle) = \frac{1}{2} (\langle c_{i\downarrow} c_{j\uparrow} \rangle - \langle c_{i\uparrow} c_{j\downarrow} \rangle) \tag{C.12}$$

Calculating its absolute square value yields

$$\begin{aligned}
\widetilde{\Delta}^*_{ij} \widetilde{\Delta}_{ij} &= \frac{1}{4} (\langle c^\dagger_{j\uparrow} c^\dagger_{i\downarrow} \rangle - \langle c^\dagger_{j\downarrow} c^\dagger_{i\uparrow} \rangle)(\langle c_{i\downarrow} c_{j\uparrow} \rangle - \langle c_{i\uparrow} c_{j\downarrow} \rangle) \\
&= \frac{1}{4} \Big(\langle c^\dagger_{j\uparrow} c^\dagger_{i\downarrow} \rangle \langle c_{i\downarrow} c_{j\uparrow} \rangle - \langle c^\dagger_{j\uparrow} c^\dagger_{i\downarrow} \rangle \langle c_{i\uparrow} c_{j\downarrow} \rangle - \langle c^\dagger_{j\downarrow} c^\dagger_{i\uparrow} \rangle \langle c_{i\downarrow} c_{j\uparrow} \rangle + \langle c^\dagger_{j\downarrow} c^\dagger_{i\uparrow} \rangle \langle c_{i\uparrow} c_{j\downarrow} \rangle \Big)
\end{aligned} \tag{C.13}$$

Comparing this with the result of Eq. (C.11) shows

$$\langle \boldsymbol{S}_i \cdot \boldsymbol{S}_j - \frac{1}{4} n_i n_j \rangle = -2 \widetilde{\Delta}^*_{ij} \widetilde{\Delta}_{ij} \tag{C.14}$$

With this approximation the mean-field expression for the energy expectation value reads

$$E_{\mathrm{mf}} = \langle H \rangle_{\mathrm{mf}} = -\sum_{(ij)s} t_{ij} (\widetilde{\chi}^*_{ijs} + \mathrm{h.c.}) - 2J \sum_{\langle ij \rangle} \widetilde{\Delta}^*_{ij} \widetilde{\Delta}_{ij} \tag{C.15}$$

where $\widetilde{\chi}^*_{ijs} \equiv \langle c^\dagger_{is} c_{js} \rangle$.

C.2.2. One-particle hamiltonian

Consider now explicitly a variational wave function $|\psi_0\rangle$. All expectation values used above and in particular the energy are now taken as evaluated in $|\psi_0\rangle$. In order to obtain the best approximation of the ground-state of the system the energy in Eq. (C.15) is minimized with respect to the free parameters $\{\Delta_{ij}\}$ fulfilling certain physical constraints.[4] Therefore

[3] In some cases only one field is relevant and all other possible fields in the decomposition can be neglected. For example, in a paramagnetic model, the antiferromagnetic order parameter is zero.

[4] These constraints can be summarized to the constraint that we employ a normalized one-particle wave function. This leads directly to the Fermi- or the Bose-function for the evaluation of expectation values.

$|\psi_0\rangle \equiv |\psi_0(\boldsymbol{\Delta})\rangle$, where $\boldsymbol{\Delta} \equiv (\dots, \Delta_{ij}, \dots)^T$ is a vector of length equal to the number of pairs nearest of neighbors on the lattice. The corresponding stationarity condition, the variation with respect to the trial wave function, reads

$$\frac{\delta E_{\mathrm{mf}}}{\delta\langle\psi_0|} + \mathcal{E}\frac{\delta(1-\langle\psi_0|\psi_0\rangle)}{\delta\langle\psi_0|} = 0 \tag{C.16}$$

Here the normalization condition $\langle\psi_0|\psi_0\rangle = 1$ was introduced via the Lagrange multiplier $\mathcal{E}$.

To evaluate Eq. (C.16) we have to take the functional derivative e.g. as in the term

$$\frac{\delta\Delta_{ij}^*}{\delta\langle\psi_0|} = \frac{1}{2}\frac{\delta(\langle\psi_0|c_{i\downarrow}^\dagger c_{j\uparrow}^\dagger - c_{i\uparrow}^\dagger c_{j\downarrow}^\dagger|\psi_0\rangle)}{\delta\langle\psi_0|} = \frac{1}{2}(c_{j\uparrow}^\dagger c_{i\downarrow}^\dagger - c_{j\downarrow}^\dagger c_{i\uparrow}^\dagger)|\psi_0\rangle \tag{C.17}$$

The formal procedure applied in the preceding equation can be justified by explicitly using the one-particle structure of $|\psi_0\rangle$. Apart from that it allows an unrestricted functional form for $|\psi_0\rangle$. Using this the evaluation of all terms is simple, e.g.

$$\frac{\delta(\Delta_{ij}^*\Delta_{ij})}{\delta\langle\psi_0|} = \Delta_{ij}\frac{\delta\Delta_{ij}^*}{\delta\langle\psi_0|} + \text{h.c.} = \Delta_{ij}(c_{j\uparrow}^\dagger c_{i\downarrow}^\dagger - c_{j\downarrow}^\dagger c_{i\uparrow}^\dagger)|\psi_0\rangle + \text{h.c.} \tag{C.18}$$

and leads to the evaluated expression for Eq. (C.16)

$$\Big(-\sum_{(ij)s} t_{ij}(c_{is}^\dagger c_{js} + \text{h.c.}) - J\sum_{\langle ij\rangle}(\Delta_{ij}(c_{j\uparrow}^\dagger c_{i\downarrow}^\dagger - c_{j\downarrow}^\dagger c_{i\uparrow}^\dagger) + \text{h.c.})\Big)|\psi_0\rangle = \mathcal{E}|\psi_0\rangle \tag{C.19}$$

Clearly, the expression on the left hand side defines the a one particle hamiltonian, such that in general one can define

$$H_{\mathrm{eff}} \equiv \frac{\delta E_{\mathrm{mf}}}{\delta\langle\psi_0|} \tag{C.20}$$

Furthermore, we already know that Eq. (C.20) is equivalent to the BdG equation Eq. (3.6) and with that we showed the equivalence of the BdG framework and a variational calculation.[5]

Finally, to obtain the effective one-particle hamiltonian used in this thesis we only have to employ another decomposition for the spin interaction. For this we cite Wang *et al.* (2006) and give[6]

$$\langle \boldsymbol{S}_i \cdot \boldsymbol{S}_j\rangle_0 = -\frac{3}{4}(\widetilde{\chi}_{ij}^*\widetilde{\chi}_{ij} + \widetilde{\Delta}_{ij}^*\widetilde{\Delta}_{ij}) \quad , \qquad \frac{1}{4}\langle\hat{n}_i\hat{n}_j\rangle_0 = \frac{1}{4}(-\widetilde{\chi}_{ij}^*\widetilde{\chi}_{ij} + \widetilde{\Delta}_{ij}^*\widetilde{\Delta}_{ij}) \tag{C.22}$$

[5] Eq. (C.20) can also be obtained by directly employing the decomposition of Eq. (C.1) in the t-J-hamiltonian of Eq. (C.5) without going through the variational calculation by just dropping the fluctuation and the scalar term in the operator expression. But this procedure does not clarify, why the energy should be minimal in a self-consistent solution of the BdG equation.

[6] In reference Wang *et al.* (2006) the expression reads

$$\langle \boldsymbol{S}_i \cdot \boldsymbol{S}_j\rangle_0 = -m_i m_j - \frac{3}{4}(\widetilde{\chi}_{ij}^*\widetilde{\chi}_{ij} + \widetilde{\Delta}_{ij}^*\widetilde{\Delta}_{ij}) \tag{C.21}$$

where $m_i = \frac{1}{2}(n_{i\uparrow} - n_{i\downarrow})$. In the whole theses only cases are examined in which $m_i = 0$ such that we can drop this

which leads to

$$E_{\mathrm{mf}} = -\sum_{(ij)s} t_{ij}(\widetilde{\chi}^*_{ijs} + \mathrm{h.c.}) - \sum_{\langle ij\rangle} \tfrac{1}{2} J_{ij} \widetilde{\chi}^*_{ij} \widetilde{\chi}_{ij} - \sum_{\langle ij\rangle} J_{ij} \widetilde{\Delta}^*_{ij} \widetilde{\Delta}_{ij} \tag{C.23}$$

and finally to

$$H_{\mathrm{RMFT}} = -\sum_{(ij)s} t_{ij} c^\dagger_{is} c_{js} + \mathrm{h.c.} - \sum_{\langle ij\rangle} \tfrac{1}{2} J_{ij} \widetilde{\chi}^*_{ij} c^\dagger_{i\uparrow} c_{j\uparrow} + \mathrm{h.c.} - \sum_{\langle ij\rangle} J_{ij} \widetilde{\Delta}_{ij} c^\dagger_{j\uparrow} c^\dagger_{i\downarrow} + \mathrm{h.c.} \tag{C.24}$$

where summations are over pairs of nearest neighbors $\langle ij\rangle$ and pairs of nearest and next-nearest neighbors (ij).

Our justification of the approach is exclusively based on a phenomenological viewpoint: we know from experience that a system is well described by a "hamiltonian" consisting of certain fields.[7] We can obviously state that the effective hamiltonian does not have anything to do with the corresponding microscopic hamiltonian that consists only of operators. The hamiltonian incorporating fields can rather be considered a Hamilton function for a classical problem, respecting the Fermi- or Bose-statistics and energetical features of the system — and no quantum correlations at all.

[7] Take again BCS: the picture of an electron gas of non-interacting pairs of electrons must be a realistic one taking into account the successfull description of experimental results. Not only that it yields reliable results, but also BCS is a much more clear description of the phenomen of superconductivity as a hypothetical exact one: If one included the interaction in a mathematically correct way one would end up with a veritable many-body Hilbert space, where the notion of electron pairs is completely useless being based on the notion of single particles. We see that in this case, the human-comprehensible, intuitive picture of electron pairs, is a very good description of nature — providing a physical understanding that would not be possible with a rigorous quantum mechanical treatment of the problem

D. The super cell method

D.1. Generalization of the Bloch theorem to an arbitrary elementary cell

We present the form of the Bloch theorem for a lattice with an elementary cell that contains several lattice sites. Such a lattice is called a super-lattice consisting of N_s super cells, i.e. N_s elementary cells. The following is based on the second proof of the Bloch theorem in Ashcroft and Mermin (1976, Ch. 9).

Given a hamiltonian on such a one-dimensional lattice of spacing a with N_s super cells, $L = N_s R$ lattice sites that is periodic in the super cells: $H(x + Ra) = H(x)$. Let us further impose periodic boundary conditions for the full lattice (a torus of N_s super cells): $\psi(x + La) = \psi(x)$. We can then write H and ψ in terms of their fourier transformations[1]

$$H(x) = \sum_K \mathrm{e}^{iKx} H(K) \quad \text{with} \quad K \in \mathcal{R} \equiv \{0, \tfrac{2\pi}{Ra}, 2\tfrac{2\pi}{Ra}, ..., (R-1)\tfrac{2\pi}{Ra}\} \tag{D.1}$$

$$\psi(x) = \sum_k \mathrm{e}^{ikx} \psi(k) \quad \text{with} \quad k \in \mathcal{BZ} \equiv \{0, \tfrac{2\pi}{La}, 2\tfrac{2\pi}{La}, ..., (L-1)\tfrac{2\pi}{La}\} \tag{D.2}$$

The eigenvalue equation (stationary Schroedinger equation) then reads

$$\begin{aligned}
&\big(H(x) - E\big)\psi(x) = 0 && \text{(D.3)}\\
&\Leftrightarrow \sum_{kK} \mathrm{e}^{i(K+k)x} H(K)\psi(k) - E\sum_k \mathrm{e}^{ikx}\psi(k) = 0\\
&\Leftrightarrow \sum_{kK} \mathrm{e}^{ikx} H(K)\psi(k-K) - E\sum_k \mathrm{e}^{ikx}\psi(k) = 0\\
&\Leftrightarrow \sum_k \mathrm{e}^{ikx}\big(\sum_K H(K)\psi(k-K) - E\psi(k)\big) = 0\\
&\Leftrightarrow \sum_K H(K)\psi(k-K) - E\psi(k) = 0 && \text{(D.4)}
\end{aligned}$$

The last line shows that for a value of $k \in \mathcal{BZ}$ all fourier coefficients $\psi(k)$ which differ from it by $K \in \mathcal{R}$ are coupled, i.e., the sum of these forms one solution of the eigenvalue problem. By choosing a second value for k that does not differ from the first one by a vector K, we find another independent solution, and so on. By inspection of $\mathcal{BZ}$ (and remembering $L = N_\mathrm{s} R$)

[1] Note that the restriction to a finite number of wave vectors in the sets $\mathcal{R}$, $\mathcal{BZ}$ is easily justified by noting that x can only take discrete values (multiples of a) on a lattice such that any value of $K_a = (n_1 R + n_2)\frac{2\pi}{Ra}$, where $n_1, n_2 \in \mathrm{N}$ and $n_2 < R$ yields the same phase factor as the value $K_b = n_2 \frac{2\pi}{Ra}$ both in the calculation of the coefficents $H(K_a) = \frac{1}{R}\sum_x \mathrm{e}^{-iK_a x} H(x) = \frac{1}{R}\sum_x \mathrm{e}^{-iK_b x} H(x) = H(K_b)$ as in the Fourier expansion $H(x) = \sum_K \mathrm{e}^{iKx} H(K)$ such that any other values as those listed in $\mathcal{R}$ are redundant. Analogous for $\mathcal{BZ}$.

it is clear that we can only find N_s sets of values of k that are independent in the just stated sense. This leads to a reduction of the Brillouin Zone (the set of wave vectors that provide independent solutions of the eigenvalue problem) such that all independent solutions that can be calculated from Eq. (D.4) have the form

$$\psi_k(x) := \sum_K \mathrm{e}^{i(k+K)x}\psi(k+K) = \mathrm{e}^{ikx}\sum_K \mathrm{e}^{iKx}\psi(k+K)$$
$$\text{with} \quad k \in \mathcal{BZ}^* \equiv \{0, \tfrac{2\pi}{La}, 2\tfrac{2\pi}{La}, ..., (N_s-1)\tfrac{2\pi}{La}\} \quad \text{(D.5)}$$

This is the Bloch theorem for an elementary cell consisting of an arbitrary number of lattice sites, as obviously: $u(x) = \sum_K \mathrm{e}^{iKx}\psi(k+K) = u(x+R)$. Note that the equation Eq. (D.4) has in general many solutions ψ_k for one value of k.

The generalization to higher dimensional lattices is trivial when employing the concept of the reciprocal lattice.

D.2. Fast Fourier transform matrix diagonalization

We consider the case of a hamiltonian with periodicity $H(x+Ra) = H(x)$ as above (one dimensional lattice of N_s super cells, $L = N_sR$), the eigenfunctions of which can be written as

$$\psi_{nk}(x) = \mathrm{e}^{ikx}u_n(x) \quad \text{where} \quad u_{nk}(x+Ra) = u_{nk}(x)$$
$$\text{with} \quad k \in \mathcal{BZ}^* \equiv \{0, \tfrac{2\pi}{La}, 2\tfrac{2\pi}{La}, ..., (N_s-1)\tfrac{2\pi}{La}\} \quad \text{(D.6)}$$

where we introduced a further index n anticipating that there are more solutions to be classified. Take now the concrete case of a hamiltonian the action of which is defined as: $H\psi(x) = \sum_\tau T(x,\tau)\psi(x+\tau) + V(x)\psi(x)$, where the term depending on the neighbors τ of the site x, $T(x,\tau)$ and a potential term $V(x)$ have the periodicity of the super cell, i.e., $T(x+Ra,\tau) = T(x,\tau)$, $V(x+Ra) = V(x)$. The hamilton operator can be written in matrix form as

$$H \equiv (H_{xy})_{x,y=0}^{L-1} \quad \text{with} \quad H_{xy} = \delta_{\tau y}T(x,\tau) + \delta_{xy}V(x) \quad \text{(D.7)}$$

when writing the state vector as $\psi = (\psi(0), \psi(1), ..., \psi(L-1))^T$. With this notation the eigenvalue equation Eq. (D.3) can be written with Eq. (D.6) in the following way

$$(H-E_{nk})\begin{pmatrix}\psi_{nk}(0)\\ \psi_{nk}(1)\\ \vdots\\ \psi_{nk}(L-1)\end{pmatrix} = 0 \quad \Leftrightarrow \quad (H-E_{nk})\begin{pmatrix}u_{nk}(0)\\ \mathrm{e}^{ik}u_{nk}(1)\\ \vdots\\ \mathrm{e}^{ik(L-1)}u_{nk}(L-1)\end{pmatrix} = 0 \quad \text{(D.8)}$$

Employing the periodicity condition for $u_{nk}(x)$ yields

$$(H - E_{nk}) \begin{pmatrix} \tilde{\mathbf{u}}_{nk} \\ \mathrm{e}^{ikR}\tilde{\mathbf{u}}_{nk} \\ \vdots \\ \mathrm{e}^{ik(N_s-1)R}\tilde{\mathbf{u}}_{nk} \end{pmatrix} = 0 \quad \text{where} \quad \tilde{\mathbf{u}}_{nk} \equiv \begin{pmatrix} u_{nk}(0) \\ \mathrm{e}^{ik}u_{nk}(1) \\ \vdots \\ \mathrm{e}^{ik(R-1)}u_{nk}(R-1) \end{pmatrix} \tag{D.9}$$

Let us write down the equations for the Mth supercell, i.e. for $x \in \{MR, ..., (M+1)R-1\}$, of the matrix equation:

$$\begin{aligned} & T(x,\tau)\mathrm{e}^{ik(M+\sigma(\tau))R}\tilde{u}_{nk}(\tau) + (V(x) - E_{nk})\mathrm{e}^{ikMR}\tilde{u}_{nk}(x) = 0 \\ \Leftrightarrow \quad & T(x,\tau)\mathrm{e}^{ik\sigma(\tau)R}\tilde{u}_{nk}(\tau) + (V(x) - E_{nk})\tilde{u}_{nk}(x) = 0 \end{aligned} \tag{D.10}$$

where

$$\sigma(\tau) = \begin{cases} 1 & \text{if } \tau \text{ in upper super cell} \\ 0 & \text{if } \tau \text{ in same super cell} \\ -1 & \text{if } \tau \text{ in lower super cell} \end{cases} \tag{D.11}$$

As in Eq. (D.10) $T(x+R,\tau) = T(x,\tau)$, $V(x+R) = V(x)$, i.e. the coefficients in the equation are the same for each super cell (also the function $\sigma(\tau)$ is the same for the whole lattice). It is therefore sufficient to calculate $\tilde{u}_{nk}$ via (D.10) (the reduced eigenvalue problem) to obtain the full eigenvector ψ_{nk}.

Let us put this in a form one would use in a program code, such that the procedure to calculate all $L = N_s R$ eigenvalues and vectors of the Hamilton operator is as follows. Solve the reduced eigenvalue problem Eq. (D.10) and Eq. (D.12) for a fixed value of k by diagonalizing the matrix[2]

$$H^k_{\text{reduced}} \equiv (H_{xy})^{R-1}_{x,y=0} \quad \text{with} \quad H_{xy} = \delta_{\tau y}\mathrm{e}^{ik\sigma(\tau)R}T(x,\tau) + \delta_{xy}V(x) \tag{D.12}$$

which yields a set of R eigenvalues $\{E_{0k}, E_{1k}, ..., E_{(R-1)k}\}$ and vectors $\{\tilde{\mathbf{u}}_{0k}, \tilde{\mathbf{u}}_{1k}, ..., \tilde{\mathbf{u}}_{(R-1)k}\}$. The set of R eigenvectors for the wave vector k of the full hamiltonian is then obtained as

$$\psi_{nk} = \begin{pmatrix} \tilde{\mathbf{u}}_{nk} \\ \mathrm{e}^{ikR}\tilde{\mathbf{u}}_{nk} \\ \vdots \\ \mathrm{e}^{ik(N_s-1)R}\tilde{\mathbf{u}}_{nk} \end{pmatrix} \tag{D.13}$$

Repeat the procedure for the next value of $k \in \mathcal{BZ}^*$ to obtain the next set of R eigenvalues and vectors, and so on. This yields finally $L = N_s R$ solutions.

The generalization to more than one dimension is straightforward using the concept of the reciprocal lattice. A derivation of the preceding in a completely different is found in e.g. Ghosal *et al.* (2002).

[2]Note that as $k \in \mathcal{BZ}^*$ the phase factor in Eq. (D.10) and Eq. (D.12) reads: $\mathrm{e}^{ik\sigma(\tau)R} = \mathrm{e}^{i2\pi\sigma(\tau)m/N_s}$ where $m \in \{0, 1, ..., N_s - 1\}$ ($k = m\frac{2\pi}{N_s R}$) so that in the program one will employ a parametrization in terms of the integer numbers m instead of the wave vectors k.

Bibliography

Andersen, B. M., Y. S. Barash, S. Graser, and P. J. Hirschfeld, 2008, Phys. Rev. B **77**, 054501.

Anderson, P. W., 1973, Mater. Res. Bull. **8**, 153.

Anderson, P. W., 1987, Science **235**, 1196.

Anderson, P. W., P. A. Lee, M. Randeria, T. M. Rice, N. Trivedi, and F. C. Zhang, 2004, J. Phys.: Condens. matter **16**, R755.

Ashcroft, N. W., and N. D. Mermin, 1976, *Solid State Physics* (Brooks Cole).

Brinkman, W. F., and T. M. Rice, 1970, Phys. Rev. B **2**, 4302.

Datta, S., and P. F. Bagwell, 2008, Superlattices and Microstructures **25**, 1233.

Dimos, D., P. Chaudhari, J. Mannhart, and F. K. LeGoues, 1988, Phys. Rev. Lett. **61**, 219.

Edegger, B., V. N. Muthukumar, and C. Gros, 2007, Advances in Physics **56**, 927.

Fazekas, P., and P. W. Anderson, 1974, Phil. Mag. **30**, 432.

Forster, O., 2008, *Analysis 2* (Vieweg+Teubner, Wiesbaden), 8th edition.

Freericks, J. K., 2006, *Transport in Multilayered Nanostructures: The Dynamical Mean-Field Theory Approach* (Imperial College Press).

Freericks, J. K., 2010, Nat. Phys. **6**, 559.

Fukushima, N., 2008, Phys. Rev. B **78**, 115105.

Fukushima, N., C.-P. Chou, and T. K. Lee, 2009, Phys. Rev. B **79**, 184510.

Garg, A., M. Randeria, and N. Trivedi, 2008, Nat. Phys. **4**, 762.

Ghosal, A., C. Kallin, and A. J. Berlinsky, 2002, Phys. Rev. B **66**, 214502.

Graser, S., P. J. Hirschfeld, T. Kopp, R. Gutser, B. M. Andersen, and J. Mannhart, 2010, Nat. Phys. **6**, 609.

Gurevich, A., and E. A. Pashitskii, 1998, Phys. Rev. B **57**, 13878.

Gutzwiller, M. C., 1963, Phys. Rev. Lett. **10**, 159.

Gutzwiller, M. C., 1964, Phys. Rev. **134**, A923.

Gutzwiller, M. C., 1965, Phys. Rev. **137**, A1726.

Hammerl, G., H. Bielefeldt, S. Leitenmeier, A. Schmehl, C. Schneider, A. Weber, and J. Mannhart, 2002, Eur. Phys. J. B **27**, 299.

Hammerl, G., A. Schmehl, R. R. Schulz, B. Goetz, H. Bielefeldt, C. W. Schneider, H. Hilgenkamp, and J. Mannhart, 2000, Nature (London) **407**, 162.

Hilgenkamp, H., and J. Mannhart, 2002, Rev. Mod. Phys. **74**, 485.

Hubbard, J., 1963, Proc. R. Soc. London., Ser. A **276**, 238.

Jaksch, D., C. Bruder, J. I. Cirac, C. W. Gardiner, and P. Zoller, 1998, Phys. Rev. Lett. **81**, 3108.

Jaksch, D., V. Venturi, J. I. Cirac, C. J. Williams, and P. Zoller, 2002, Phys. Rev. Lett. **89**(4), 040402.

Kanamori, J., 1963, Prog. Theor. Phys. **30**, 238.

Ko, W.-H., C. P. Nave, and P. A. Lee, 2007, Phys. Rev. B **76**, 245113.

Li, C., S. Zhou, and Z. Wang, 2006, Phys. Rev. B **73**, 060501.

Metzner, W., and D. Vollhardt, 1988, Phys. Rev. B **37**, 7382.

Mineev, V. P., and K. V. Samokhin, 1999, *Introduction to unconventional superconductivity* (Gordon and Breach Science Publishers, Amsterdam).

Mott, N. F., 1949, Proc. Phys. Soc. A **62**, 416.

Ogata, M., and H. Fukuyama, 2008, Rep. Prog. Phys. **71**, 036501.

Ogata, M., and A. Himeda, 2003, Journal of the Physical Society of Japan **72**, 374.

Ogawa, T., K. Kanda, and T. Matsubara, 1975, Prog. Theor. Phys. **53**, 614.

Pennycook, S. J., C. Prouteau, M. F. Chisholm, D. K. Christen, D. Verebelyi, D. P. Norton, M. Kim, N. D. Browning, J. P. Buban, Y. Pan, and J. F. Hamet, 2000, *Studies of High Temperature Superconductors: Microstructures and Related Studies of High Temperature Superconductors-II*, volume 30 (Nova Science Publishers).

Raczkowski, M., and D. Poilblanc, 2009, Phys. Rev. Lett. **103**, 027001.

Schwingenschlögl, U., and C. Schuster, 2009, Phys. Rev. B **79**, 092505.

Sigrist, M., 2006, *Unkonventionelle Supraleitung* (Lecture Notes, ETH Zürich), URL `http://www.itp.phys.ethz.ch/education/prev_lectures/ws05/ucsc`.

Stolbov, S. V., M. K. Mironova, and K. Salama, 1999, Superconductor Science and Technology **12**, 1071.

Tanaka, Y., and S. Kashiwaya, 1995, Phys. Rev. Lett. **74**, 3451.

Tsuchiura, H., Y. Tanaka, M. Ogata, and S. Kashiwaya, 1999, Journal of the Physical Society of Japan **68**, 2510.

Tsuchiura, H., Y. Tanaka, M. Ogata, and S. Kashiwaya, 2001, Phys. Rev. B **64**, 140501.

Vollhardt, D., 1984, Rev. Mod. Phys. **56**, 99.

Wang, Q.-H., Z. D. Wang, Y. Chen, and F. C. Zhang, 2006, Phys. Rev. B **73**, 092507.

Wolf, F. A., S. Graser, F. Loder, and T. Kopp, 2012, Phys. Rev. Lett. **108**, 117002.

Yokoyama, T., Y. Sawa, Y. Tanaka, and A. A. Golubov, 2007, Phys. Rev. B **75**, 020502.

Zhang, F. C., C. Gros, T. M. Rice, and H. Shiba, 1988, Supercond. Sci. Technol. **1**, 36.

Zhang, F. C., and T. M. Rice, 1988, Phys. Rev. B **37**, 3759.